

Dissertation zur Erlangung des Doktorgrades (Dr. rer. nat.)  
des Fachbereichs Mathematik/Informatik  
der Universität Osnabrück

---

# The Modification of Boolean Models in Random Network Analysis

---

Vorgelegt von

Stephan Bussmann  
aus Damme

und betreut durch  
Prof. Dr. Hanna Döring  
sowie Prof. Dr. Nils Aschenbruck.

Osnabrück, Oktober 2021



## Acknowledgments

Above all I would like to express my deepest gratitude to my family. In particular to my siblings Kathrin, Sandra and Michael and my parents Brigitte and Burkhard. They were always there for me and at all times showed their unconditional support. This provided a safe environment and allowed me to freely pursue my interests. No less, I thank Julia for her constant love and support. Her patience and motivational skills in the months preceding the final form of this manuscript were truly exceptional.

During my studies at Osnabrück University I had the pleasure to get to know a host of outstanding people. I am thankful to Christian, David, Patrick and Tim for being steadfast companions throughout my bachelor's and master's studies and whose presence in my life I thoroughly enjoy to this day. Furthermore, I thank the university funded research training group 'Graphs and Networks' for the opportunity to write this thesis. During my doctoral studies I had an incredible time at both the Institute of Computer Science and Institute of Mathematics and am thankful for the great atmosphere created by my colleagues. Alexander, Bertram, Jan, Matthias, Rissa, Stefanie, Thomas and Timmy I thank for a great time in the distributed systems group and for introducing me to the great sport of bouldering. Alex N., Alex G., Arun, Dominik, Jan-Marten, Jens, Jonathan, Katharina, Lorenzo, Markus, Marianne, Mathias and Sabine all made work at the Institute of Mathematics a blast. I am especially thankful to my academic sister Carina Betken for being both a helpful colleague and a steadfast friend.

Finally, I want to give special thanks to my doctoral advisors Hanna Döring and Nils Aschenbruck. I am thankful for the countless discussions we had which helped me finish this thesis as well as the great confidence and patience they showed towards me. In the same line I am thankful to Matthias Reitzner for always having an open door.



# Contents

<b>1</b>	<b>Introduction</b>	<b>7</b>
<b>2</b>	<b>Preliminaries</b>	<b>13</b>
2.1	General Notations . . . . .	13
2.2	Poisson point processes . . . . .	14
2.3	Basics of Graph and Percolation Theory . . . . .	18
2.3.1	Discrete Percolation . . . . .	19
2.3.2	Continuum Percolation . . . . .	20
2.4	Normal Approximation via Malliavin-Stein . . . . .	22
2.4.1	Stein's Method . . . . .	23
2.4.2	Malliavin Calculus and Poisson Functionals . . . . .	25
2.4.3	The Malliavin-Stein Method . . . . .	27
<b>3</b>	<b>The Obstructed Gilbert Graph</b>	<b>29</b>
3.1	Related Works . . . . .	29
3.2	Construction of the Graph . . . . .	30
3.2.1	The Galton-Watson Tree . . . . .	31
3.3	Critical Intensities . . . . .	32
3.4	A Central Limit Theorem for the Covered Volume . . . . .	37
<b>4</b>	<b>Time Bounded Cylinders</b>	<b>43</b>
4.1	Related Works . . . . .	43
4.2	Construction of the Cylinders . . . . .	44
4.3	Applying the Malliavin-Stein Bound . . . . .	48
4.4	Central Limit Theorems . . . . .	52
4.4.1	Proof for the Covered Volume . . . . .	54
4.4.2	Proof for the Isolated Nodes . . . . .	57
4.4.3	Proof for the Euler Characteristic . . . . .	59
4.5	Stacked Time Bounded Cylinders . . . . .	60
4.5.1	Construction of the Cylinderstacks . . . . .	61
4.5.2	Covered Volume . . . . .	63
4.5.3	Isolated Cylinders . . . . .	65
<b>5</b>	<b>Closing Remarks</b>	<b>66</b>

<b>6 Addendum - Simulation Techniques</b>	<b>68</b>
6.1 Poisson Point Processes . . . . .	68
6.2 Connected components . . . . .	70
6.3 The Carcassonne Grid . . . . .	71
<b>List of Figures</b>	<b>75</b>
<b>Bibliography</b>	<b>77</b>

# Chapter 1

## Introduction

*Abstract:* In this manuscript we perform a rigorous mathematical investigation of the behavior opportunistic network models exhibit when two major real-world problems are taken into account. The first problem considered is *obstruction*. Here we model the network using an **obstructed Gilbert graph** which is a classical Gilbert graph but where there exist zones where no nodes are allowed to be placed. We take a look at percolation properties of this model, that is we investigate random graph configurations for which a component of infinite size has strictly positive probability to be created. The second problem considered in this thesis is *mobility*. Of course mobility in and of itself is not a problem but a feature in any network that follows the store-carry-forward paradigm. However it can be problematic to properly handle in a mathematical model. In the past this has been done by modelling movement by a series of static network configurations. However, with this technique it can be difficult to get a grasp on some of the time sensitive properties of the network. In this work we introduce the **time bounded cylinder** model which enables an analysis over a complete timeframe. We provide normal approximations for important properties of the model, like its covered volume and the number of isolated nodes.

As we are using rigorous mathematics to tackle problems which computer scientists working in the field of distributed systems are faced with, we bring the two fields closer together.

### The Boolean model and random networks

In this thesis we are interested in opportunistic networks. These are defined by a network topology where the status of a communications channel is unpredictable.

Think of some software that is installed on a mobile device and is communicating via Bluetooth with other devices that have the same software installed. It is easy to see that the network topology in this setting is constantly changing, as Bluetooth provides a limited communication range and the mobile nodes are frequently entering and leaving each others communication radius. Consult [MFM<sup>+</sup>14] for an extensive introduction into opportunistic networks. We care about this setting as it portrays the network topology oftentimes used in emerging technologies, like the Internet of Things [LJ19] or device-to-device communication.

Mathematically, opportunistic networks are modelled by placing a deterministic or random number of points randomly in Euclidean space and declare a communications channel between these points open if they fulfill some proximity threshold. The classical approach for theoretical studies of these telecommunication networks is to consider the **Boolean model** (see [JK20] or [LP18] for reference) where participants are represented by the nodes and their communication zone is given by a ball around these nodes. Representing connections between nodes by an edge the considered graph model is the Gilbert graph, also known as random geometric graph.

Probably the most common and fruitful way to introduce randomness in this model is creating the nodes by using a Poisson point process. That is a random point set with convenient independence properties, which make it accessible to an extensive mathematical toolset. Most notably it is highly modifiable via the use of markings, as we will see in detail in Chapter 2.

### Obstruction

A shortcoming of using the (homogeneous) Poisson model for placing the participants of the networks is that geographical restrictions are not considered. Works as [JBRAS05] and more recently [SA19] clearly show by simulation that the introduction of restrictions like this have a great influence on the connectivity of a network. One approach to tackle this is the Poisson Hole Process [Hae12] where we model obstructions by a secondary, independent Poisson point process. We use this setting to define the obstructed Gilbert graph: Imagine two Poisson point processes  $\eta_N$  and  $\eta_O$  as well as proximity thresholds  $r_N > 0$  and  $r_O > 0$ . The vertices of our graph are the points of  $\eta_N$  with a distance of at least  $r_O$  to any point in  $\eta_O$ . Two vertices are connected if their distance is below or equal to  $r_N$ . In this work we are firstly interested in percolation thresholds of this model. That means we look for configurations by which the graph has strictly positive probability to create a component of infinitely many nodes. These thresholds are of particular interest as how readily a network percolates is a good indicator for its robustness (see [New10, Chapter 16] for example). In Theorem 3.4 we give a bound on the subcritical regime that is configurations by which the probability of percolation is



zero. Under strict assumptions we then look at the supercritical regime in Theorem 3.6 that is configurations by which the probability of percolation is above zero. We give a bound by which the graph is certain to be in this regime, thus proving the existence of a phase transition from subcritical to the supercritical regime.

After that we let  $Z_N$  and  $Z_O$  denote the random sets given by the Boolean models associated to  $\eta_N$  and  $\eta_O$  respectively. We are interested in the covered volume  $Z_N \setminus Z_O$  restricted to some window of observation. Let  $W_s = [-\frac{s}{2}, \frac{s}{2}]^d$  denote said window and  $\mathcal{N}(0, 1)$  the standard normal distribution. We present the following theorem:

**Theorem 1.1.** *Assume  $0 < \gamma_N, \gamma_O, r_N, r_O < \infty$ . As  $s \rightarrow \infty$ , the distribution of the standardized covered volume of the random set  $(Z_N \setminus Z_O) \cap W_s$  satisfies*

$$\frac{\lambda_d((Z_N \setminus Z_O) \cap W_s) - \mathbb{E}[\lambda_d((Z_N \setminus Z_O) \cap W_s)]}{\sqrt{\mathbb{V}[\lambda_d((Z_N \setminus Z_O) \cap W_s)]}} \xrightarrow{d} \mathcal{N}(0, 1).$$

We additionally prove that the rate of convergence in this case is  $1/\sqrt{\lambda_d(W_s)}$ .

## Mobility

In the domain of telecommunication network performance evaluation, one of the oldest models used for the dynamics of moving nodes is the random direction mobility model (for reference see [RMSM01] or [CBD02]). Nowadays, it is available within standard evaluation frameworks surveyed in [DFHO<sup>+</sup>18]. The random direction model belongs to the group of standard, basic models used in nearly every performance evaluation to understand the elementary properties in well-known standard scenarios before considering more sophisticated and more realistic ones. Within a performance analysis, it is common to analyze series of states of the model indexed by time. However, for networks that are delay tolerant, such as opportunistic networks, longer periods of time are more interesting. Opportunistic networks follow the store-carry-forward paradigm, where the movement of the devices is used to carry the messages to their destinations. In this domain, it is particularly interesting to answer certain questions for a longer period of time such as:

- (1) Will a message reach a node (at all)?
- (2) Does a node stay isolated?

Since it is clear that mobility changes the properties of a network, there are first results to consider the dynamics of mobile communication networks, see e.g., [DMPG09] starting with discrete snapshots of the random walk model on the torus. In [DFK16], the nodes of the telecommunication network move according to the random waypoint model and the connection time of two random nodes is

studied. The very recent work [HJC21] also deals with a dynamic Boolean model, where Hirsch, Jahnel and Cali consider two different kinds of movement, small movements with a small velocity and a few large movements with a high velocity. They derive asymptotic formulas for the percolation time and the  $k$ -hop connection time.

In this thesis we propose the time bounded cylinder (TBC) model which enables an analysis over a complete timeframe by modeling the movement in  $\mathbb{R}^d$  and the resulting communication capabilities via cylinders in  $\mathbb{R}^d \times [0, T]$ . Our first step will be to establish the theory for a rigid movement model where nodes pick a direction and velocity at random and keep these for the complete timeframe. In a second step we will propose a method to introduce changes in direction and velocity.

The following is a slightly simplified construction, which will be made more precise in Chapter 4. We take a set of points in  $\mathbb{R}^d \times \{0\}$  sampled from a homogeneous Poisson point process with intensity  $0 < \gamma < \infty$ . For each of these points  $p_0$  we randomly choose a vector  $v$  from the upper half of the  $d + 1$ -dimensional unit sphere. Then we fix some  $T \geq 0$  and look at  $p_0 + v \in \mathbb{R}^{d+1}$ . This vector defines a line from  $p_0$  to some point  $p_T \in \mathbb{R}^d \times \{T\}$ . We fix some radius  $r > 0$  and for every point  $x$  on this line consider the ball  $\mathbb{B}_d(x, r)$ . The union of these balls defines the time bounded cylinder on  $p$  in direction  $v$ . Let  $Z$  denote the union of all cylinders created this way for some Poisson process and let  $W_s = [-\frac{s}{2}, \frac{s}{2}]^d \times [0, T]$ . Our first main finding in Chapter 4 is this:

**Theorem 1.2.** *As  $s \rightarrow \infty$ , the standardized covered volume of the TBC model as defined in Chapter 4 satisfies*

$$\frac{\lambda_{d+1}(Z \cap W_s) - \mathbb{E}[\lambda_{d+1}(Z \cap W_s)]}{\sqrt{\mathbb{V}[\lambda_{d+1}(Z \cap W_s)]}} \xrightarrow{d} \mathcal{N}(0, 1).$$

Moreover, in Theorem 4.12 we see that the rate of convergence in the Wasserstein distance is of order  $1/\sqrt{\lambda_{d+1}(W_s)}$ . Theorem 4.21 gives an analogous result in the setting allowing for changes in direction. The covered volume is a very interesting quantity in network simulation as it gives some insight into the connectedness of the model. Less volume means more overlap of the communication zones which, in turn, implies greater connectivity. Since the TBC model considers the complete timeframe, its covered volume actually gives insight into the achievable throughput of the network.

The next property considered is the number of isolated nodes, which means cylinders that do not intersect with the rest of the model within the timeframe.

**Theorem 1.3.** *Assume  $d = 2$  and let  $\text{Iso}_Z(s)$  denote the number of cylinders with basepoint in  $[-\frac{s}{2}, \frac{s}{2}]^2$  that do not intersect with any cylinder in the TBC model as defined in Chapter 4. Then*

$$\frac{\text{Iso}_Z(s) - \mathbb{E}[\text{Iso}_Z(s)]}{\sqrt{\mathbb{V}[\text{Iso}_Z(s)]}} \xrightarrow{d} \mathcal{N}(0, 1)$$

as  $s \rightarrow \infty$ .

As before we additionally offer a rate of convergence (see Theorem 4.13) and a version for changeable directions (see Theorem 4.22). These nodes are of particular interest in opportunistic networks as one can not communicate with them. Let us assume a sensor node (e.g. deployed for wildlife monitoring [ABV<sup>+</sup>12]) that can store the sensor data for some time, but has to transmit the data before it runs out of memory. If this node stays isolated for too long, it results in loss of data (e.g. inaccuracies in the wildlife tracking trace). Lastly we come to a quantity of more theoretical significance and present a limit theorem for the Euler characteristic of the model, a precise definition of which is given in Chapter 4.

**Theorem 1.4.** *Assume  $d = 2$  and let  $s \rightarrow \infty$ , then the Euler characteristic  $\chi$  of the TBC model  $Z$  restricted to a window  $W_s = [-\frac{s}{2}, \frac{s}{2}]^2$  satisfies a central limit theorem, namely*

$$\frac{\chi(Z \cap W_s) - \mathbb{E}[\chi(Z \cap W_s)]}{\sqrt{\mathbb{V}[\chi(Z \cap W_s)]}} \xrightarrow{d} \mathcal{N}(0, 1).$$

Since the Euler characteristic can be defined as the alternating sum of Betti numbers, we see this result as an incentive for further mathematical studies of the Betti numbers of the TBC model. These would give great insight into the topological structure of the model, such as the number of connected components or the number of holes. From a computer science perspective, both of these would be of special interest.

## Structure of the Thesis

### Chapter 2: Preliminaries

Here we prepare the toolset needed to understand the main chapters of this thesis. We will start with some general notation. After that, we provide what we need to know about Poisson point processes. In Section 2.2 we give a rigorous definition and present theorems which will prove useful later on. We do the same for the basic principles of percolation theory in Section 2.3. Section 2.4 then gives some background on the Malliavin-Stein method, which provides us with our main tool for proving central limit theorems.

### Chapter 3: The Obstructed Gilbert Graph

In this chapter we first give a concise definition of the graph considered in this setting and then introduce the Galton-Watson tree which is a special graph structure that will prove useful when proving the main results of the chapter. Our main findings regarding the obstructed Gilbert graph will be presented and proven in

Section 3.3.

#### **Chapter 4: Time Bounded Cylinders**

This is the major chapter of this thesis where we introduce our novel approach to modelling mobility in random networks. Again, we first give concise instructions on how our model is created. After that, in Section 4.3, we prove the lemma we use to derive our central limit theorems. It is an application of results from the Malliavin-Stein method tailored to fit our setting. Section 4.4 then presents these results and gives the necessary proofs. In Section 4.5 we then propose a modification of our model that allows for changes in direction. We proceed to present and prove modifications of our main results from the section before.

#### **Addendum: Simulation Techniques**

In the spirit of bringing mathematics and computer science closer together we introduce algorithms for simulating the concepts presented throughout this thesis. First we introduce our used algorithm for creating Poisson point processes which, in particular, allows for the creation of inhomogeneous processes. After that we present algorithms to evaluate the structure of a graph and introduce another modified Boolean model named the Carcassonne grid.

# Chapter 2

## Preliminaries

In this chapter we present and explain the most important tools and concepts used throughout this thesis. We also establish most of the symbolism and notation used in later chapters. However, it is assumed that the reader has some basic knowledge on probability theory and the theory of point processes.

### 2.1. General Notations

We start with the set of natural numbers excluding zero which we denote by  $\mathbb{N}$ . Furthermore, we set  $\mathbb{N}_0 := \mathbb{N} \cup \{0\}$ . Let  $\mathbb{Z}$  denote the set of integers,  $\mathbb{R}$  the set of real numbers and  $\mathbb{R}_+ = [0, \infty)$ . As we will primarily be working in the Euclidean space  $\mathbb{R}^d$ , we set  $\|\cdot\|$  as the Euclidean norm, that is

$$\|v\| := \|v\|_2 = \sqrt{v_1^2 + v_2^2 + \cdots + v_d^2}$$

for any vector  $v = (v_1, \dots, v_d) \in \mathbb{R}^d$ . We define the closed  $d$ -dimensional ball of radius  $r \in \mathbb{R}_+$  centered at  $x \in \mathbb{R}^d$  by

$$\mathbb{B}_d(x, r) := \{y \in \mathbb{R}^d \mid \|x - y\| \leq r\}.$$

For a ball centered at the origin we abbreviate this notation to  $\mathbb{B}_d(r)$ . Let  $\lambda_d$  denote the Lebesgue-measure on  $\mathbb{R}^d$ . The volume of the  $d$ -dimensional unit ball is given by

$$\kappa_d := \lambda_d(\mathbb{B}_d(1)) = \frac{\pi^{\frac{d}{2}}}{\Gamma(\frac{d}{2} + 1)}$$

where  $\Gamma$  denotes the gamma function. The  $(d - 1)$ -dimensional unit sphere is the boundary of the unit ball,

$$S^{d-1} := \partial\mathbb{B}_d(1) = \{x \in \mathbb{R}^d \mid \|x\| = 1\}.$$

Given any set  $A$  we denote by  $\mathcal{P}(A)$  its power set and by  $\mathcal{B}(A)$  the Borel- $\sigma$ -algebra over  $A$ . For  $B \subset A$  we write  $\mathbb{1}_B$  for the indicator function of  $B$ , that is

$$\mathbb{1}_B : A \rightarrow \{0, 1\} \text{ with } \mathbb{1}_B(x) = \begin{cases} 1, & x \in B \\ 0, & x \notin B \end{cases}.$$

Finally, for some measurable space  $(\mathbb{X}, \mathcal{X})$  and  $(x, B) \in \mathbb{X} \times \mathcal{X}$ , we define by  $\delta_x(B) := \mathbb{1}_B(x)$  the Dirac measure concentrated on  $x \in \mathbb{X}$ .

## 2.2. Poisson point processes

The central concept in this thesis is the Poisson point process. We will now give the necessary definitions and present some useful results that will prove useful later on. For this, we follow [LP18] and fix some probability space  $(\Omega, \mathbb{P}, \mathcal{A})$  and a measurable space  $(\mathbb{X}, \mathcal{X})$ .

**Definition 2.1.** Consider a  $\sigma$ -finite intensity measure  $\Lambda$  on  $\mathbb{X}$ . A point process  $\eta$  on  $\mathbb{X}$  is called a Poisson point process with intensity measure  $\Lambda$  if

- we have that  $\mathbb{P}[\eta(A) = k] = \frac{\Lambda(A)^k}{k!} e^{-\Lambda(A)}$  for all  $A \in \mathcal{X}$  and  $k \in \mathbb{N}_0$ ,
- for  $m \in \mathbb{N}$  and a vector of pairwise disjoint sets  $(A_1, \dots, A_m) \in \mathbb{X}^m$ , we have that  $(\eta(A_1), \dots, \eta(A_m)) \in \mathbb{N}^m$  is a vector of independent random variables.

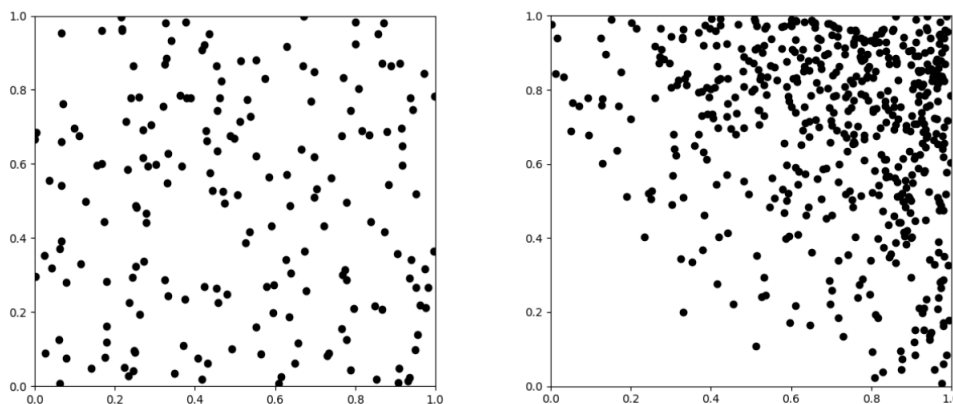


Figure 2.1: Two realizations of Poisson point processes observed in the cube  $[0, 1]^2$ . To the left we see the stationary case with intensity 200. To the right we see the case where the intensity measure is given by  $\Lambda(A) = 200 \cdot \int_A (x + y)^3 d(x, y)$ ,  $A \subset [0, 1]^2$ .

We take special interest in the case  $\mathbb{X} = \mathbb{R}^d$  and  $\Lambda(A) = \gamma \cdot \lambda_d(A)$  where  $\gamma$  denotes a real constant, i.e.  $\gamma \in (0, \infty)$ . In this case we refer to the Poisson point process as **stationary**. Since the Lebesgue measure is invariant under translations, the point process shows the same behavior no matter where in  $\mathbb{R}^d$  we choose to evaluate it. This is why in the stationary case they are sometimes also referred to as homogeneous.

Poisson point processes admit the following characterization, known as the Mecke equation. Here we denote by  $\mathcal{N}(\mathbb{X})$  the space of all measures that can be constructed by a countable sum of finite counting measures on  $\mathbb{X}$ .

**Theorem 2.2** (Mecke Equation). *Consider a  $\sigma$ -finite intensity measure  $\Lambda$  on  $\mathbb{X}$  and a point process  $\eta$  on  $\mathbb{X}$ . The following items are equivalent:*

- $\eta$  is a Poisson point process with intensity measure  $\Lambda$ .
- $\mathbb{E} \left[ \int_{\mathbb{X}} f(x, \eta) \eta(dx) \right] = \int_{\mathbb{X}} \mathbb{E} [f(x, \eta + \delta_x)] \Lambda(dx)$  for all measurable functions  $f$  on  $\mathbb{X} \times \mathcal{N}(\mathbb{X})$  with values in  $[0, \infty]$ .

We will not give a proof here but refer to [LP18, p.27]. A core concept throughout this thesis will be the marking of Poisson processes, as we use it to establish the models that will be analysed in later chapters. To understand markings we have to prepare with the following item.

**Definition 2.3.** *Consider measurable spaces  $(\mathbb{X}, \mathcal{X})$  and  $(\mathbb{Y}, \mathcal{Y})$ . A function*

$$f : \mathbb{X} \times \mathcal{Y} \rightarrow [0, 1]$$

*such that  $f(x, Y)$  becomes a probability measure for each choice of  $x \in \mathbb{X}$  and a measurable function for each  $Y \in \mathcal{Y}$  is called a **Markov kernel** from  $\mathbb{X}$  to  $\mathbb{Y}$ .*

Note that in the cited literature, that is [LP18], Markov kernels are referred to as *probability kernels*. Let us give an elementary example to better understand the nature of this construction.

**Example 2.4.** Consider a random walk on  $\mathbb{Z}$  and let  $p$  denote the probability of an increment. Then we can write the transition probability from  $n \in \mathbb{Z}$  to  $m \in \mathbb{Z}$  by

$$f(n, \{m\}) = p \cdot \mathbb{1}_{\{m\}}(n+1) + (1-p) \cdot \mathbb{1}_{\{m\}}(n-1).$$

By

$$f(n, B) := \sum_{m \in B} f(n, \{m\})$$

for  $B \in \mathcal{P}(\mathbb{Z})$  the transition probabilities define a Markov kernel from  $\mathbb{Z}$  to  $\mathbb{Z}$ .

With knowledge of Markov kernels at hand, we are now ready to give the definition of a marking. As stated before, this is a key concept in this thesis.

**Definition 2.5.** Consider a point process  $\mu$  on  $\mathbb{X}$  with intensity measure  $\Theta$  and a Markov kernel  $f$  from  $\mathbb{X}$  to  $\mathbb{Y}$ . For each  $x \in \mu$  we independently choose a random element in  $\mathbb{Y}$ , with distribution given  $x$  defined by the probability measure  $f(x, \cdot)$ . The resulting point process on  $\mathbb{X} \times \mathbb{Y}$  is called a  **$f$ -marking** of  $\mu$ .

**Lemma 2.6** ([LP18, Proposition 5.5]). Consider a marked point process as constructed in Definition 2.5. Its intensity measure is given by

$$\Theta \otimes f(A) := \int \int \mathbb{1}_A(x, y) f(x, dy) \Theta(dx)$$

where  $A \in \mathcal{X} \times \mathcal{Y}$ .

In case the marks are not dependent on the points of  $\mathbb{X}$ , which means there exists a probability measure  $\mathbb{Q}$  with  $f(x, \cdot) = \mathbb{Q}$  for all  $x \in \mathbb{X}$ , we speak of an **independent  $\mathbb{Q}$ -marking**. In this case the intensity measure simplifies to the product measure. This is the case we are particularly interested in. In this thesis we exclusively consider markings of Poisson point processes. This is convenient because of the following remarkable result.

**Theorem 2.7** ([LP18, Theorem 5.6]). An  $f$ -marking on a Poisson point process is again Poisson.

This theorem is tremendously valuable, as it tells us that the convenient properties of Poisson processes as well as the rich theory established for them can be used on the marked process. Let us highlight the versatility of markings with a few examples.

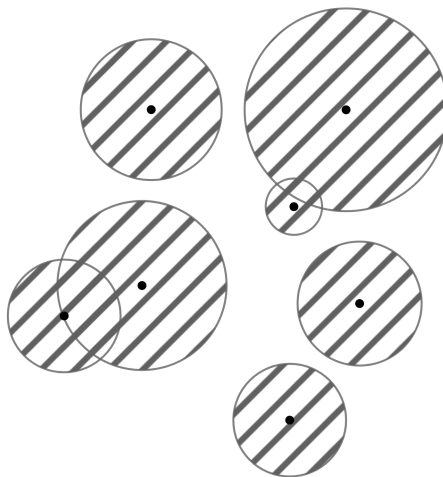


Figure 2.2: Excerpt of a Boolean model in  $\mathbb{R}^2$ .



**Example 2.8.** Consider a Poisson point process  $\eta$  on  $\mathbb{R}^d$  and an independent probability measure  $\mathbb{Q}$  on  $\mathbb{R}_+$ . Let  $\xi$  denote an independent  $\mathbb{Q}$ -marking of  $\eta$ . Each element  $y \in \xi$  is of the form  $y = (x, r)$ , with  $x \in \mathbb{R}^d$  and  $r \in \mathbb{R}_+$ . We can use this information to create the random set

$$Z(\xi) = \bigcup_{(x,r) \in \xi} \mathbb{B}_d(x, r),$$

which is the classical **Boolean model** with radius distribution  $\mathbb{Q}$ .

Sometimes it is desirable to dismiss points or select only a subset of points of a process in a random fashion. For these tasks, **thinnings** are a convenient tool and an important piece in the theory of point processes. They can be defined using markings, as the following example shows.

**Example 2.9.** Let  $p \in [0, 1]$  and consider the Markov kernel from  $\mathbb{X}$  to  $\{0, 1\}$  given by

$$f(x, \cdot) := (1 - p)\delta_0 + p\delta_1.$$

With this kernel we construct an  $f$ -marking of a point process  $\mu$  as above and denote the resulting marked process by  $\xi$ . Thus every point created by  $\mu$  gets marked with either a zero or a one, with probability  $1 - p$  and  $p$  respectively. The point process  $\mu_p = \xi(\cdot \times \{1\})$  counts only the points of  $\mu$  which received a one as marking and is called a  $p$ -**thinning** of  $\mu$ . Analogously we call  $\mu_{1-p} = \xi(\cdot \times \{0\})$  a  $(1 - p)$ -**thinning**.

By thinning our process  $\mu$  this way we thus create two new point processes. Note that if we thin out a Poisson process this way the resulting processes retain their Poisson properties. In this case this is not due to Theorem 2.7, but rather to the so called Restriction Theorem which we will not reiterate here. Instead we again refer to [LP18] and state the following.

**Theorem 2.10** ([LP18, Theorem 5.8]). *If the process  $\mu$  in Example 2.9 is a Poisson point process, then we have that the thinnings  $\mu_p$  and  $\mu_{1-p}$  are also independent Poisson point processes.*

Note that in the cited work [LP18] the thinning probability is allowed to depend on the position of the point, which in turn allows for a richer and more versatile theory. For the purposes of this work however, we are content with the simplified concept as introduced above. The last item in our toolset regarding Poisson point processes is the so called Superposition Theorem.

**Theorem 2.11** ([LP18, Theorem 3.3]). *We consider a series of independent Poisson point processes  $(\eta_i)_{i \in \mathbb{N}}$ , each defined on  $\mathbb{X}$  with intensity measure  $\Lambda_i$ . Their superposition is the sum*

$$\eta := \sum_{i=1}^{\infty} \eta_i.$$

$\eta$  is a Poisson point process with intensity measure  $\Lambda = \sum_{i=1}^{\infty} \Lambda_i$ .

This tells us that the union of countably many Poisson point processes form another Poisson process with an intensity that can be easily computed. Between the superposition, thinning and more generally marking of Poisson point processes note the remarkable resilience of their defining properties.

### 2.3. Basics of Graph and Percolation Theory

In this section we collect some of the basic definitions we need from graph theory and use them to reiterate the necessary background on percolation theory needed in this thesis. We start by recalling some of the most important vocabulary when discussing graphs.

**Definition 2.12.** *This collection is phrased in accordance with [Die18, p. 2 et seq.].*

- A (undirected) **graph** is defined as a pair  $G = (V, E)$  where  $V$  denotes some set and  $E \subset \{\{x, y\} \mid x \in V, y \in V\}$ .  $V$  is called the set of **vertices** or sometimes set of **nodes**.  $E$  is called the set of **edges**.
- The **order** of a graph is the cardinality of its set of vertices. We call a graph **finite** if  $|V| < \infty$  and **infinite** otherwise.
- A graph  $G^* = (V^*, E^*)$  is called a **subgraph** of  $G = (V, E)$  if  $V^* \subset V$  and  $E^* \subset E$ .
- $x \in V$  and  $y \in V$  are called **neighbours** or **adjacent** if  $\{x, y\} \in E$ .
- A graph is called **complete** if all of its vertices are pairwise adjacent.
- The **degree** of a vertex  $x \in V$  in  $G$  is the number of edges containing  $x$ , denoted by  $\deg_G(x) = |\{e \in E \mid x \in e\}|$ .
- A non-empty subgraph  $P = (V^P, E^P)$  of  $G$  that is of the form
 
$$V^P = \{x_0, \dots, x_k\} \quad E^P = \{\{x_0, x_1\}, \{x_1, x_2\}, \dots, \{x_{k-1}, x_k\}\}$$
 is called a **path** of length  $k$  in  $G$ .
- The **distance** of two vertices  $x$  and  $y$  of  $G$  is the minimal number of edges among all paths from  $x$  to  $y$ . It is denoted by  $d_G(x, y)$ .
- The **diameter** of a graph  $G = (V, E)$  is given by

$$\text{diam}(G) = \max\{d_G(x, y) \mid x \in V, y \in V\}.$$

This list is not exhaustive with respect to this Thesis as we will introduce additional items as we need them. But for now we can start our short survey of percolation theory and start with the discrete case.

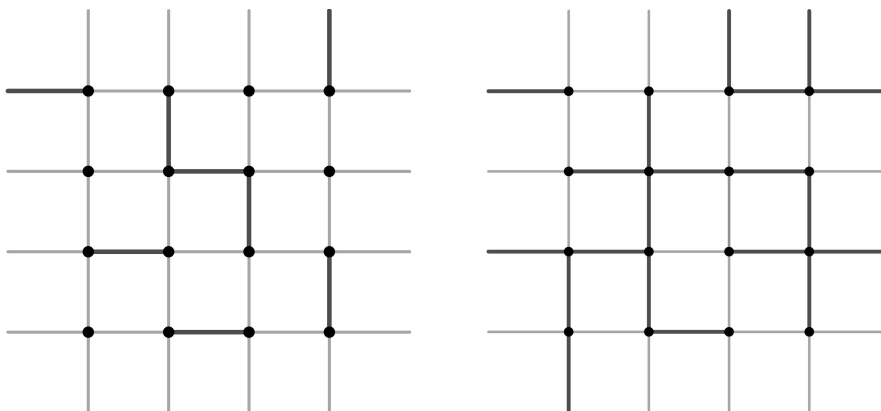


Figure 2.3: Visualization of the bond percolation model on the 2-dimensional lattice. The black bonds are open, the grey ones closed. On the left we have  $p = 0.2$ , to the right  $p = 0.5$ .

### 2.3.1. Discrete Percolation

For this introduction we slightly modify [MR96, p.3]. Consider some infinite graph  $G = (V, E)$ . In the language of percolation theory we refer to its vertices as **sites** and its edges as **bonds**. Each bond can be either open or closed. Subsequently, an open path from  $x \in V$  to  $y \in V$  is a path in  $V$  consisting only of open bonds. A closed path is defined analogously. We say that two vertices are **connected** if there exists an open path between them.

Now consider some probability space  $(\Omega, \mathbb{P}, \mathcal{A})$  and assume each bond independently open with some probability and closed otherwise. Realizing this probability for each bond gives us an open subgraph of  $G$ . Percolation theory is interested in the question under what conditions the probability of creating a subgraph of infinite diameter is greater than zero. This is best explained with an example.

**Example 2.13.** Consider  $V = \mathbb{Z}^d$  and  $E = \{\{x, y\} \mid (x, y) \in \mathbb{Z}^d \times \mathbb{Z}^d, \|x - y\| = 1\}$ . Each bond is open with probability  $p \in [0, 1]$  and closed otherwise. This setting is known as integer lattice percolation and one of the oldest studied percolation models. Let  $G(0)$  denote the subgraph of open bonds containing the origin. We define the **critical probability** of percolation by

$$p_c(d) = \inf\{p \mid \mathbb{P}(\text{diam}(G(0)) = \infty) > 0\}.$$

In [MR96, Theorem 1.1] it is proven that  $0 < p_c(d) < 1$  for all  $d \geq 2$ . Also it is noted that  $p_c(1) = 1$  which is a common property among percolation models and usually referred to as one-dimensional triviality. In [Kes80] Harry Kesten showed that  $p_c(2) = \frac{1}{2}$ , a statement that might seem natural but is actually the result of a long and complicated proof.

The setting where we refer to bonds as being open or closed is called the **bond percolation** model. Another approach is the **site percolation** model where we also attribute the vertices with these properties. There, each site is independently open with some probability. An edge is open if both of its corresponding vertices have this property.

**Example 2.14.** Consider a triangular lattice of points in  $\mathbb{R}^2$  where the triangles have some side length  $r > 0$ . We know from [Kes82, p.52] that the site percolation model on this lattice has critical probability  $p = \frac{1}{2}$ , that is if a bond is open with probability  $p > \frac{1}{2}$  we have a strict positive probability for a subgraph of infinite diameter to exist.

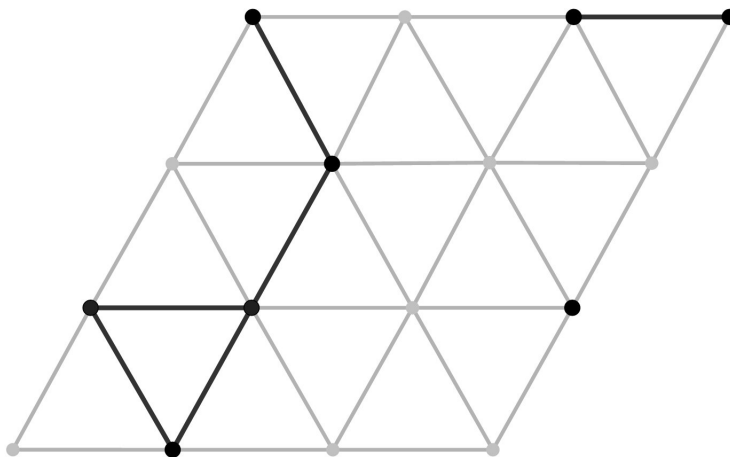


Figure 2.4: Illustration of site percolation on a triangular lattice. The black vertices are open, grey ones are closed. Same for the edges.

### 2.3.2. Continuum Percolation

Next we take a look at percolation on a random model driven by a Poisson point process. Remember the Boolean model as presented in Example 2.8. Let us additionally present its definition as introduced in [MR96, p. 17].

**Definition 2.15.** Consider a stationary Poisson point process  $\eta$  in  $\mathbb{R}^d$  with intensity  $\gamma > 0$  and some independent random variable  $R$  taking values in the interval  $[0, \infty)$ . The triple  $(\eta, R, \gamma)$  is called the **Boolean model** with density  $\gamma$  and radius random variable  $R$ .

The random set  $Z(\xi)$  as introduced in Example 2.8 is an associated quantity when setting  $\mathbb{Q}$  as the law of  $R$ . Without risk of confusion we will use the name

Boolean model for both  $(\eta, R, \gamma)$  and the implicated random set  $Z(\xi)$ . Note that  $Z(\xi)$  can be broken down into a collection of connected components, that is subsets that cannot be divided into disjoint non-empty closed sets. Analogous to the discrete case, continuum percolation now investigates under what conditions there exists a connected component  $C \subset Z(\xi)$  of infinite diameter, that is

$$\text{diam}(C) = \sup_{x,y \in C} \|x - y\|.$$

Consider the connected component containing the origin and label it  $C(0)$ . We define the **critical intensity** of the Boolean model by

$$\gamma_c(d) := \inf\{\gamma \mid \mathbb{P}(\text{diam}(C(0)) = \infty) > 0\}.$$

It is known that in the case  $d = 1$  the probability for an unbounded component to emerge is zero, see [MR96, Theorem 3.1]. For  $d = 2$  and a deterministic radius  $R \equiv 1$ , we have that

$$0.174 < \gamma_c < 0.843,$$

see [MR96, Theorem 3.10]. An intriguing feature of the Boolean model is the uniqueness of the unbounded component.

**Theorem 2.16** ([MR96, Theorem 3.6]). *In the Boolean model  $(\eta, R, \gamma)$  as described above, there is at most one unbounded component  $\mathbb{P}$ -a.s..*

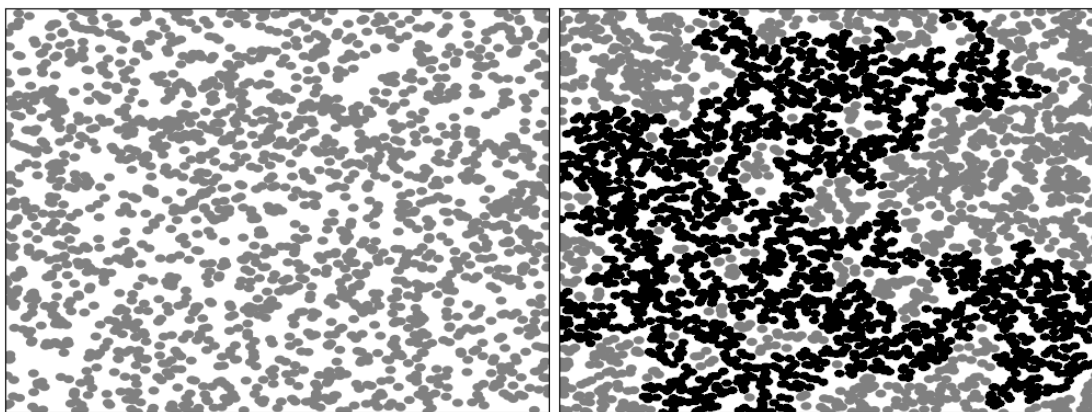


Figure 2.5: Two Boolean models with identical radius. The left one has too low intensity to form an unbounded component. The right, denser one has formed one, which is marked in black.

## 2.4. Normal Approximation via Malliavin-Stein

Now that we know about Poisson point processes, we would like a tool to derive central limit theorems for functionals based on those. Fortunately, tools like that exist and are the result of a rather fruitful combination of two concepts called **Stein's method** and **Malliavin calculus**. In this section we will give brief introductions to both of these and then explain how they can be combined to give rise to aforementioned limit theorems. Note however, that this a rather extensive field which we will not explore in depth here. For a more detailed introduction into Stein's method we refer the reader to the excellent survey paper [Ros11]. For more information on Malliavin calculus and how it connects to Stein's method we advise to consult [PR16].

To talk about the approximation of distributions, we first need a notion of distance between them. For this we use the *Wasserstein* distance, cf. [BP16].

**Definition 2.17.** *Let  $\nu_1$  and  $\nu_2$  denote probability measures on  $\mathbb{R}^d$  and  $\mathcal{H}$  a set of functions  $h : \mathbb{R}^d \rightarrow \mathbb{R}$  satisfying the following property: For any pair of random elements  $X, Y$  in  $\mathbb{R}^d$  satisfying  $\mathbb{E}[|h(X)|] < \infty$  and  $\mathbb{E}[|h(Y)|] < \infty$  we have that*

$$\mathbb{E}[h(X)] = \mathbb{E}[h(Y)] \Rightarrow X \stackrel{d}{\sim} Y.$$

*We can then define the probabilistic distance of the probability measures by*

$$d_{\mathcal{H}}(\nu_1, \nu_2) := \sup_{h \in \mathcal{H}} \left| \int h(t) \nu_1(dt) - \int h(t) \nu_2(dt) \right|.$$

**Example 2.18.** In the case of  $\mathcal{H} = \{\mathbb{1}_{(-\infty, x]}(\cdot) : x \in \mathbb{R}\}$  and  $\mathbb{R}$ -valued random variables  $X$  and  $Y$  we define the **Kolmogorov** distance of their respective laws by

$$d_{\mathbb{K}}(X, Y) = \sup_{x \in \mathbb{R}} |\mathbb{P}(X \leq x) - \mathbb{P}(Y \leq x)|.$$

**Example 2.19.** In the case of  $\mathcal{H} = \{h : \mathbb{R} \rightarrow \mathbb{R} : |h(x) - h(y)| \leq |x - y|\}$  and  $\mathbb{R}$ -valued random variables  $X$  and  $Y$  with  $\mathbb{E}[|X|] < \infty$  and  $\mathbb{E}[|Y|] < \infty$  we define the **Wasserstein** distance of their respective laws by

$$d_{\mathbb{W}}(X, Y) = \sup_{h \in \mathcal{H}} |\mathbb{E}[h(X)] - \mathbb{E}[h(Y)]|.$$

While  $d_{\mathbb{K}}$  may be the more intuitive metric,  $d_{\mathbb{W}}$  is more advantageous to work with. The following Lemma however implies that a bound in the Wasserstein distance implies a bound in  $d_{\mathbb{K}}$ .

**Lemma 2.20.** *Consider random variables  $X$  and  $Y$  where  $Y$  possesses a Lebesgue-density bounded by  $c \in \mathbb{R}$ . Then we have that*

$$d_{\mathbb{K}}(X, Y) \leq \sqrt{2c \cdot d_{\mathbb{W}}(X, Y)}.$$

A proof can be found in [Ros11]. In case of normal approximation we get the following bound.

**Lemma 2.21.** *Consider random variables  $X$  and  $Y$ , where the law of  $Y$  shall be a standard normal distribution. Then we have that*

$$d_K(X, Y) \leq \left(\frac{2}{\pi}\right)^{\frac{1}{4}} \cdot \sqrt{d_W(X, Y)}.$$

*Proof.* Let  $f$  denote the density function of standard normal distributed random variable and  $x \in \mathbb{R}$ . We have that

$$f(x) = \frac{1}{\sqrt{2\pi}} e^{-\frac{x^2}{2}} \leq \frac{1}{\sqrt{2\pi}}.$$

The asserted statement thus follows from Lemma 2.20 with  $c = \frac{1}{\sqrt{2\pi}}$ .  $\square$

### 2.4.1. Stein's Method

Let us take a first look into Stein's original idea. It begins with the observation that for any bounded function  $f$  with bounded first derivative and for a standard normal random variable  $N$  we have that

$$\mathbb{E}[f'(N) - Nf(N)] = 0.$$

This can be easily verified by a short integration of parts:

$$\begin{aligned} \mathbb{E}[f'(N) - Nf(N)] &= \mathbb{E}[f'(N)] - \mathbb{E}[Nf(N)] \\ &= \frac{1}{\sqrt{2\pi}} \int_{-\infty}^{\infty} f'(x) e^{-\frac{x^2}{2}} dx - \frac{1}{\sqrt{2\pi}} \int_{-\infty}^{\infty} x f(x) e^{-\frac{x^2}{2}} dx \\ &= \left[ \frac{1}{\sqrt{2\pi}} f(x) e^{-\frac{x^2}{2}} \right]_{-\infty}^{\infty} = 0. \end{aligned}$$

This simple calculation gave rise to a method which was introduced 1972 by Charles Stein in [Ste72]. At its heart we have the following result:

**Lemma 2.22** ([Ros11, Lemma 2.2]). *Let  $\Phi$  denote the distribution function of a standard normal distributed random variable. For the differential equation*

$$f'_x(w) - wf_x(w) = \mathbb{1}[w \leq x] - \Phi(x),$$

where  $w, x \in \mathbb{R}$ , exists a unique, bounded solution.

In the cited source [Ros11] the asserted solution is explicitly given. Its existence however is enough to formulate the following corollary.

**Corollary 2.23.** *Let  $f_x$  denote the solution mentioned in Lemma 2.22 and  $W$  some random variable. Then we have*

$$|\mathbb{P}(W \leq x) - \Phi(x)| = |\mathbb{E}[f'_x(W) - W f_x(W)]|.$$

Given a series of random variables  $(W_n)_{n \in \mathbb{N}}$  we can thus prove asymptotic normality by using

$$|\mathbb{P}(W_n \leq x) - \Phi(x)| = |\mathbb{E}[f'_x(W_n) - W_n f_x(W_n)]|$$

and by estimating the right hand side of this equation. This is Stein's method.

The challenge in this technique is obviously to control the function  $f_x$ . It turns out that using the Wasserstein distance, see Definition 2.17, offers some advantages in that regard. Let  $\mathcal{H}$  denote some set of functions.

**Lemma 2.24** ([Ros11, Lemma 2.5]). *Let  $N$  denote a standard normally distributed random variable. For the differential equation*

$$f'_h(w) - w f_h(w) = h(w) - \mathbb{E}[h(N)]$$

where  $h \in \mathcal{H}$  and  $w \in \mathbb{R}$  exists a bounded solution. It has the following properties:

- In case  $h$  is bounded it follows that

$$\|f_h\| \leq \sqrt{\frac{\pi}{2}} \|h(\cdot) - \mathbb{E}[h(N)]\| \text{ and } \|f'_h\| \leq 2 \|h(\cdot) - \mathbb{E}[h(N)]\|.$$

- In case  $h$  is absolutely continuous we have

$$\|f_h\| \leq 2 \|h'\|, \quad \|f_h\| \leq \sqrt{\frac{\pi}{2}} \|h'\| \text{ and } \|f''_h\| \leq 2 \|h'\|.$$

This lemma now allows us to connect Stein's method to Definition 2.17.

**Lemma 2.25.** *Let  $W$  and  $N$  denote random variables and assume  $N$  to be standard normally distributed. Let  $f_h$  be the solution as presented in Lemma 2.24. Then*

$$d_{\mathcal{H}}(W, N) = \sup_{h \in \mathcal{H}} |\mathbb{E}[f'_h(W) - W f_h(W)]|.$$

*Proof.* Let  $\nu_1$  and  $\nu_2$  denote the laws of  $W$  and  $N$  respectively. By Definition 2.17 we have

$$\begin{aligned} d_{\mathcal{H}}(W, N) &= \sup_{h \in \mathcal{H}} \left| \int h(x) \nu_1(dx) - \int h(x) \nu_2(dx) \right| \\ &= \sup_{h \in \mathcal{H}} |\mathbb{E}[h(W)] - \mathbb{E}[h(N)]| \\ \boxed{\text{Lemma 2.24}} &= \sup_{h \in \mathcal{H}} |\mathbb{E}[f'_h(W) - W f_h(W)]|. \end{aligned}$$

□



These results show the value of using the Wasserstein distance. Using this metric, all considered functions  $h \in \mathcal{H}$  are Lipschitz continuous with constant 1. This implies  $\|h'\| \leq 1$  and the estimates in Lemma 2.24 take the form  $\|f_h\| \leq 2$ ,  $\|f'_h\| \leq \sqrt{\frac{2}{\pi}}$  and  $\|f''_h\| \leq 2$ . This leads to the final theorem of this section.

**Theorem 2.26** ([Ros11, Theorem 3.1]). *Let  $W$  and  $N$  denote random variables and assume  $N$  to be standard normally distributed. Let  $\mathcal{F}$  denote the set of functions  $f$  with  $\|f\| \leq 2$ ,  $\|f'\| \leq \sqrt{\frac{2}{\pi}}$  and  $\|f''\| \leq 2$ . Then we have*

$$d_W(W, N) \leq \sup_{f \in \mathcal{F}} \mathbb{E}[f'(W) - Wf(W)].$$

This bound forms the basis for further refinement using Malliavin calculus.

### 2.4.2. Malliavin Calculus and Poisson Functionals

Malliavin calculus is a set of techniques named after the French mathematician Paul Malliavin introduced in [Mal78]. Among other things it gives a framework enabling integration by parts of random variables. Particularly, it gives a notion of the derivative of a random variable which we will call the **Malliavin derivative**. The idea in this section is to show that, if the random variable in question is a function of a Poisson point process, there are certain conditions under which the Malliavin derivative admits a convenient representation. This representation can then be used to handle the bound in Theorem 2.26.

First we need to know what Poisson functionals are and how to work with them. We follow the general definition in [LP18, Chapter 18] and consider a measurable space  $(\mathbb{X}, \mathcal{X})$  and denote by  $\mathbf{N}$  the space of all locally finite counting measures on  $\mathbb{X}$ . Let  $\eta$  denote a Poisson process on  $\mathbb{X}$  with  $\sigma$ -finite intensity measure  $\Lambda$ .

**Definition 2.27.** *A random variable  $F$  such that  $F = f(\eta)$   $\mathbb{P}$ -a.s. for some measurable function  $f : \mathbf{N} \rightarrow \mathbb{R}$  is called a **Poisson functional**. In this notion  $f$  is called a representative of  $F$ .*

Our aim is to refine the bound in Theorem 2.26 in case the considered random variable is a Poisson functional. To that end, we now define an operator which can be seen as a discrete analogue to classical derivatives.

**Definition 2.28.** *For  $x \in \mathbb{X}$  we define a map  $D_x f : \mathbf{N} \rightarrow \mathbb{R}$  by*

$$D_x f := f(\mu + \delta_x) - f(\mu), \quad \mu \in \mathbf{N}.$$

*This map is called the **difference** (or **add-one-cost**) **operator** of  $f(\mu)$ . We can extend this definition inductively for  $n \geq 2$  and  $(x_1, \dots, x_n) \in \mathbb{X}^n$  by setting  $D^1 := D$  and defining  $D_{x_1, \dots, x_n}^n f : \mathbf{N} \rightarrow \mathbb{R}$  by*

$$D_{x_1, \dots, x_n}^n f := D_{x_1}^1 D_{x_2, \dots, x_n}^{n-1} f.$$

*We then call  $D_{x_1, \dots, x_n}^n f$  the **n-th order difference operator**.*

The idea now is to show that under certain conditions this operator coincides with the Malliavin derivative of the Poisson functional. To do so we follow [Las16] and, for some measure  $\mu$ , denote by  $L^2(\mu)$  the space of square-integrable functions with respect to that measure. Furthermore, we define by  $\langle \cdot, \cdot \rangle_\mu$  the scalar product in this space and by  $\|\cdot\|_\mu$  the associated norm. Given  $n \in \mathbb{N}$ , we identify  $L_s^2(\mu^n)$  as the subset containing the symmetric functions in  $L^2(\mu^n)$ .

**Lemma 2.29.** *The difference operator as presented in Definition 2.28 has the following properties:*

- For  $n \in \mathbb{N}$  and  $(x_1, \dots, x_n) \in \mathbb{X}^n$  the  $n$ -th order difference operator is symmetric.
- The map  $(x_1, \dots, x_n, \mu) \mapsto D_{x_1, \dots, x_n}^n f(\mu)$  is measurable for all  $\mu \in \mathbb{N}$  and  $(x_1, \dots, x_n) \in \mathbb{X}^n$ .

*Proof.* Both items follow from the representation

$$D_{x_1, \dots, x_n}^n f(\mu) = \sum_{J \subset \{1, \dots, n\}} (-1)^{n-|J|} f\left(\mu + \sum_{j \in J} \delta_{x_j}\right),$$

see [Las16, p.5]. □

We can now define measurable and symmetric functions

$$\begin{aligned} T_n f : \quad & \mathbb{X}^n \rightarrow L_s^2(\Lambda^n) \\ (x_1, \dots, x_n) & \mapsto \mathbb{E}[D_{x_1, \dots, x_n}^n f(\eta)]. \end{aligned}$$

By definition we set  $T_0 f := \mathbb{E}[f(\eta)]$ . We need one more item before we can get to the heart of the technique presented in this section.

**Definition 2.30.** *Consider some  $n \geq 1$ ,  $\eta$  the Poisson point process as above and  $f \in L^1(\Lambda^n)$ . The  **$n$ -th order Wiener-Itô integral** is given by*

$$I_n(f) = \sum_{J \subset [n]} (-1)^{n-|J|} \int \int f(x_1, \dots, x_n) \eta^{|J|}(\mathrm{d}x_J) \Lambda^{n-|J|}(\mathrm{d}x_{J^c})$$

where  $x_J := (x_j)_{j \in J}$ .

Now we are ready for the following Theorem, which is known as the Wiener-Itô Chaos Expansion. It gives a representation of Poisson functionals which will lead us to the connection of difference operators and Malliavin calculus.

**Theorem 2.31** ([Las16, Theorem 2]). *Consider some  $f \in L_\eta^2$ . We have that*

$$f(\eta) = \sum_{n=0}^{\infty} \frac{1}{n!} I_n(T_n f).$$

*This series converges in  $L^2(\mathbb{P})$ .*

Defining  $g_n := \frac{1}{n!} \mathbb{E}[D^n f(\eta)]$  this gives the representation

$$f(\eta) = \mathbb{E}[f(\eta)] + \sum_{n=1}^{\infty} I_n(g_n). \quad (2.1)$$

Now consider some Poisson functional  $F$  with representative  $f$ . By Theorem 2.31  $F$  admits some representation as given in (2.1). Assume that this representation satisfies

$$\sum_{n=1}^{\infty} nn! \|g_n\|_{\Lambda^n}^2 < \infty$$

and that  $\mathbb{E}[|F|^2] < \infty$ . These are the conditions under which we can identify the difference operator as given by Definition 2.28 with the Malliavin derivative of  $F$ . This statement is proven in [Las16, Theorem 3]. Furthermore, it is proven that

$$\sum_{n=1}^{\infty} nn! \|g_n\|_{\Lambda^n}^2 < \infty \Leftrightarrow \mathbb{E} \left[ \int (D_x F)^2 \Lambda(dx) \right] < \infty.$$

So for any Poisson functional  $F$  with  $\mathbb{E}[|F|^2] < \infty$  and  $\mathbb{E} \left[ \int (D_x F)^2 \Lambda(dx) \right] < \infty$  the Malliavin derivative coincides with its difference operator. This opens the door for the toolset of Malliavin calculus to be applied to simplify the right-hand side of Theorem 2.26, making it more convenient to deal with in the setting of Poisson functionals.

### 2.4.3. The Malliavin-Stein Method

Since the last section was somehow technical let us reiterate how we got here. Our goal is normal approximation of a Poisson functional.

- Stein's method gives us a bound in the Wasserstein distance, see Theorem 2.26.
- Malliavin calculus would allow us to further refine this bound, if we had a feasible way to express the Malliavin derivative.
- We show that the Malliavin derivative is under certain conditions given by the difference operator, see Definition 2.28.
- We apply Malliavin calculus and derive a bound involving these operators.

This strategy of applying Malliavin calculus on a bound derived by Stein's method was first successfully applied by [PSTU10]. However, application of their theorem requires the computation of the chaos expansion and thus of the  $n$ -th

order Wiener-Itô integral. This makes it rather inconvenient to use. The theorem we present next eliminates this problem and gives a bound which solely relies on the first and second-order difference operators. Although it was first presented in [LPS16], the form we give here can be found in [LP18].

**Theorem 2.32** ([LP18, Theorem 21.3]). *Let  $\eta$  denote a Poisson process with intensity measure  $\Lambda$ . Consider a Poisson functional  $F$  on  $\eta$  with  $\mathbb{E}[|F|^2] < \infty$ ,  $\mathbb{E}[F] = 0$  and  $\mathbb{V}[F] = 1$ .  $N$  shall denote a standard normal random variable. If  $\mathbb{E}[\int (\mathbb{D}_x F)^2 \Lambda(dx)] < \infty$  then there are constants*

$$\begin{aligned}\alpha_1(F) &= \int \sqrt{\mathbb{E}[(\mathbb{D}_x F)^2 (\mathbb{D}_y F)^2]} \cdot \sqrt{\mathbb{E}[(D_{x,z}^2 F)^2 (D_{y,z}^2 F)^2]} \Lambda^3(d(x, y, z)), \\ \alpha_2(F) &= \int \mathbb{E}[(D_{x,z}^2 F)^2 (D_{y,z}^2 F)^2] \Lambda^3(d(x, y, z)), \\ \alpha_3(F) &= \int \mathbb{E}[|\mathbb{D}_x F|^3] \Lambda(dx),\end{aligned}$$

such that

$$d_W(F, N) \leq 2\sqrt{\alpha_1(F)} + \sqrt{\alpha_2(F)} + \alpha_3(F).$$

# Chapter 3

## The Obstructed Gilbert Graph

In this chapter we introduce a variation of the well known Gilbert graph first introduced in [Hae12]. There it was named the **Poisson hole process**. Essentially it is a Cox process, that is a Poisson point process in a random environment. In the model they have two independent, stationary Poisson point processes in  $\mathbb{R}^d$  on the same probability space: One of them is labeled the primary and the other one the secondary process. We reject all points of the secondary process if they are placed too close to a point of the primary process with respect to the Euclidean distance.

In this chapter we study percolation properties on a very similar model, which we name the **obstructed Gilbert graph** to emphasize the close relatedness to Gilberts original setting from 1961. The first section will give a short survey over existing research on related models and work done on the Poisson hole process in particular. After this we give a concise definition of the model studied in this chapter and introduce the Galton-Watson tree, which will prove an useful tool for analysing percolation properties of the model. In the next section we then present and prove theorems which give thresholds on the subcritical and supercritical regimes. In the final section we study the asymptotic distribution of the covered volume of the communication zones of the obstructed nodes and present a central limit theorem.

### 3.1. Related Works

After its introduction in [Gil61], the Gilbert graph has enjoyed a great deal of attention. This graph uses a Poisson point process in Euclidean space as vertex set and creates an edge whenever two vertices satisfy some proximity threshold. Since the graph structure depends on the Euclidean coordinates of the vertices

it is also called the random geometric graph. A fundamental work summarizing much of the research done up until 2003 is [Pen03]. In opportunistic networks the communication between two close participants might not always be possible due to geographic obstruction, which we would like to take into account by introducing obstacles into the model. As mentioned, the setting studied in this chapter was introduced in [Hae12], by name of **Poisson Hole process**. The most notable contribution related to this thesis is [YSBRL19], where the authors consider a slightly modified five parameter model. They consider a Poisson point process  $\eta_p$  in  $\mathbb{R}^2$  with intensity  $\lambda_p$ , called the primary process. Primary nodes are connected if their Euclidean distance is below a threshold  $d_p$ . Similarly, the secondary Poisson process  $\eta_s$  in  $\mathbb{R}^2$  with intensity  $\lambda_s$  is introduced. Secondary nodes are connected if their Euclidean distance is below a threshold  $d_s$  and if there is no primary node within distance  $d_g$  from either of them. The vector  $(d_p, d_s, d_g, \lambda_p, \lambda_s)$  defines the model. The authors proceed to study necessary conditions for simultaneous percolation in both the primary and secondary network. This is similar to our result in Theorem 3.4, but our technique involving a branching tree construction is not restricted to dimension  $d = 2$ . The last result in [YSBRL19] is a sufficient condition for simultaneous percolation. They compare their continuous model to a dependent site percolation model, that is the probability for a site to be declared open may be dependent on the states of neighbouring sites. In our Theorem 3.6 we similarly introduce a sufficient condition for percolation in  $\mathbb{R}^2$ , which is also derived by comparison with site percolation. However our approach uses independent site percolation, resulting in a more streamlined bound. Our strategy also results in much more strict conditions, however. It nonetheless affirms the result of [YSBRL19] that percolation in such a restricted environment is indeed achievable.

Another noteworthy setting is the one presented in [HJC19]. As mentioned the Poisson hole process can be seen as Poisson point process in a random environment, that is a Cox process. Indeed, Example 2.1 in their work includes exactly this setting. They show the existence of phase transitions for Cox processes which are required to fulfill a stabilizing property and certain requirements regarding connectedness of their support. This connectedness property however is not fulfilled in our model, which bars us from using their technique.

## 3.2. Construction of the Graph

Let us start with the following idea of a random graph as introduced by [Gil61].

**Definition 3.1.** *Consider a stationary Poisson point process  $\eta$  in  $\mathbb{R}^d$  with intensity  $\gamma > 0$  and some real number  $r > 0$ . Given a realisation of  $\eta$  we take its support as the set of vertices  $V$  and denote the set of edges by  $E$ . We have*

$$(x, y) \in E \Leftrightarrow \|x - y\| \leq r.$$

The resulting graph  $G = (V, E)$  is known as the **Gilbert graph** or also **random geometric graph** (see [Pen03] for instance).

It is clear that the Gilbert graph and the Boolean model  $(\eta, \frac{r}{2}, \gamma)$  (see Definition 2.15 and Example 2.8) are closely related. If for all pairs  $x, y \in \eta$  we draw an edge if  $\mathbb{B}(x, \frac{r}{2}) \cap \mathbb{B}(y, \frac{r}{2}) \neq \emptyset$  we get the corresponding Gilbert graph with distance parameter  $r$ . In the following we will frequently exploit this duality and switch between the random set given by the Boolean model and the implied graph structure. We will now define the graph structure studied in this chapter. All point processes presented operate on the same shared probability space.

**Definition 3.2.** Consider two stationary Poisson point processes  $\eta_N$  and  $\eta_O$  in  $\mathbb{R}^d$  with intensity  $\gamma_N > 0$  and  $\gamma_O \geq 0$  respectively. Also consider two real numbers  $r_N > 0$  and  $r_O > 0$ . Given realizations of the point processes we define

$$V := \{x \in \eta_N \mid \|x - y\| > r_O \ \forall y \in \eta_O\}$$

as the set of vertices of a graph with  $G = (V, E)$ , where

$$(x, y) \in E \Leftrightarrow \|x - y\| \leq r_N.$$

In this case we call  $G$  the **obstructed Gilbert graph**.

### 3.2.1. The Galton-Watson Tree

The process introduced in this section was originally conceived in 1874 by Francis Galton and Henry W. Watson to study the extinction of family names in British aristocracy but has since then become a valuable tool in the study of random graphs. We will follow [Bla17, p.11] and introduce the process as a random tree, that is a graph of special structure constructed as follows.

We fix some node and label it the **root** of our tree. Then we take a  $\mathbb{N}_0$  valued random variable  $X$  whose law we refer to as **offspring distribution**. We create a random number, distributed according to  $X$ , of vertices and connect them to the root. For each newly created node we place a random number, **independently** and with respect to the offspring distribution, of nodes adjacent to it. Iteration of this procedure yields the tree. We collect all nodes at distance  $n$  to the root in a set labeled  $G_{n+1}$  and called  **$n + 1$ -th generation** of the tree. Thus the root itself is the only element of  $G_1$ , the first generation.

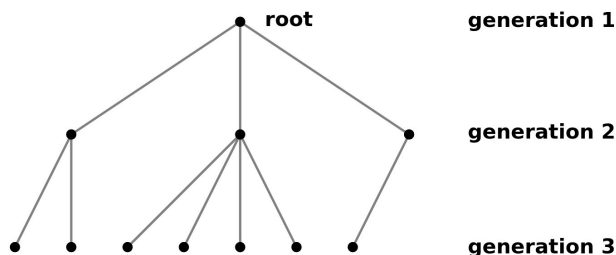


Figure 3.1: An example of a tree and its generations.

We set the total number of nodes in our tree as

$$S := \sum_{k=1}^{\infty} |G_k|$$

and define the **extinction probability** by  $\mathbb{P}(S < \infty)$ .

**Theorem 3.3** ([Bla17, Corollary 2.1.2]). *Let  $X$  be a random variable driven by the offspring distribution and  $S$  the total number of nodes in the associated Galton-Watson tree. Then the following implications hold true:*

- $\mathbb{E}[X] < 1 \Rightarrow \mathbb{P}(S < \infty) = 1$ ,
- $\mathbb{E}[X] > 1 \Rightarrow \mathbb{P}(S < \infty) < 1$ ,
- $\mathbb{E}[X] = 1$  and  $\mathbb{P}(X = 0) = 0 \Rightarrow \mathbb{P}(S < \infty) = 0$ ,
- $\mathbb{E}[X] = 1$  and  $\mathbb{P}(X = 0) > 0 \Rightarrow \mathbb{P}(S < \infty) = 1$ .

### 3.3. Critical Intensities

Our first main finding of this chapter provides some insight into how the two intensities of the obstructed Gilbert graph interact. It gives us a threshold by which we are sure to be in the **subcritical regime**, which means that we have a configuration in which unbounded components will not emerge  $\mathbb{P}$ -a.s..

**Theorem 3.4.** *Consider the obstructed Gilbert graph as presented in Definition 3.2. If*

$$\gamma_N \cdot r_N^d < \frac{e^{\gamma_O \cdot \kappa_d r_O^d}}{2^d \kappa_d}$$

*the probability for an unbounded component to emerge is 0.*

This Theorem allows for an interesting observation. Increasing the intensity of the obstacles increases this threshold exponentially. This means if we place just a few more obstacles we have to add a large number of nodes just to retain some hope of reaching criticality. To proof this we need the following result.



**Lemma 3.5** ([LP18, p.168]). *Let  $(\eta, r, \gamma)$  be a Boolean model as presented in Definition 2.15 and  $Z$  denote the associated random set. We have that*

$$\mathbb{P}(x \in Z) = 1 - e^{-\gamma \lambda_d(\mathbb{B}_d(r))}.$$

This interesting property of the Boolean model is due to its **capacity functional**, a concept we introduce more in-depth later when talking about the time bounded cylinder model.

*Proof of Theorem 3.4.* We construct a random tree representing a component in the obstructed Gilbert graph as follows. Consider a node  $v_0$  in the origin, which we will take as the root of our tree. The second generation is the set

$$G_2 = \{v \in \eta_N \mid 0 < \|v - v_0\| \leq 2r_N, \|v - o\| > r_O \forall o \in \eta_O\}.$$

Next consider a  $k \in \mathbb{N}$  and  $G_2 = \{v_1, \dots, v_k\}$ . The members of the third generation adjacent to  $v_i$  are the points in  $v \in \eta_N$  that are not covered by a ball  $o + \mathbb{B}(r_O)$ ,  $o \in \eta_O$ , are in communication range, that is  $\|v - v_i\| \leq 2r_N$  and are not included in the tree yet. That is the set

$$G_3^i := \{v \in \eta_N \mid \|v - v_i\| \leq 2r_N, \|v - o\| > r_O \forall o \in \eta_O, v \notin G_3^j \forall j < i, v \notin G_k \forall k < 3\}.$$

Consequently we have

$$G_3 = \bigcup_{i=1}^k G_3^i.$$

Iterating this procedure yields the tree. Note that this is not a Galton-Watson tree as the independence property of the offspring distribution is not fulfilled. However we can use a technique deployed in the proof of [MR96, Theorem 3.2] and compare the tree representing a component in the obstructed Gilbert graph with a Galton-Watson tree constructed as follows. We get the second generation  $\overline{G}_2 = G_2$  in the same way as before. Now for each  $v_i \in \overline{G}_2$  we introduce independent copies  $\eta_N^i$  of  $\eta_N$  and  $\eta_O^i$  of  $\eta_O$ . The members of the third generation adjacent to  $v_i$  are then

$$\overline{G}_3^i := \{v \in \eta_N^i \mid \|v - v_i\| \leq 2r_N, \|v - o\| > r_O \forall o \in \eta_O^i\}$$

Again, iterating this procedure yields the tree. Note that by this construction we have that

$$\mathbb{E}[|G_k^i|] \leq \mathbb{E}[|\overline{G}_2|].$$

for all  $k \in \mathbb{N}$ . Let  $X$  denote a random variable driven by the offspring distribution in the constructed Galton-Watson tree. We have

$$\mathbb{P}(X = k) = \mathbb{P}\left(\eta_N\left(\mathbb{B}(2r_N) \setminus \bigcup_{o \in \eta_O} (o + \mathbb{B}(r_O))\right) = k\right).$$

Furthermore we get by the law of total expectation that

$$\begin{aligned} \mathbb{E}[X] &= \mathbb{E}[|\overline{G}_2|] = \mathbb{E}\left[\eta_N\left(\mathbb{B}(2r_N)\setminus\bigcup_{o\in\eta_O}(o+\mathbb{B}(r_O))\right)\right] \\ \boxed{Z_O := \bigcup_{o\in\eta_O} o + \mathbb{B}(r_O)} &= \mathbb{E}[\mathbb{E}[\eta_N(\mathbb{B}(2r_N)\setminus Z_O) \mid Z_O]] \\ &= \gamma_N \cdot \mathbb{E}[\lambda_d(\mathbb{B}(2r_N)\setminus Z_O)]. \end{aligned}$$

For the expectation on the right hand side we can use Fubini's theorem and receive

$$\begin{aligned} \mathbb{E}[\lambda_d(\mathbb{B}(2r_N)\setminus Z_O)] &= \mathbb{E}\left[\int_{\mathbb{B}(2r_N)} \mathbb{1}(x \notin Z_O) dx\right] \\ \boxed{\text{Fubini}} &= \int_{\mathbb{B}(2r_N)} \mathbb{P}(x \notin Z_O) dx \\ \boxed{\text{Capacity functional}} &= \int_{\mathbb{B}(2r_N)} e^{-\gamma_O \lambda_d(\mathbb{B}(r_O))} dx \\ &= \lambda_d(\mathbb{B}(2r_N)) e^{-\gamma_O \lambda_d(\mathbb{B}(r_O))}. \end{aligned}$$

This gives us

$$\mathbb{E}[X] = \mathbb{E}[|\overline{G}_2|] = \gamma_N \cdot \lambda_d(\mathbb{B}(2r_N)) e^{-\gamma_O \lambda_d(\mathbb{B}(r_O))}$$

and by Theorem 3.3 we see that if this expectation is below 1, the extinction probability in the Galton-Watson tree is 1. This in turn implies the extinction of the tree representing a component in the obstructed Gilbert graph.  $\square$

Now that we know under what conditions the obstructed graph does not percolate, the next result deals with the existence of a **supercritical** regime. That is conditions under which an unbounded component emerges with probability greater than zero. To do this we restrict ourselves to the case  $d = 2$  and small obstacles, that is  $r_O < \frac{r_N}{2}$ . Note that in the case  $d = 1$  the obstructed graph does not percolate  $\mathbb{P}$ -a.s.. This follows immediately from the one-dimensional triviality for the Boolean model, see [MR96, Theorem 3.1].

**Theorem 3.6.** *Consider the obstructed Gilbert graph as presented in Definition 3.2. Assume  $d = 2$  and  $r_O < \frac{r_N}{2}$ . If*

$$\gamma_N > \frac{-\ln\left(1 - \frac{e^{0.822661 \cdot \gamma_O r_N^2}}{2}\right)}{0.822662 \cdot (r_N - 2r_O)^2}$$

and  $\gamma_O < \frac{\ln(2)}{0.822662 r_N^2}$ , then the graph is in the supercritical regime.

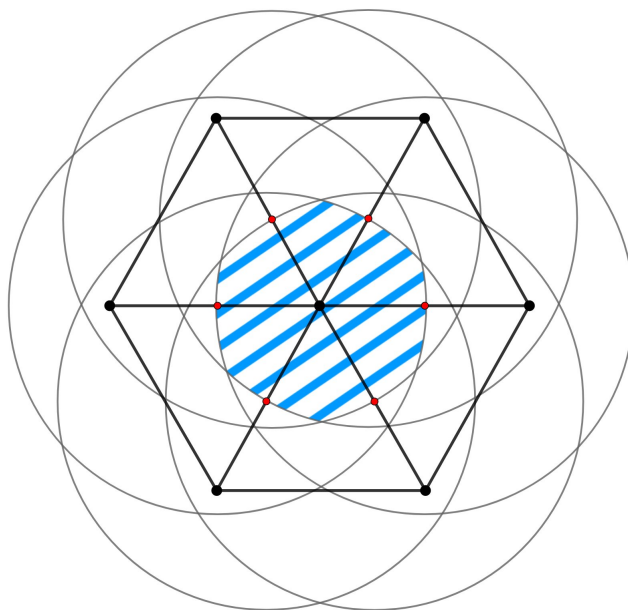


Figure 3.2: Illustration of the construction used in the proof of Theorem 3.6. In the center we have the point  $x$  and the blue shaded area is the mentioned intersection  $A_x$  of open balls.

*Proof of Theorem 3.6.* We employ a strategy to used by [MR96, p.87] and consider a triangular lattice of points in  $\mathbb{R}^2$  where the triangles have side length  $r_N$ . Our aim is to compare the obstructed Gilbert graph to a site percolation model on this lattice. Take some site  $x$  and imagine six circles of radius  $r_N$  centered on the midpoints of the edges adjacent to  $x$ . The area inside of all six circles shall be called  $A_x$ . See Figure 3.2 for an illustration.

Thus, for adjacent sites  $x$  and  $y$ , if we take points  $x' \in A_x$  and  $y' \in A_y$ , we have that  $\mathbb{B}(x', r_N) \cap \mathbb{B}(y', r_N) \neq \emptyset$ . So if we would declare some site  $x$  open if  $\eta_N(A_x) > 0$  we could deduce from site percolation on the lattice that the Boolean model  $(\eta_N, r_N, \gamma_N)$  would percolate as well. We still have to take the obstacles into account however.

To match our model, we declare a site  $x$  open if there is no obstacle present in  $A_x$  and at least one node present in the set  $A'_x$  which is constructed analogously to  $A_x$  but where the circles are centered on the adjacent edges to  $x$  with distance  $\frac{r_N}{2} - r_O$ . Then, since  $\eta_N$  and  $\eta_O$  are independent Poisson processes, the probability for a site  $x$  to be declared open is

$$\mathbb{P}(\eta_N(A'_x) > 0) \cdot \mathbb{P}(\eta_O(A_x) = 0) = (1 - e^{-\gamma_N \cdot \lambda_2(A'_x)}) \cdot e^{-\gamma_O \cdot \lambda_2(A_x)}. \quad (3.1)$$

To compute the volume necessary to further evaluate this probability, we consider the triangular lattice where the triangles have some side length  $r$ . Let us assume

a site in the origin and compute the volume of  $A_0(r)$  which is the construction as seen above but for the site in the origin and given side length  $r$ . In a first step, we compute the distance from the origin to an intersection of two of the circles, which amounts to

$$d_0 = \frac{\sqrt{15} - \sqrt{3}}{4}r.$$

Then we calculate the area of a regular hexagon with side length  $d_0$  which is

$$A_H = \frac{\sqrt{3}(\sqrt{45} - 3)^2}{32}r^2.$$

After this it remains to compute the area of the circular segments which are cut off by the hexagon, each given by

$$A_C = \frac{r^2}{2} \left( \cos^{-1} \left( 1 - \frac{(\sqrt{15} - \sqrt{3})^2}{32} \right) - \sin \left( \cos^{-1} \left( 1 - \frac{(\sqrt{15} - \sqrt{3})^2}{32} \right) \right) \right).$$

This gives us

$$\lambda_2(A_0(r)) = A_H + 6 \cdot A_C \approx 0.8226612 \cdot r^2.$$

With this we can compute the volumes

$$A_x = A_0(r_N) \text{ and } A'_x = A_0(r_N - 2r_O). \quad (3.2)$$

As we have seen in Example 2.14, the site percolation model on this lattice has critical probability  $p = \frac{1}{2}$ . Thus if the probability given in (3.1) exceeds this threshold we can safely say that the obstructed Gilbert graph percolates. For  $\gamma_O < \frac{\ln(2)}{0.822662r_N^2}$  this gives us the condition

$$\begin{aligned} & \mathbb{P}(\eta_N(A'_x) > 0) \cdot \mathbb{P}(\eta_O(A_x) = 0) > \frac{1}{2} \\ \Leftrightarrow & 1 - e^{-\gamma_N \cdot \lambda_2(A'_x)} > \frac{e^{\gamma_O \cdot \lambda_2(A_x)}}{2} \\ \Leftrightarrow & e^{-\gamma_N \cdot \lambda_2(A'_x)} < 1 - \frac{e^{\gamma_O \cdot \lambda_2(A_x)}}{2} \\ \Leftrightarrow & \gamma_N \cdot \lambda_2(A'_x) > -\ln \left( 1 - \frac{e^{\gamma_O \cdot \lambda_2(A_x)}}{2} \right) \\ \Leftrightarrow & \gamma_N > \frac{-\ln \left( 1 - \frac{e^{\gamma_O \cdot \lambda_2(A_x)}}{2} \right)}{\lambda_2(A'_x)}. \end{aligned}$$

Taking up (3.2) we receive the asserted statement.  $\square$

### 3.4. A Central Limit Theorem for the Covered Volume

Next we consider the  $d$ -dimensional random sets  $Z_N$  created by the Boolean model  $(\eta_N, r_N, \gamma_N)$  and  $Z_O$  created by  $(\eta_O, r_O, \gamma_O)$ . We are interested in the asymptotic distribution of the volume of the random set  $Z_N \setminus Z_O$  restricted to a window of observation  $W_s := [-\frac{s}{2}, \frac{s}{2}]^d$  and prove Theorem 1.1 by proving the following stronger result.

**Theorem 3.7.** *Let  $N$  denote a standard normally distributed random variable. Assume  $0 < \gamma_N, \gamma_O, r_N, r_O < \infty$ . Then there exists a constant  $c \in \mathbb{R}_+$  such that*

$$d_W \left( \frac{\lambda_d((Z_N \setminus Z_O) \cap W_s) - \mathbb{E}[\lambda_d((Z_N \setminus Z_O) \cap W_s)]}{\sqrt{\mathbb{V}[\lambda_d((Z_N \setminus Z_O) \cap W_s)]}}, N \right) \leq \frac{c}{\sqrt{\lambda_d(W_s)}}.$$

In the proof of this theorem and further along in Chapter 4 we will use the following well-known estimate.

**Lemma 3.8.** *Consider  $a, b \in \mathbb{R}$  and  $q \geq 1$ . Then we have that*

$$|a + b|^q \leq 2^{q-1}(|a|^q + |b|^q).$$

*Proof.* Note that for  $q \geq 1$  the function  $x^q$  is clearly convex for  $x \geq 0$ . First using the triangle inequality and then the definition of convexity now get us

$$|a + b|^q = \left| \frac{2a}{2} + \frac{2b}{2} \right|^q \leq \left| \frac{|2a|}{2} + \frac{|2b|}{2} \right|^q \leq \frac{|2a|^q}{2} + \frac{|2b|^q}{2} = 2^{q-1}(|a|^q + |b|^q).$$

□

*Proof of Theorem 3.7.* Let  $\eta_S$  denote the superposition of  $\eta_N$  and  $\eta_O$  and consider the random variable  $R_S$  with  $\mathbb{P}[R_S = r_N] = \frac{\gamma_N}{\gamma_N + \gamma_O} = 1 - \mathbb{P}[R_S = r_O]$ . This defines the Boolean model  $(\eta_S, R_S, \gamma_N + \gamma_O)$ . We aim to use Theorem 2.32 on the Poisson functional  $F$  with representative

$$f(\eta_S) := \frac{\lambda_d((Z_N \setminus Z_O) \cap W_s) - \mathbb{E}[\lambda_d((Z_N \setminus Z_O) \cap W_s)]}{\sqrt{\mathbb{V}[\lambda_d((Z_N \setminus Z_O) \cap W_s)]}}.$$

We first derive a non-trivial lower bound on the variance  $\mathbb{V}[\lambda_d((Z_N \setminus Z_O) \cap W_s)]$ . This will confirm that the prerequisites of Theorem 2.32 are met. By Fubini's Theorem we have that

$$\begin{aligned} & \mathbb{V}[\lambda_d((Z_N \setminus Z_O) \cap W_s)] \\ &= \mathbb{E} \left[ \int_{W_s^2} \mathbb{1}(x \in Z_N \setminus Z_O, y \in Z_N \setminus Z_O) \lambda_d^2(d(x, y)) \right] - \mathbb{E} \left[ \int_{W_s} \mathbb{1}(x \in Z_N \setminus Z_O) \lambda_d(dx) \right]^2 \end{aligned}$$

$$= \int_{W_s^2} \mathbb{P}(x \in Z_N \setminus Z_O, y \in Z_N \setminus Z_O) - \mathbb{P}(x \in Z_N \setminus Z_O) \mathbb{P}(y \in Z_N \setminus Z_O) \lambda_d^2(d(x, y)).$$

To evaluate this integral, we first see that

$$\begin{aligned} \mathbb{P}(x \in Z_N \setminus Z_O) &= \mathbb{P}(\eta_N(\mathbb{B}_d(x, r_N)) > 0, \eta_O(\mathbb{B}_d(x, r_O)) = 0) \\ \boxed{\text{Independence of } \eta_N \text{ and } \eta_O} &= \mathbb{P}(\eta_N(\mathbb{B}_d(x, r_N)) > 0) \mathbb{P}(\eta_O(\mathbb{B}_d(x, r_O)) = 0) \\ \boxed{\text{Lemma 3.5}} &= (1 - e^{-\gamma_N \lambda_d(\mathbb{B}_d(r_N))}) e^{-\gamma_O \lambda_d(\mathbb{B}_d(r_O))}. \end{aligned}$$

Furthermore,

$$\begin{aligned} &\mathbb{P}(x \in Z_N \setminus Z_O, y \in Z_N \setminus Z_O) \\ &= \mathbb{P}(\eta_N(\mathbb{B}_d(x, r_N)) > 0, \eta_N(\mathbb{B}_d(y, r_N)) > 0, \eta_O(\mathbb{B}_d(x, r_O)) = 0, \eta_O(\mathbb{B}_d(y, r_O)) = 0) \\ &= \mathbb{P}(\eta_N(\mathbb{B}_d(x, r_N)) > 0, \eta_N(\mathbb{B}_d(y, r_N)) > 0) \mathbb{P}(\eta_O(\mathbb{B}_d(x, r_O)) = 0, \eta_O(\mathbb{B}_d(y, r_O)) = 0). \end{aligned}$$

We now apply DeMorgan's laws and get

$$\begin{aligned} &\mathbb{P}(\eta_N(\mathbb{B}_d(x, r_N)) > 0, \eta_N(\mathbb{B}_d(y, r_N)) > 0) \\ &= 1 - \mathbb{P}(\{\eta_N(\mathbb{B}_d(x, r_N)) = 0\} \cup \{\eta_N(\mathbb{B}_d(y, r_N)) = 0\}). \end{aligned}$$

By the additivity of probability measures this gives us

$$\begin{aligned} &\mathbb{P}(\eta_N(\mathbb{B}_d(x, r_N)) > 0, \eta_N(\mathbb{B}_d(y, r_N)) > 0) \\ &= 1 - 2 \cdot \mathbb{P}(\eta_N(\mathbb{B}_d(r_N)) = 0) + \mathbb{P}(\eta_N(\mathbb{B}_d(x, r_N)) = 0, \eta_N(\mathbb{B}_d(y, r_N)) = 0) \\ &= 1 - 2 \cdot \mathbb{P}(\eta_N(\mathbb{B}_d(r_N)) = 0) + \mathbb{P}(\eta_N(\mathbb{B}_d(x, r_N) \cup \mathbb{B}_d(y, r_N)) = 0). \end{aligned}$$

These results lead us to

$$\begin{aligned} &\mathbb{P}(x \in Z_N \setminus Z_O, y \in Z_N \setminus Z_O) \\ &= (1 - 2 \cdot e^{-\gamma_N \lambda_d(\mathbb{B}_d(r_N))} + e^{-\gamma_N \lambda_d(\mathbb{B}_d(x, r_N) \cup \mathbb{B}_d(y, r_N))}) e^{-\gamma_O \lambda_d(\mathbb{B}_d(x, r_O) \cup \mathbb{B}_d(y, r_O))}. \end{aligned}$$

Now let us denote by  $H_w^d(z)$  the cap of a  $d$ -dimensional hypersphere with radius  $z$  and height  $w$ . See Figure 3.3 for an illustration. For a method to explicitly compute its volume we refer to [Li11].

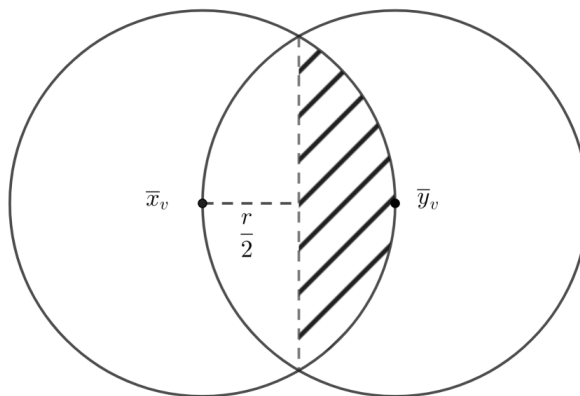


Figure 3.3: Variance estimation for  $d = 2$ . The shaded area marks  $H_{\frac{r}{2}}^2(r)$ .

For  $x, y \in \mathbb{R}^d$  satisfying  $\|x - y\| \leq r$  we have

$$\lambda_d(\mathbb{B}_d(r)) \leq \lambda_d(\mathbb{B}_d(x, r) \cup \mathbb{B}_d(y, r)) \leq 2\lambda_d(\mathbb{B}_d(r)) - 2\lambda_d(H_{\frac{r}{2}}^d).$$

Now let  $r_- = \min(r_N, r_O)$ .

$$\begin{aligned} & \mathbb{V}[\lambda_d((Z_N \setminus Z_O) \cap W_s)] \\ &= \int_{W_s} \int_{W_s} \mathbb{P}(x \in Z_N \setminus Z_O, y \in Z_N \setminus Z_O) - \mathbb{P}(x \in Z_N \setminus Z_O)\mathbb{P}(y \in Z_N \setminus Z_O) \, dy \, dx \\ &\geq \int_{W_s} \int_{\mathbb{B}(x, r_-)} (1 - 2 \cdot e^{-\gamma_N \lambda_d(\mathbb{B}_d(r_N))} + e^{-\gamma_N \lambda_d(\mathbb{B}_d(x, r_N) \cup \mathbb{B}_d(y, r_N))}) e^{-\gamma_O \lambda_d(\mathbb{B}_d(x, r_O) \cup \mathbb{B}_d(y, r_O))} \\ &\quad - (1 - e^{-\gamma_N \lambda_d(\mathbb{B}_d(r_N))})^2 e^{-2\gamma_O \lambda_d(\mathbb{B}_d(r_O))} \, dy \, dx \\ &= \int_{W_s} \int_{\mathbb{B}(x, r_-)} (1 - 2 \cdot e^{-\gamma_N \lambda_d(\mathbb{B}_d(r_N))} + e^{-\gamma_N \lambda_d(\mathbb{B}_d(x, r_N) \cup \mathbb{B}_d(y, r_N))}) e^{-\gamma_O \lambda_d(\mathbb{B}_d(x, r_O) \cup \mathbb{B}_d(y, r_O))} \\ &\quad - (1 - 2 \cdot e^{-\gamma_N \lambda_d(\mathbb{B}_d(r_N))} + e^{-2\gamma_N \lambda_d(\mathbb{B}_d(r_N))}) e^{-2\gamma_O \lambda_d(\mathbb{B}_d(r_O))} \, dy \, dx \\ &\geq \int_{W_s} \int_{\mathbb{B}(x, r_-)} (1 - 2 \cdot e^{-\gamma_N \lambda_d(\mathbb{B}_d(r_N))} + e^{-2\gamma_N \cdot \lambda_d(\mathbb{B}_d(r_N))} e^{2\lambda_d(H_{\frac{r_-}{2}}^d)}) e^{-2\gamma_O \cdot \lambda_d(\mathbb{B}_d(r_O))} e^{2\lambda_d(H_{\frac{r_-}{2}}^d)}) \\ &\quad - (1 - 2 \cdot e^{-\gamma_N \lambda_d(\mathbb{B}_d(r_N))} + e^{-2\gamma_N \lambda_d(\mathbb{B}_d(r_N))}) e^{-2\gamma_O \lambda_d(\mathbb{B}_d(r_O))} \, dy \, dx \end{aligned}$$

Since  $e^x > 1$  for  $x > 0$  it is clear that the integrand in that lower bound is a positive constant. It follows that there is a  $c_1 > 0$  such that

$$\mathbb{V}[\lambda_d((Z_N \setminus Z_O) \cap W_s)] \geq c_1 \cdot \lambda_d(W_s). \quad (3.3)$$

This, along with  $\lambda_d((Z_N \setminus Z_O) \cap W_s) < \infty$  for all  $s \in \mathbb{R}$ , gives  $\mathbb{E}[|F|^2] < \infty$  and thus the first prerequisite of Theorem 2.32.

Next we take a look at the difference operator  $D_x \lambda_d((Z_N \setminus Z_O) \cap W_s)$ . Since the presence of an additional node does not change the volume if it is too far away from the area of observation, the operator gives zero in that case. That is

$$|x| > s + r_N \Rightarrow D_x \lambda_d((Z_N \setminus Z_O) \cap W_s) = 0 \quad \mathbb{P}\text{-a.s.} \quad (3.4)$$

Additionally seeing that for all  $x \in \mathbb{R}^d$  we have

$$\begin{aligned} |D_x F| &= \frac{|D_x \lambda_d((Z_N \setminus Z_O) \cap W_s)|}{\sqrt{\mathbb{V}[\lambda_d((Z_N \setminus Z_O) \cap W_s)]}} \\ &\leq \frac{|D_x \lambda_d((Z_N \setminus Z_O) \cap W_s)|}{\sqrt{c_1 \lambda_d(W_s)}} \quad \mathbb{P}\text{-a.s.} \end{aligned} \quad (3.5)$$

we conclude that  $\mathbb{E}[\int (D_x F)^2 \gamma_N \lambda_d(dx)] < \infty$  and thus that Theorem 2.32 is applicable. We have to give bounds on  $\alpha_1(F)$ ,  $\alpha_2(F)$  and  $\alpha_3(F)$ . We first use

$$|D_x \lambda_d((Z_N \setminus Z_O) \cap W_s)| \leq \lambda_d(\mathbb{B}_d(r_N)) \quad \mathbb{P}\text{-a.s.} \quad (3.6)$$

to extend the previous estimate to

$$|D_x F| \leq \frac{\lambda_d(\mathbb{B}_d(r_N))}{\sqrt{c_1 \lambda_d(W_s)}} \quad \mathbb{P}\text{-a.s.} \quad (3.7)$$

By the stationarity of  $\eta_S$  we have for  $x, y \in \mathbb{R}^d$

$$\mathbb{E}[(D_x F)^2 (D_y F)^2] \leq \frac{\lambda_d(\mathbb{B}_d(r_N))^4}{c_1^2 \lambda_d(W_s)^2},$$

which gives us a bound on the first term in  $\alpha_1(F)$ . For the second one we have to deal with the second order operator. We aim to use the Cauchy-Schwarz inequality and will then have to derive fourth moment bounds on  $D_{x,y}^2 F$ . We first see that

$$\begin{aligned} D_{x,y}^2 \lambda_d((Z_N \setminus Z_O) \cap W_s) &= D_x D_y \lambda_d((Z_N \setminus Z_O) \cap W_s) \\ &= D_x (\lambda_d(((Z_N \cup \mathbb{B}_d(y, r_N)) \setminus Z_O) \cap W_s) - \lambda_d((Z_N \setminus Z_O) \cap W_s)) \\ \boxed{\text{Linearity of Diff. Op.}} &= D_x \lambda_d(((Z_N \cup \mathbb{B}_d(y, r_N)) \setminus Z_O) \cap W_s) - D_x \lambda_d((Z_N \setminus Z_O) \cap W_s) \end{aligned}$$

$\mathbb{P}$ -a.s.. This implies that when  $\|x - y\| > 2r_N$  we have that  $\mathbb{B}_d(x, r_N) \cap \mathbb{B}_d(y, r_N) = \emptyset$  and thus

$$\mathbb{E}[(D_{x,y}^2 F)^4] = 0. \quad (3.8)$$

In case  $\|x - y\| \leq 2r_N$  we can use Lemma 3.8 and (3.3) to get

$$\mathbb{E}[(D_{x,y}^2 F)^4] = \frac{\mathbb{E}[(D_{x,y}^2 \lambda_d((Z_N \setminus Z_O) \cap W_s))^4]}{\mathbb{V}[\lambda_d((Z_N \setminus Z_O) \cap W_s)]^2}$$



$$\leq \frac{2^3 \cdot (\mathbb{E}[(D_x \lambda_d((Z_N \cup \mathbb{B}_d(y, r_N)) \setminus Z_O) \cap W_s))^4] + \mathbb{E}[(D_x \lambda_d((Z_N \setminus Z_O) \cap W_s))^4]}{c_1^2 \cdot \lambda_d(W_s)^2}$$

By using the bound (3.6) this reduces to

$$\mathbb{E}[(D_{x,y}^2 F)^4] \leq \frac{2^4 \cdot \lambda_d(\mathbb{B}_d(r_N))^4}{c_1^2 \cdot \lambda_d(W_s)^2}. \quad (3.9)$$

Next let  $W_{s,r_N} = [-\frac{s}{2}, \frac{s}{2}]^d + \mathbb{B}_d(r_N)$ . It follows from (3.4), (3.7) and the Cauchy-Schwarz inequality that

$$\alpha_1(F) = \gamma_N^3 \cdot \int_{(\mathbb{R}^d)^3} \sqrt{\mathbb{E}[(D_x F)^2 (D_y F)^2]} \sqrt{\mathbb{E}[(D_{x,z}^2 F)^2 (D_{y,z}^2 F)^2]} \lambda_d^3(d(x, y, z))$$

$$\boxed{(3.4)} = \gamma_N^3 \cdot \int_{W_{s,r_N}^3} \sqrt{\mathbb{E}[(D_x F)^2 (D_y F)^2]} \sqrt{\mathbb{E}[(D_{x,z}^2 F)^2 (D_{y,z}^2 F)^2]} \lambda_d^3(d(x, y, z))$$

$$\boxed{(3.7)} \leq \gamma_N^3 \cdot \int_{W_{s,r_N}^3} \frac{\lambda_d(\mathbb{B}_d(r_N))^2}{c_1 \cdot \lambda_d(W_s)} \cdot \sqrt{\mathbb{E}[(D_{x,z}^2 F)^2 (D_{y,z}^2 F)^2]} \lambda_d^3(d(x, y, z))$$

$$\boxed{\text{C.-S.}} \leq \frac{\gamma_N^3 \lambda_d(\mathbb{B}_d(r_N))^2}{c_1 \cdot \lambda_d(W_s)} \cdot \int_{W_{s,r_N}^3} \sqrt[4]{\mathbb{E}[(D_{x,z}^2 F)^4]} \sqrt[4]{\mathbb{E}[(D_{y,z}^2 F)^4]} \lambda_d^3(d(x, y, z)).$$

Taking (3.8) into account yields

$$\begin{aligned} & \int_{W_{s,r_N}^3} \sqrt[4]{\mathbb{E}[(D_{x,z}^2 F)^4]} \sqrt[4]{\mathbb{E}[(D_{y,z}^2 F)^4]} \lambda_d^3(d(x, y, z)) \\ &= \int_{W_{s,r_N}} \int_{\mathbb{B}_d(z, 2r_N)} \int_{\mathbb{B}_d(z, 2r_N)} \sqrt[4]{\mathbb{E}[(D_{x,z}^2 F)^4]} \sqrt[4]{\mathbb{E}[(D_{y,z}^2 F)^4]} \lambda_d(dx) \lambda_d(dy) \lambda_d(dz). \end{aligned}$$

Note that for the volume of  $W_{s,r_N}$  we have by Lemma 3.8 that

$$\begin{aligned} \lambda_d(W_{s,r_N}) &\leq (2r_N + s)^d \leq 2^{d-1} (2^d r_N^d + s^d) \leq 2^{d-1} (2^d r_N^d + 1) s^d \quad (3.10) \\ &= 2^{2d-1} \left( r_N^d + \frac{1}{2^d} \right) \lambda_d(W_s) =: c_{d,r_N} \cdot \lambda_d(W_s) \end{aligned}$$

and thus, using (3.9),

$$\begin{aligned} & \int_{W_{s,r_N}^3} \sqrt[4]{\mathbb{E}[(D_{x,z}^2 F)^4]} \sqrt[4]{\mathbb{E}[(D_{y,z}^2 F)^4]} \lambda_d^3(d(x, y, z)) \\ & \leq \lambda_d(W_{s,r_N}) \frac{2^2 \cdot \lambda_d(\mathbb{B}_d(2r_N))^2 \cdot \lambda_d(\mathbb{B}_d(r_N))^2}{c_1 \cdot \lambda_d(W_s)} \\ & \leq \frac{2^{2(d+1)} c_{d,r_N} \lambda_d(\mathbb{B}_d(r_N))^4}{c_1}. \end{aligned}$$

This gives us

$$\alpha_1(F) \leq \frac{\gamma_N^3 \cdot 2^{2(d+1)} c_{d,r_N} \lambda_d(\mathbb{B}_d(r_N))^6}{c_1^2 \cdot \lambda_d(W_s)}.$$

Next we deal with  $\alpha_2(F)$ . Applying the Cauchy-Schwarz inequality yields

$$\begin{aligned} \alpha_2(F) &= \gamma_N^3 \int_{(\mathbb{R}^d)^3} \mathbb{E}[(D_{x,z}^2 F)^2 (D_{y,z}^2 F)^2] \lambda_d^3(d(x, y, z)) \\ \boxed{\text{C.-S.}} &\leq \gamma_N^3 \int_{W_{s,r_N}^3} \sqrt{\mathbb{E}[(D_{x,z}^2 G)^4]} \sqrt{\mathbb{E}[(D_{y,z}^2 G)^4]} \lambda_d^3(d(x, y, z)). \end{aligned}$$

With the same arguments used before this now gives us

$$\begin{aligned} \alpha_2(F) &\leq \gamma_N^3 \lambda_d(W_{s,r_N}) \cdot \lambda_d(\mathbb{B}_d(2r_N))^2 \frac{2^4 \cdot \lambda_d(\mathbb{B}_d(r_N))^4}{c_1^2 \lambda_d(W_s)^2} \\ &\leq \frac{\gamma_N^3 2^{2d+4} c_{d,r_N} \lambda_d(\mathbb{B}_d(r_N))^6}{c_1^2 \lambda_d(W_s)}. \end{aligned}$$

Only  $\alpha_3(F)$  remains. Note that (3.6) implies

$$\mathbb{E}[|D_x \lambda_d((Z_N \setminus Z_O) \cap W_s)|^3] \leq 1 + \lambda_d(\mathbb{B}_d(r_N))^3.$$

This gives us

$$\begin{aligned} \alpha_3(F) &\leq \gamma_N \int_{W_{s,r_N}} \mathbb{E}[|D_x F|^3] \lambda_d(dx) \\ \boxed{(3.5)} &= \gamma_N \int_{W_{s,r_N}} \mathbb{E} \left[ \frac{|D_x \lambda_d((Z_N \setminus Z_O) \cap W_s)|^3}{\sqrt{\mathbb{V}[\lambda_d((Z_N \setminus Z_O) \cap W_s)]^3}} \right] \lambda_d(dx) \\ \boxed{(3.3) \ \& \ (3.6)} &\leq \gamma_N \int_{W_{s,r_N}} \frac{1 + \lambda_d(\mathbb{B}_d(r_N))^3}{c_1^{\frac{3}{2}} \lambda_d(W_s)^{\frac{3}{2}}} \lambda_d(dx) \\ &\leq \frac{\gamma_N (1 + \lambda_d(\mathbb{B}_d(r_N))^3) c_{d,r_N}}{c_1^{\frac{3}{2}} \sqrt{\lambda_d(W_s)}}. \end{aligned}$$

Using these estimates in Theorem 2.32 now gives the statement.  $\square$

As we have seen the proof is enabled by the lower bound on the variance, which has heavy influence on the constant  $c$  in Theorem 3.7. The variance in turn depends on the interplay between the point processes  $\eta_N$  and  $\eta_O$ . The higher the intensity or radius of obstacles, the bigger our observation window has to be in order to come close to normality of the volume distribution.

# Chapter 4

## Time Bounded Cylinders

The purpose of this chapter is to rigorously introduce our cylinder model and to prove asymptotic distributions of certain functionals operating on it. The first section will give a short survey of existing work in the field of cylinder processes. We then begin our exploration into the time bounded cylinder model by giving detailed instructions on how to construct it. In section 4.3 we will prove the central tool for deriving the main results, which is an adaptation of Theorem 2.32 to our novel setting. Then we come to the main, original achievements of this chapter presented in section 4.4. It contains central limit theorems derived for functions on the time bounded cylinder model. The final section will introduce a modification to the setting where the cylinders are allowed to change directions at predetermined times. We then proceed to present results derived for the modified model.

The contents of this chapter were first published in the preprint [ABD21] and draw heavily from it.

### 4.1. Related Works

By the definition of Weil, see [Wei87], a cylinder in  $\mathbb{R}^d$  is constructed by choosing a  $q$ -dimensional,  $0 \leq q \leq d - 1$ , linear subspace of  $\mathbb{R}^d$  and taking the Minkowski sum of this subspace and a set taken from its orthogonal complement. A Poisson cylinder process is then simply a Poisson process on the space of these cylinders. The union  $Z$  of the cylinders created by such a process in the stationary case has been subject to recent study. In [HS09] Heinrich and Spiess derive a central limit theorem for the  $d$ -dimensional volume of  $Z$  restricted to a growing window of observation by taking into account the long-range dependencies and applying the method of cumulants.

In [HS13] the authors modified that limit theorem using weakened assumptions on

the cylinder bases and proved a new central limit theorem for the surface content of the model. In [BBGT20] Baci et al. were able to derive concentration inequalities for the volume and the intrinsic volumes of the model, again restricted to a compact window of observation. Assumptions of convexity on the cylinder bases and isotropy of  $Z$  were made. The special case of  $q = 1$  and spherical cylinder bases is studied in [BT16] where Broman and Tykesson focus on connectivity properties. The main difference in the time bounded cylinder point of view is the restriction to the timeframe as well as the absence of horizontally running cylinders. In their recent preprint [FH21], Flimmel and Heinrich also followed the idea of cylinders constructed by marked point processes, but they restrict the underlying point process to lie on the real line. They determine the asymptotic limit for the variance of the covered area for stripes of random thickness and prove a law of large numbers. In conclusion, cylinder models have enjoyed a great deal of attention recently. We see the model proposed in the next chapter as a fruitful addition to existing research and an important step towards application for dynamic telecommunication networks.

## 4.2. Construction of the Cylinders

We start with a stationary Poisson process  $\eta$  in  $\mathbb{R}^d$  with intensity  $\gamma \in (0, \infty)$ , see Definition 2.1. We will refer to its points as the **basepoints** of the cylinders we are about to construct. In terms of random networks think of these points as the positions of our nodes at time 0. To model a movement, the basepoints need a direction and a velocity. We get both of these quantities by choosing a point on the upper half of the  $d + 1$ -dimensional unit sphere at random: Let  $h \in (0, 1)$  denote a real constant, we define

$$\mathbb{M}_h^d := \{v \in S^d : v_{d+1} > h\}$$

and let  $\mathbb{Q}$  denote a probability measure on  $\mathbb{M}_h^d$ . We shall refer to points chosen according to this measure as the **directions** of our cylinders.

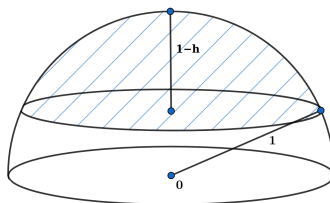


Figure 4.1: The blue shaded area is the set of possible directions when  $d = 2$ .

To construct a cylinder fix some  $T \in [0, \infty)$ . We call this parameter the *time horizon* of the model. For  $(x_1, \dots, x_d) \in \mathbb{R}^d$  and  $u \in \mathbb{R}$  we set  $\hat{x}_u = (x_1, \dots, x_d, u) \in$

$\mathbb{R}^{d+1}$ . Given a basepoint  $p \in \mathbb{R}^d$  and a direction  $v \in \mathbb{M}_h^d$ , we define a time bounded cylinder as a union of Minkowski sums. Remember that  $\mathcal{C}^d$  denotes the system of compact subsets of  $\mathbb{R}^d$ .

**Definition 4.1.** *Given a radius  $r \geq 0$  and a time horizon  $T$ , the value of the function*

$$\begin{aligned} \text{Cyl}_{r,T} : \mathbb{R}^d \times \mathbb{M}_h^d &\rightarrow \mathcal{C}^{d+1} \\ (p, v) &\mapsto \bigcup_{t \in [0,1]} \left( \left( \frac{tT}{v_{d+1}} \cdot v + \hat{p}_0 \right) + \mathbb{B}_d(r) \right) \end{aligned}$$

is called a **time bounded cylinder**.

The first  $d$  entries of a vector  $v \in \mathbb{M}_h^d$  thus encode the direction a node is moving in. The entry with index  $d+1$  encodes the velocity at which that node is traveling. We can now see that  $v_{d+1} = 1$  means a node remains in place, while smaller values for  $v_{d+1}$  imply faster movement.  $v_{d+1} = 0$  would imply infinite velocity which, in turn, would imply cylinders of infinite length. Thus we need the restriction  $v_{d+1} > h$  to limit the movement speed of nodes.

Since  $r$  and  $T$  are constant in our model, we define  $\text{Cyl}(p, v) := \text{Cyl}_{r,T}(p, v)$  for ease of notation. It will prove fruitful to think of the cylinders themselves as elements of a Poisson point process. To that end, we take the points of  $\eta$  and attach the directions as markings.

**Definition 4.2.** *Let  $\eta$  and  $\mathbb{Q}$  be defined as above. Mark every point in the support of  $\eta$  with a direction from  $\mathbb{M}_h^d$ , randomly chosen i.i.d. according to  $\mathbb{Q}$ . The resulting marked point process  $\xi$ , defined on  $\mathbb{R}^d \times \mathbb{M}_h^d$ , is called the **process of time bounded cylinders**.*

**Lemma 4.3.**  *$\xi$  is a Poisson point process with intensity measure  $\Lambda = \gamma \lambda_d \otimes \mathbb{Q}$ .*

*Proof.* By Definition 2.5,  $\xi$  is an independent  $\mathbb{Q}$ -marking. The asserted statement now follows directly from Theorem 2.7.  $\square$

We are now in a position to define our model:

**Definition 4.4.** *With the point process  $\xi$  given as above, the **time bounded cylinder (TBC) model** is the random set*

$$Z(\xi) := \bigcup_{(p,v) \in \xi} \text{Cyl}(p, v).$$

*In this notation we identify the random measure  $\xi$  with its support.*

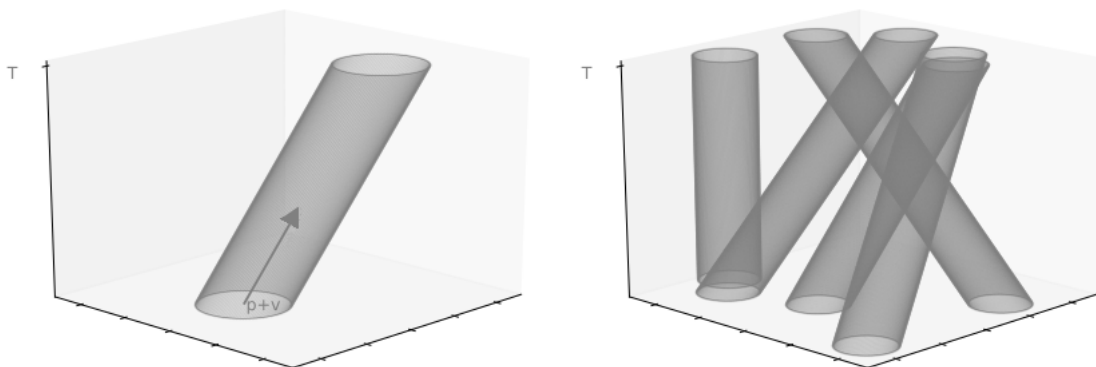


Figure 4.2: In the left picture we see a cylinder with basepoint  $\hat{p}_0$  and direction  $v$ . The arrow marks the displaced vector  $p + v$ . To the right we have an excerpt of a TBC model  $Z$  constructed on  $\mathbb{R}^2$ .

A helpful tool in the study of random closed sets in general and in particular when proving the main results presented in this chapter are capacity functionals. These can be seen as analogues to the distribution functions of real-valued random variables for random closed sets, see [SW08] for reference.

**Definition 4.5.** The **capacity functional** of a random closed set  $Z \subset \mathbb{R}^d$  is a mapping defined by the probability

$$\mathbb{P}(Z \cap C \neq \emptyset)$$

with argument  $C \in \mathcal{C}^d$ .

To derive the capacity functional of our model we will need the following definition.

**Definition 4.6.** Given a set  $C \in \mathbb{R}^d \times [0, T]$  and a direction  $v \in \mathbb{M}_h^d$  we denote by  $\overline{C}_v$  the **v-shadow** of  $C$  onto  $\mathbb{R}^d$ , that is the set

$$\overline{C}_v := \left\{ x - \frac{x_{d+1}}{v_{d+1}} v \mid x \in C \right\} \subset \mathbb{R}^d \times \{0\}.$$

Intuitively speaking, the  $v$ -shadow of a point  $x \in \mathbb{R}^{d+1}$  is the point of intersection of the line  $\{x + s \cdot v \mid s \in \mathbb{R}\}$  and  $\mathbb{R}^d \times \{0\}$ . That is the projection of  $x$  on  $\mathbb{R}^d \times \{0\}$  along  $v$ . With this we can formulate our next lemma which gives a concise form of the capacity functional for the TBC model.

**Lemma 4.7.** For  $Z(\xi)$  as in Definition 4.4 and a compact  $C \subset \mathbb{R}^d \times [0, T]$  we have

$$\mathbb{P}(Z(\xi) \cap C \neq \emptyset) = 1 - \exp \left( - \gamma \cdot \int_{\mathbb{M}_h^d} \lambda_d(\overline{C}_v + \mathbb{B}_d(r)) \mathbb{Q}(dv) \right).$$

*Proof.* Define the set

$$A_C := \{(p, v) \in \mathbb{R}^d \times \mathbb{M}_h^d \mid \text{Cyl}(p, v) \cap C \neq \emptyset\}.$$

By Lemma 4.3  $\xi$  is a Poisson point process. Thus we have that

$$\mathbb{P}(Z(\xi) \cap C \neq \emptyset) = 1 - \mathbb{P}(\xi(A_C) = 0) = 1 - \exp(-\Lambda(A_C)).$$

Note that for any fixed  $v \in \mathbb{M}_h^d$  and  $x \in \mathbb{R}^d \times [0, T]$  there exists a ball of radius  $r$  in  $\mathbb{R}^d$  such that a cylinder with direction  $v$  will include  $x$  if and only if its basepoint is included in that ball. The union of these balls for all points  $x \in C$  coincides with the set  $\overline{C}_v + \mathbb{B}_d(r)$ . We get

$$\begin{aligned} \Lambda(A_C) &= \gamma \int_{\mathbb{M}_h^d} \int_{\mathbb{R}^d} \mathbb{1}(\text{Cyl}(p, v) \cap C \neq \emptyset) \lambda_d(dp) \mathbb{Q}(dv) \\ &= \gamma \int_{\mathbb{M}_h^d} \int_{\overline{C}_v + \mathbb{B}_d(r)} \mathbb{1} \lambda_d(dp) \mathbb{Q}(dv) = \gamma \int_{\mathbb{M}_h^d} \lambda_d(\overline{C}_v + \mathbb{B}_d(r)) \mathbb{Q}(dv). \end{aligned}$$

□

If one wants to express the probability that a particular point  $x \in \mathbb{R}^d \times [0, T]$  gets hit by the set of cylinders, then Lemma 4.7 with  $C := \{x\}$  yields

$$\mathbb{P}(x \in Z(\xi)) = 1 - \exp(-\gamma \cdot r^d \kappa_d) \quad (4.1)$$

where  $\kappa_d$  denotes the volume of the  $d$ -dimensional unit ball. To give bounds on the capacity functional we sometimes need the following definition.

**Definition 4.8.** Given a pair  $(p, v) \in \mathbb{R}^d \times \mathbb{M}_h^d$ , we call the distance from basepoint  $(p_1, \dots, p_d, 0)$  to endpoint  $\frac{T}{v_{d+1}}(v_1, \dots, v_{d+1}) + (p_1, \dots, p_d, 0)$ ,

$$R_v := \left\| \frac{T}{v_{d+1}}(v_1, \dots, v_{d+1}) \right\| = \frac{T}{v_{d+1}},$$

the **scope** of the corresponding cylinder  $\text{Cyl}(p, v)$ . We denote the maximum scope of cylinders in our model by  $R_h := \frac{T}{h}$ .

Think of the scope of a cylinder as the radius of its  $d$ -dimensional area of influence. For  $(p, v), (q, w) \in \mathbb{R}^d \times \mathbb{M}_h^d$  the cylinders  $\text{Cyl}(p, v)$  and  $\text{Cyl}(q, w)$  can intersect if and only if  $\|p - q\| \leq R_v + R_w + 2r \leq 2(R_h + r)$ . Now we want to estimate  $\mathbb{P}(\text{Cyl}(p, v) \cap Z(\xi) \neq \emptyset)$ . Notice that  $\lambda_d(\overline{\text{Cyl}(p, v)}_w + \mathbb{B}_d(r))$  takes its minimum in the case  $w = v$ . Then we have that  $\overline{\text{Cyl}(p, v)}_v = \mathbb{B}_d(p, r)$ . The maximum is reached when  $v$  and  $w$  have opposite directions while  $w_{d+1} = h$ . Then it follows that

$$\lambda_d(\overline{\text{Cyl}(0, v)}_w + \mathbb{B}_d(r)) \leq 2(R_h + r) \cdot \lambda_d(\mathbb{B}_d(2r)) < \infty$$

for all  $v \in \mathbb{M}_h^d$ . We get

$$0 < (2r)^d \kappa_d \leq \lambda_d(\overline{\text{Cyl}(p, v)_w} + \mathbb{B}_d(r)) \leq (R_h + r)2^{d+1}r^d \kappa_d$$

and thus by Lemma 4.7

$$1 - \exp(-\gamma(2r)^d \kappa_d) \leq \mathbb{P}(\text{Cyl}(p, v) \cap Z(\xi) \neq \emptyset) \leq 1 - \exp(-\gamma(R_h + r)2^{d+1}r^d \kappa_d). \quad (4.2)$$

### 4.3. Applying the Malliavin-Stein Bound

Our aim is to derive asymptotic distributions of functionals on  $Z(\xi)$ . Our main tool to do this will be the following Lemma which is a generalization of the arguments we gave in the proof of Theorem 3.7 applied to this new setting. While in the proof before we used that the second-order difference operator vanishes far enough outside the observation window, we managed to soften this assumption and now only require a fast enough decay.

**Lemma 4.9.** *Let  $f : \mathcal{C}^{d+1} \rightarrow \mathbb{R}$ ,  $s \geq 1$  and  $W_s = [-\frac{s}{2}, \frac{s}{2}]^d \times [0, T]$ . Assume that  $|f(A)| < \infty$  for all  $A \in \mathcal{C}^{d+1}$  and that there exist constants  $c_1, c_2, c_3$  and  $R \in \mathbb{R}$  such that the following conditions are met for all  $x = (p, v), y = (q, w) \in \mathbb{R}^d \times \mathbb{M}_h^d$ :*

- (A)  $D_x f(Z(\xi) \cap W_s) = 0$   $\mathbb{P}$ -a.s. for  $\|p\| > R + s$ ,
- (B)  $\mathbb{V}[f(Z(\xi) \cap W_s)] \geq c_1 \cdot \lambda_{d+1}(W_s)$ ,
- (C)  $\max\{\mathbb{E}[D_x f(Z(\xi) \cap W_s)^4], \mathbb{E}[D_x f(Z(\xi + \delta_y) \cap W_s)^4]\} \leq c_2$ ,
- (D)  $\|p - q\| > R \Rightarrow \mathbb{E}[(D_{x,y}^2 f(Z(\xi) \cap W_s))^4] \leq \frac{c_3}{\lambda_{d+1}(W_s)^4}$ .

Then, there is a constant  $c \in \mathbb{R}$  such that

$$d_w\left(\frac{f(Z(\xi) \cap W_s) - \mathbb{E}[f(Z(\xi) \cap W_s)]}{\sqrt{\mathbb{V}[f(Z(\xi) \cap W_s)]}}, N\right) \leq \frac{c}{\sqrt{\lambda_{d+1}(W_s)}}.$$

The proof of this lemma gives insight into the composition of  $c$ , which is quite complex. When proving our main results however, we will always set  $c_3 = 0$ . In that case the constant is reduced to the following:

**Remark 4.10.** *Let  $c_3 = 0$ . In that case the constant  $c$  in Lemma 4.9 is given by*

$$c = \frac{\gamma \sqrt{c_{d,R,T}}}{c_1^{\frac{3}{2}}} \left(8\sqrt{\gamma c_1 c_2} \lambda_d(\mathbb{B}_d(R)) + (1 + c_2) \sqrt{c_{d,R,T}}\right)$$

where  $c_{d,R,T} = \frac{2^{2d-1}(R^d + \frac{1}{2^d})}{T}$ . Note however, that  $R$  will depend on  $T$ .



An interesting fact is that under these assumptions the lemma implies an upper bound on the variance, which is of the same order as the lower bound.

**Remark 4.11.** *Since (C) implies  $\mathbb{E}[D_x f(Z(\xi) \cap W_s)^2] \leq 1 + c_2$ , the Poincaré inequality gives us the upper bound*

$$\mathbb{V}[f(Z(\xi) \cap W_s)] \leq \int_{W_s \times \mathbb{M}_h^d} \mathbb{E}[D_x f(Z(\xi) \cap W_s)^2] \Lambda(dx) \leq (1 + c_2) \cdot \lambda_{d+1}(W_s).$$

*Proof of Lemma 4.9.* We start by defining

$$g(\xi) := \frac{f(Z(\xi) \cap W_s) - \mathbb{E}[f(Z(\xi) \cap W_s)]}{\sqrt{\mathbb{V}[f(Z(\xi) \cap W_s)]}}$$

and aim to use Theorem 2.32 on the Poisson functional  $G$  with representative  $g$ . First let us check if the prerequisites are met. From the finiteness of  $f$  and condition (B) it follows that  $\mathbb{E}[|G|^2] < \infty$ . As we have seen before, as a function of  $f$  the difference operator is linear. This leads to

$$|D_x G| = \frac{|D_x f(Z(\xi) \cap W_s)|}{\sqrt{\mathbb{V}[f(Z(\xi) \cap W_s)]}} \quad \mathbb{P}\text{-a.s.} \quad (4.3)$$

It follows now from conditions (A) and (B) that  $\mathbb{E}[f(D_x G)^2 \Lambda(dx)] < \infty$ . Thus we can apply the theorem and must now derive bounds for  $\alpha_1(G)$ ,  $\alpha_2(G)$  and  $\alpha_3(G)$ . So let  $x, y \in \mathbb{R}^d \times \mathbb{M}_h^d$ . By the Cauchy-Schwarz inequality, (4.3) and stationarity of the Poisson process we have

$$\begin{aligned} \mathbb{E}[(D_x G)^2 (D_y G)^2] &\leq \sqrt{\mathbb{E}[(D_x G)^4]} \sqrt{\mathbb{E}[(D_y G)^4]} \\ \boxed{\text{(4.3) and stationarity}} &= \frac{\mathbb{E}[(D_x f(Z(\xi) \cap W_s))^4]}{\sqrt{\mathbb{V}[f(Z(\xi) \cap W_s)]^4}} \\ \boxed{\text{(B) and (C)}} &\leq \frac{c_2}{c_1^2 \cdot \lambda_{d+1}(W_s)^2}. \end{aligned} \quad (4.4)$$

To get a bound on the second order operators, we use the linearity of the difference operator and then Lemma 3.8.

$$\begin{aligned} \mathbb{E}[|D_{x,y}^2 G|^4] &= \frac{\mathbb{E}[|D_{x,y}^2 f(Z(\xi) \cap W_s)|^4]}{\mathbb{V}[f(Z(\xi) \cap W_s)]^2} \\ \boxed{\text{Lemma 3.8 and (B)}} &\leq \frac{2^3 \cdot (\mathbb{E}[|D_x f(Z(\xi + \delta_y) \cap W_s)|^4] + \mathbb{E}[|D_x f(Z(\xi) \cap W_s)|^4])}{c_1^2 \cdot \lambda_{d+1}(W_s)^2} \\ \boxed{\text{(C)}} &\leq \frac{2^4 \cdot c_2}{c_1^2 \cdot \lambda_{d+1}(W_s)^2}. \end{aligned} \quad (4.5)$$

Condition (D) sharpens this estimate to

$$\mathbb{E}[|D_{x,y}^2 G|^4] = \frac{\mathbb{E}[|D_{x,y}^2 f(Z(\xi) \cap W_s)|^4]}{\mathbb{V}[f(Z(\xi) \cap W_s)]^2} \leq \frac{c_3}{c_1^2 \cdot \lambda_{d+1}(W_s)^6}. \quad (4.6)$$

Now let  $\overline{W}_{R,s} = [-\frac{s}{2}, \frac{s}{2}]^d + \mathbb{B}_d(R)$ . It follows from condition (A), (4.4) and Cauchy-Schwarz that

$$\begin{aligned} \alpha_1(G) &= \int_{(\mathbb{R}^d \times \mathbb{M}_h^d)^3} \sqrt{\mathbb{E}[(D_x G)^2 (D_y G)^2]} \sqrt{\mathbb{E}[(D_{x,z}^2 G)^2 (D_{y,z}^2 G)^2]} \Lambda^3(d(x, y, z)) \\ \boxed{\text{(A)}} &= \int_{(\overline{W}_{R,s} \times \mathbb{M}_h^d)^3} \sqrt{\mathbb{E}[(D_x G)^2 (D_y G)^2]} \sqrt{\mathbb{E}[(D_{x,z}^2 G)^2 (D_{y,z}^2 G)^2]} \Lambda^3(d(x, y, z)) \\ \boxed{\text{(4.4)}} &\leq \int_{(\overline{W}_{R,s} \times \mathbb{M}_h^d)^3} \frac{\sqrt{c_2}}{c_1 \cdot \lambda_{d+1}(W_s)} \cdot \sqrt{\mathbb{E}[(D_{x,z}^2 G)^2 (D_{y,z}^2 G)^2]} \Lambda^3(d(x, y, z)) \\ \boxed{\text{C.-S.}} &\leq \int_{(\overline{W}_{R,s} \times \mathbb{M}_h^d)^3} \frac{\sqrt{c_2}}{c_1 \cdot \lambda_{d+1}(W_s)} \cdot \sqrt[4]{\mathbb{E}[(D_{x,z}^2 G)^4]} \sqrt[4]{\mathbb{E}[(D_{y,z}^2 G)^4]} \Lambda^3(d(x, y, z)). \end{aligned}$$

We will now disassemble the domain of integration in order to properly apply our conditions. To that end, set  $A_x = \mathbb{B}_d(x_1, R) \times \mathbb{M}_h^d$  and  $A_x^C = \overline{W}_{R,s} \setminus \mathbb{B}_d(x_1, R) \times \mathbb{M}_h^d$ . This gives us the decomposition

$$\begin{aligned} &\int_{(\overline{W}_{R,s} \times \mathbb{M}_h^d)^3} \sqrt[4]{\mathbb{E}[(D_{x,z}^2 G)^4]} \sqrt[4]{\mathbb{E}[(D_{y,z}^2 G)^4]} \Lambda^3(d(x, y, z)) \quad (4.7) \\ &= \int_{\overline{W}_{R,s} \times \mathbb{M}_h^d} \int_{A_x} \int_{A_x} \sqrt[4]{\mathbb{E}[(D_{x,z}^2 G)^4]} \sqrt[4]{\mathbb{E}[(D_{y,z}^2 G)^4]} \Lambda(dx) \Lambda(dy) \Lambda(dz) \\ &\quad + \int_{\overline{W}_{R,s} \times \mathbb{M}_h^d} \int_{A_x} \int_{A_x^C} \sqrt[4]{\mathbb{E}[(D_{x,z}^2 G)^4]} \sqrt[4]{\mathbb{E}[(D_{y,z}^2 G)^4]} \Lambda(dx) \Lambda(dy) \Lambda(dz) \\ &\quad + \int_{\overline{W}_{R,s} \times \mathbb{M}_h^d} \int_{A_x^C} \int_{A_x} \sqrt[4]{\mathbb{E}[(D_{x,z}^2 G)^4]} \sqrt[4]{\mathbb{E}[(D_{y,z}^2 G)^4]} \Lambda(dx) \Lambda(dy) \Lambda(dz) \\ &\quad + \int_{\overline{W}_{R,s} \times \mathbb{M}_h^d} \int_{A_x^C} \int_{A_x^C} \sqrt[4]{\mathbb{E}[(D_{x,z}^2 G)^4]} \sqrt[4]{\mathbb{E}[(D_{y,z}^2 G)^4]} \Lambda(dx) \Lambda(dy) \Lambda(dz). \end{aligned}$$

The first summand on the right hand side of (4.7) can now be bounded using (4.5). This yields

$$\begin{aligned} &\int_{\overline{W}_{R,s} \times \mathbb{M}_h^d} \int_{A_x} \int_{A_x} \sqrt[4]{\mathbb{E}[(D_{x,z}^2 G)^4]} \sqrt[4]{\mathbb{E}[(D_{y,z}^2 G)^4]} \Lambda(dx) \Lambda(dy) \Lambda(dz) \\ \boxed{\text{(4.5)}} &\leq \lambda_d(\overline{W}_{R,s}) \lambda_d(\mathbb{B}_d(R))^2 \frac{4\gamma^3 \sqrt{c_2}}{c_1 \cdot \lambda_{d+1}(W_s)}. \end{aligned}$$

By Fubini's Theorem, the second and third summand are the same. Note that the implication in condition (D) applies to all pairs  $(x, w)$  with  $w \in A_x^C$ , since the

required distance is met. Thus we can bound these summands by using (4.5) and (4.6) which gets us

$$2 \cdot \int_{\overline{W}_{R,s} \times \mathbb{M}_h^d} \int_{A_z} \int_{A_z^C} \sqrt[4]{\mathbb{E}[(D_{x,z}^2 G)^4]} \sqrt[4]{\mathbb{E}[(D_{y,z}^2 G)^4]} \Lambda(dx) \Lambda(dy) \Lambda(dz)$$

$$\boxed{(4.5) \text{ and } (4.6)} \leq 2\gamma^3 \cdot \lambda_d(\mathbb{B}_d(R)) \lambda_d(\overline{W}_{R,s})^2 \frac{2\sqrt[4]{c_2}}{\sqrt{c_1} \cdot \sqrt{\lambda_{d+1}(W_s)}} \frac{\sqrt[4]{c_3}}{\sqrt{c_1} \cdot \lambda_{d+1}(W_s)^{\frac{3}{2}}}.$$

Another application of (4.6) gives us a bound on the last summand.

$$\int_{\overline{W}_{R,s} \times \mathbb{M}_h^d} \int_{A_z^C} \int_{A_z^C} \sqrt[4]{\mathbb{E}[(D_{x,z}^2 G)^4]} \sqrt[4]{\mathbb{E}[(D_{y,z}^2 G)^4]} \Lambda(dx) \Lambda(dy) \Lambda(dz)$$

$$\boxed{(4.6)} \leq \lambda_d(\overline{W}_{R,s})^3 \frac{\gamma^3 \sqrt{c_3}}{c_1 \cdot \lambda_{d+1}(W_s)^3}.$$

Next we note that for the volume of  $\overline{W}_{R,s}$  we have

$$\lambda_d(\overline{W}_{R,s}) \leq (2R + s)^d \leq 2^{d-1}(2^d R^d + s^d) \leq 2^{d-1}(2^d R^d + 1)s^d \quad (4.8)$$

$$= \frac{2^{2d-1}(R^d + \frac{1}{2^d})}{T} \lambda_{d+1}(W_s) =: c_{d,R,T} \cdot \lambda_{d+1}(W_s).$$

Using these results, we can now further estimate  $\alpha_1(G)$  by

$$\alpha_1(G) \leq \frac{\sqrt{c_2}}{c_1 \cdot \lambda_{d+1}(W_s)} \cdot \int_{(\overline{W}_{R,s} \times \mathbb{M}_h^d)^3} \sqrt[4]{\mathbb{E}[(D_{x,z}^2 G)^4]} \sqrt[4]{\mathbb{E}[(D_{y,z}^2 G)^4]} \Lambda^3(d(x, y, z))$$

$$\boxed{\text{decomp.}} \leq \lambda_d(\overline{W}_{R,s}) \lambda_d(\mathbb{B}_d(R))^2 \frac{4\gamma^3 c_2}{c_1^2 \cdot \lambda_{d+1}(W_s)^2}$$

$$+ 2 \cdot \lambda_d(\mathbb{B}_d(R)) \lambda_d(\overline{W}_{R,s})^2 \frac{2\gamma^3 c_2^{\frac{3}{4}} \sqrt[4]{c_3}}{c_1^2 \cdot \lambda_{d+1}(W_s)^3}$$

$$+ \lambda_d(\overline{W}_{R,s})^3 \frac{\gamma^3 \sqrt{c_2} \sqrt{c_3}}{c_1^2 \cdot \lambda_{d+1}(W_s)^4}$$

$$\boxed{(4.8)} = \frac{\gamma^3 c_{d,R,T} \sqrt{c_2}}{c_1^2 \cdot \lambda_{d+1}(W_s)} (4\sqrt{c_2} \lambda_d(\mathbb{B}_d(R))^2 + 4\sqrt[4]{c_2 c_3} c_{d,R,T} \lambda_d(\mathbb{B}_d(R)) + \sqrt{c_3} c_{d,R,T}^2).$$

Next we take care of  $\alpha_2(G)$ . We use the Cauchy-Schwarz inequality to get

$$\alpha_2(G) = \int_{(\mathbb{R}^d \times \mathbb{M}_h^d)^3} \mathbb{E}[(D_{x,z}^2 G)^2 (D_{y,z}^2 G)^2] \Lambda^3(d(x, y, z))$$

$$\boxed{\text{C.-S.}} \leq \int_{(\overline{W}_{R,s} \times \mathbb{M}_h^d)^3} \sqrt{\mathbb{E}[(D_{x,z}^2 G)^4]} \sqrt{\mathbb{E}[(D_{y,z}^2 G)^4]} \Lambda^3(d(x, y, z))$$

and apply the same decomposition argument as in the treatment of  $\alpha_1(G)$ .

$$\begin{aligned}
\alpha_2(G) &\leq \lambda_d(\overline{W}_{R,s}) \lambda_d(\mathbb{B}_d(R))^2 \frac{2^4 \gamma^3 \cdot c_2}{c_1^2 \cdot \lambda_{d+1}(W_s)^2} \\
&\quad + 2 \cdot \lambda_d(\mathbb{B}_d(R)) \lambda_d(\overline{W}_{R,s})^2 \frac{4\gamma^3 \sqrt{c_2}}{c_1 \cdot \lambda_{d+1}(W_s)} \frac{\sqrt{c_3}}{c_1 \cdot \lambda_{d+1}(W_s)^3} \\
&\quad + \lambda_d(\overline{W}_{R,s})^3 \frac{\gamma^3 c_3}{c_1^2 \cdot \lambda_{d+1}(W_s)^6} \\
&\leq \frac{\gamma^3 c_{d,R,T}}{c_1^2 \cdot \lambda_{d+1}(W_s)} (16c_2 \lambda_d(\mathbb{B}_d(R))^2 + 8\sqrt{c_2 c_3} c_{d,R,T} \lambda_d(\mathbb{B}_d(R)) + c_3 c_{d,R,T}^2).
\end{aligned}$$

Finally, we note that (C) implies  $\mathbb{E}[|D_x f(Z(\xi \cap W_s))|^3] \leq 1 + c_2$  and thus

$$\begin{aligned}
\alpha_3(G) &\leq \int_{\overline{W}_{R,s} \times \mathbb{M}_h^d} \mathbb{E}[|D_x G|^3] \Lambda(dx) \\
\boxed{(4.3)} &= \int_{\overline{W}_{R,s} \times \mathbb{M}_h^d} \mathbb{E} \left[ \frac{|D_x f(Z(\xi \cap W_s))|^3}{\sqrt{\mathbb{V}[f(Z(\xi \cap W_s))]}^3} \right] \Lambda(dx) \\
\boxed{(B)} &\leq \int_{\overline{W}_{R,s} \times \mathbb{M}_h^d} \frac{1}{c_1^{\frac{3}{2}} \lambda_{d+1}(W_s)^{\frac{3}{2}}} \cdot \mathbb{E}[|D_x f(Z(\xi \cap W_s))|^3] \Lambda(dx) \\
\boxed{(C)} &\leq \frac{\gamma(1 + c_2) \cdot c_{d,R,T}}{c_1^{\frac{3}{2}} \sqrt{\lambda_{d+1}(W_s)}}.
\end{aligned}$$

Using these bounds, Theorem 2.32 now gives us the asserted statement.  $\square$

#### 4.4. Central Limit Theorems

We will now present the main results of this chapter, namely limit theorems on the asymptotic behaviour of  $Z(\xi)$ . We start with the volume of the union of time bounded cylinders restricted to a compact window of observation. To be more precise, we are interested in the asymptotic distribution of the random variable

$$\lambda_{d+1}(Z(\xi) \cap W_s)$$

where, as before,  $W_s := [-\frac{s}{2}, \frac{s}{2}]^d \times [0, T]$ . Additionally to Theorem 1.2 we will provide a rate of convergence and in fact prove the following:

**Theorem 4.12.** *Let  $N$  denote a standard normal random variable and  $Z(\xi)$  as in Definition 4.4. Assume  $r < s$ . Then there exists a constant  $c \in \mathbb{R}_+$  such that*

$$d_W \left( \frac{\lambda_{d+1}(Z(\xi) \cap W_s) - \mathbb{E}[\lambda_{d+1}(Z(\xi) \cap W_s)]}{\sqrt{\mathbb{V}[\lambda_{d+1}(Z(\xi) \cap W_s)]}}, N \right) \leq \frac{c}{\sqrt{\lambda_{d+1}(W_s)}}.$$

We will remark that the capacity functional of the model admits a beautiful formula for the expected volume. An application of Fubini's theorem and (4.1) immediately yield

$$\begin{aligned} \mathbb{E}[\lambda_{d+1}(Z(\xi) \cap W_s)] &= \mathbb{E}\left[\int_{W_s} \mathbb{1}(x \in Z(\xi)) \lambda_{d+1}(dx)\right] \\ &= (1 - \exp(-\gamma \cdot r^d \kappa_d)) \cdot \lambda_{d+1}(W_s). \end{aligned}$$

Our second main result in this chapter concerns itself with isolated cylinders in the case  $d = 2$ . These represent nodes that have no contact to other nodes for the time frame at all. As before, we prove Theorem 1.3 by proving a stronger result offering rates of convergence. We start by considering the point process of isolated cylinders  $\xi_{\text{Iso}}$  where

$$\xi_{\text{Iso}}(A) = \int_{\mathbb{R}^d \times \mathbb{M}_h^d} \mathbb{1}(p \in A) \cdot \mathbb{1}(\text{Cyl}(p, v) \cap Z(\xi - \delta_{(p,v)}) = \emptyset) \xi(d(p, v))$$

counts the isolated cylinders with basepoint in  $A \subset \mathbb{R}^d$ . Let us make a few remarks about its expectation. By the Mecke equation, cf. Theorem 2.2, and Lemma 4.7 we have

$$\begin{aligned} \mathbb{E}[\xi_{\text{Iso}}(A)] &= \int_{A \times \mathbb{M}_h^d} \mathbb{P}[\text{Cyl}(x) \cap Z(\xi) = \emptyset] \Lambda(dx) \\ &= \int_{A \times \mathbb{M}_h^d} 1 - \exp\left(-\gamma \cdot \int_{\mathbb{M}_h^d} \lambda_d(\overline{\text{Cyl}(x)}_w + \mathbb{B}_d(r)) \mathbb{Q}(dw)\right) \Lambda(dx) \\ &= \gamma \cdot \int_{\mathbb{M}_h^d} 1 - \exp\left(-\gamma \cdot \int_{\mathbb{M}_h^d} \lambda_d(\overline{\text{Cyl}(0, v)}_w + \mathbb{B}_d(r)) \mathbb{Q}(dw)\right) \mathbb{Q}(dv) \cdot \lambda_d(A) \end{aligned}$$

and for the intensity of the point process  $\xi_{\text{Iso}}$ . Taking (4.2) into account yields

$$\gamma \lambda_d(A) \cdot \exp(-\gamma(R_h + r)2^{d+1}r^d \kappa_d) \leq \mathbb{E}[\xi_{\text{Iso}}(A)] \leq \gamma \lambda_d(A) \cdot \exp(-\gamma(2r)^d \kappa_d).$$

As before, let  $s > 0$  and  $W_s = [-\frac{s}{2}, \frac{s}{2}]^d \times [0, T]$ . By

$$\text{Iso}_{Z(\xi)}(W_s) := \xi_{\text{Iso}}(W_s)$$

we define the random variable counting the number of isolated cylinders with basepoint in  $W_s$ . We present the following limit theorem.

**Theorem 4.13.** *Assume  $d = 2$ ,  $s \geq 6(R_h + r)$  and let  $N$  denote a standard normal random variable. There exists a constant  $c \in \mathbb{R}_+$  such that*

$$d_W\left(\frac{\text{Iso}_{Z(\xi)}(W_s) - \mathbb{E}[\text{Iso}_{Z(\xi)}(W_s)]}{\sqrt{\mathbb{V}[\text{Iso}_{Z(\xi)}(W_s)]}}, N\right) \leq \frac{c}{\sqrt{\lambda_3(W_s)}}.$$

The last main result takes a first step in analyzing the topological structure of the TBC model and gives insight into its *Euler characteristic*. By  $\mathcal{R}^d$  let us denote the convex ring over  $\mathbb{R}^d$  that is the system containing all unions of finitely many compact, convex subsets of  $\mathbb{R}^d$  (cf. [SW08, p.601]).

**Definition 4.14.** *In the context of convex geometry the **Euler characteristic** is a function*

$$\chi : \mathcal{R}^d \rightarrow \mathbb{Z}$$

with the properties

- $\chi(K) = 1$  if  $K \subset \mathbb{R}^d$  convex,
- $\chi(\emptyset) = 0$  and
- $\chi(A \cup B) = \chi(A) + \chi(B) - \chi(A \cap B)$  for all  $A, B \subset \mathbb{R}^d$ .

For reference, see [SW08, p. 625]. Since our cylinders clearly are convex sets in  $\mathbb{R}^{d+1}$  and  $\eta$  is a Poisson process with finite intensity,  $\chi(Z(\xi) \cap W_s)$  is well defined for  $W_s$  as given above. Theorem 1.4 follows from:

**Theorem 4.15.** *Assume  $d = 2$ ,  $s \geq 6(R_h + r)$  and let  $N$  denote a standard normal random variable. There exists a constant  $c \in \mathbb{R}_+$  such that*

$$d_W \left( \frac{\chi(Z(\xi) \cap W_s) - \mathbb{E}[\chi(Z(\xi) \cap W_s)]}{\sqrt{\mathbb{V}[\chi(Z(\xi) \cap W_s)]}}, N \right) \leq \frac{c}{\sqrt{\lambda_3(W_s)}}.$$

#### 4.4.1. Proof for the Covered Volume

We start with the proof of the limit theorem concerning the covered volume of  $Z(\xi)$  in  $W_s$ .

*Proof of Theorem 4.12.* We aim to use Lemma 4.9 with

$$f = \lambda_{d+1}.$$

Clearly  $\lambda_{d+1}(A) < \infty$  for all  $A \in \mathcal{C}^{d+1}$ . Next, note that for  $x = (p, v) \in \mathbb{R}^d \times \mathbb{M}_h^d$  we have  $D_x \lambda_{d+1}(Z(\xi) \cap W_s) = 0$  for  $|p| > R_h + s$  P-a.s. since in this case  $\text{Cyl}(x) \cap W_s = \emptyset$ . If we set further  $y = (q, w) \in \mathbb{R}^d \times \mathbb{M}_h^d$  we have  $D_{x,y}^2 \lambda_{d+1}(Z(\xi) \cap W_s) = 0$  for  $|p - q| > 2(R_h + r)$  P-a.s. since  $\text{Cyl}(x) \cap \text{Cyl}(y) = \emptyset$ :

$$\begin{aligned} D_{x,y}^2 \lambda_{d+1}(Z(\xi) \cap W_s) &= D_x D_y \lambda_{d+1}(Z(\xi) \cap W_s) \\ &= D_x (\lambda_{d+1}(Z(\xi + \delta_y) \cap W_s) - \lambda_{d+1}(Z(\xi) \cap W_s)) \end{aligned}$$

$$\boxed{\text{Linearity of Diff. Op.}} = D_x \lambda_{d+1}(Z(\xi + \delta_y) \cap W_s) - D_x \lambda_{d+1}(Z(\xi) \cap W_s) = 0$$

$\mathbb{P}$ -a.s.. Thus conditions (A) and (D) are fulfilled and we have  $c_3 = 0$ . Condition (C) is next. The maximum volume of any cylinder is that of one with maximal scope, see Definition 4.8. Since the scope of a cylinder  $\text{Cyl}(p, v)$  with  $v \in \mathbb{M}_h^d$  is only dependent on the last entry of  $v$ , without loss of generality we can choose  $v_h = (\sqrt{1 - h^2}, 0, \dots, 0, h)$  as a cylinder with maximum scope and receive

$$\lambda_{d+1}(\text{Cyl}(p, v)) \leq \lambda_{d+1}(\text{Cyl}(0, v_h)) \leq \frac{T \cdot r^d \kappa_d}{h} \quad (4.9)$$

for all  $(p, v) \in \mathbb{R}^d \times \mathbb{M}_h^d$ . When we add a cylinder to the model, in the extreme case it becomes a subset of  $W_s$  and intersects with none of the preexisting cylinders. In that case it adds the entirety of its volume to  $\lambda_{d+1}(Z(\xi) \cap W_s)$ . We can conclude

$$D_{(p,v)} \lambda_{d+1}(Z(\xi) \cap W_s) \leq \lambda_{d+1}(\text{Cyl}(p, v)) \quad \mathbb{P}\text{-a.s.}$$

and thus from (4.9) that

$$\mathbb{E}[|D_{(p,v)} \lambda_{d+1}(Z(\xi) \cap W_s)|^4] \leq \left( \frac{T \cdot r^d \kappa_d}{h} \right)^4 =: c_2$$

and thus get condition (C). It remains to prove the lower bound on the variance. An application of Fubini's theorem yields

$$\begin{aligned} & \mathbb{V}[\lambda_{d+1}(Z(\xi) \cap W_s)] \\ &= \mathbb{E} \left[ \int_{W_s^2} \mathbb{1}(x \in Z(\xi), y \in Z(\xi)) \lambda_{d+1}^2(d(x, y)) \right] - \mathbb{E} \left[ \int_{W_s} \mathbb{1}(x \in Z(\xi)) \lambda_{d+1}(dx) \right]^2 \\ &= \int_{W_s^2} \mathbb{P}(x \in Z(\xi), y \in Z(\xi)) - \mathbb{P}(x \in Z(\xi))\mathbb{P}(y \in Z(\xi)) \lambda_{d+1}^2(d(x, y)) \\ &= \int_{W_s^2} \mathbb{P}(x \notin Z(\xi), y \notin Z(\xi)) - \mathbb{P}(x \notin Z(\xi))\mathbb{P}(y \notin Z(\xi)) \lambda_{d+1}^2(d(x, y)), \end{aligned}$$

where the last equality follows from an application of DeMorgan's laws. To see this consider events  $A$  and  $B$ . We have

$$\begin{aligned} \mathbb{P}(A \cap B) - \mathbb{P}(A)\mathbb{P}(B) &= 1 - \mathbb{P}((A \cap B)^C) - \mathbb{P}(A)\mathbb{P}(B) \\ \boxed{\text{DeMorgan}} &= 1 - \mathbb{P}(A^C \cup B^C) - \mathbb{P}(A)\mathbb{P}(B) \\ &= 1 - \mathbb{P}(A^C) - \mathbb{P}(B^C) + \mathbb{P}(A^C \cap B^C) - \mathbb{P}(A)\mathbb{P}(B) \\ &= \mathbb{P}(A) - \mathbb{P}(B^C) + \mathbb{P}(A^C \cap B^C) - \mathbb{P}(A)\mathbb{P}(B) \\ &= \mathbb{P}(A^C \cap B^C) + \mathbb{P}(A)(1 - \mathbb{P}(B)) - \mathbb{P}(B^C) \\ &= \mathbb{P}(A^C \cap B^C) - \mathbb{P}(B^C)(1 - \mathbb{P}(A)) \\ &= \mathbb{P}(A^C \cap B^C) - \mathbb{P}(A^C)\mathbb{P}(B^C). \end{aligned}$$

Lemma 4.7 now yields

$$\begin{aligned} \mathbb{P}(x \notin Z(\xi), y \notin Z(\xi)) &= \mathbb{P}(\{x, y\} \cap Z(\xi) = \emptyset) \\ &= \exp\left(-\gamma \cdot \int_{\mathbb{M}_h^d} \lambda_d(\overline{\{x, y\}_v} + \mathbb{B}_d(r)) \mathbb{Q}(dv)\right). \end{aligned}$$

To estimate this probability, consider some  $x, y \in W_s$  and assume  $\|x - y\| \leq r$ . Then, the distance of their respective  $v$ -shadows satisfies the same, i.e.  $\|\bar{x}_v - \bar{y}_v\| \leq r$  for  $\bar{x}_v := \overline{\{x\}_v}$  and  $\bar{y}_v := \overline{\{y\}_v}$ . Also denote by  $H_w^d(z)$  the cap of a  $d$ -dimensional hypersphere with radius  $z$  and height  $w$ . Then

$$\lambda_d(\mathbb{B}_d(r)) \leq \lambda_d\left(\left(\overline{\{x\}_v} + \mathbb{B}_d(r)\right) \cup \left(\overline{\{y\}_v} + \mathbb{B}_d(r)\right)\right) \leq 2\lambda_d(\mathbb{B}_d(r)) - 2\lambda_d\left(H_{\frac{r}{2}}^d(r)\right),$$

see Figure 3.3 for an illustration in  $d = 2$ . In the proof of Theorem 3.7 we used the same argument. Since  $e^x > 1$  for all  $x > 0$  we get

$$\begin{aligned} &\mathbb{P}(x \notin Z(\xi), y \notin Z(\xi)) - \mathbb{P}(x \notin Z(\xi))\mathbb{P}(y \notin Z(\xi)) \\ &\geq \exp\left(-2\gamma\lambda_d(\mathbb{B}_d(r)) + 2\gamma \cdot \lambda_d\left(H_{\frac{r}{2}}^d(r)\right)\right) - \exp\left(-2\gamma\lambda_d(\mathbb{B}_d(r))\right) =: \tau > 0 \end{aligned}$$

for all  $x \in \mathbb{B}_{d+1}(y, r)$  and  $y \in W_s$ . Then

$$\begin{aligned} &\mathbb{V}[\lambda_{d+1}(Z(\xi) \cap W_s)] \\ &\geq \int_{W_s} \int_{\mathbb{B}_{d+1}(y, r) \cap W_s} \mathbb{P}(x \notin Z(\xi), y \notin Z(\xi)) - \mathbb{P}(x \notin Z(\xi))\mathbb{P}(y \notin Z(\xi)) \lambda_{d+1}(dx) \lambda_{d+1}(dy) \\ &\geq \int_{W_s} \int_{\mathbb{B}_{d+1}(y, r) \cap W_s} \tau \lambda_{d+1}(dx) \lambda_{d+1}(dy) \\ &= \tau \int_{W_s} \lambda_{d+1}\left(\mathbb{B}_{d+1}(y, r) \cap W_s\right) \lambda_{d+1}(dy). \end{aligned}$$

For  $y \in W_s$  we also have that

$$\begin{aligned} \lambda_{d+1}\left(\mathbb{B}_{d+1}(y, r) \cap W_s\right) &\geq \frac{1}{2^{d+1}} \cdot \lambda_{d+1}\left(\mathbb{B}_{d+1}(0, \min\{r, T\})\right) \\ &= \frac{\kappa_{d+1} \cdot \min\{r, T\}^{d+1}}{2^{d+1}}, \end{aligned}$$

where we have equality if  $y$  sits just in a corner of the observation window  $W_s$ . For instance in the case  $d = 1$ ,  $r < T$  and  $y = \left(-\frac{r}{2}, T\right)$  one quarter of  $\mathbb{B}_2(y, r)$  intersects with  $W_s$ . Now we can derive the bound

$$\begin{aligned} \mathbb{V}[\lambda_{d+1}(Z(\xi) \cap W_s)] &\geq \tau \int_{W_s} \frac{\kappa_{d+1} \cdot \min\{r, T\}^{d+1}}{2^{d+1}} \lambda_{d+1}(dy) \\ &= \frac{\tau \cdot \kappa_{d+1} \cdot \min\{r, T\}^{d+1}}{2^{d+1}} \cdot \lambda_{d+1}(W_s) =: c_1 \cdot \lambda_{d+1}(W_s). \end{aligned}$$

This shows condition (B) of Lemma 4.9 and concludes the proof.  $\square$

Taking up Remark 4.11, we note that both lower and upper bound on the variance are of the same order.



### 4.4.2. Proof for the Isolated Nodes

Next we deal with the limit theorem for the isolated cylinders.

*Proof of Theorem 4.13.* As we did for the covered volume, we aim to apply Lemma 4.9 to the function

$$\text{Iso}_{Z(\xi)} : \xi \mapsto n \in \mathbb{N}$$

counting the number of isolated cylinders created by  $\xi$ . Since the Poisson process  $\eta$  has finite intensity, it holds that  $\text{Iso}_{Z(\xi)}(A) < \infty$   $\mathbb{P}$ -a.s. for all  $A \in \mathcal{C}^3$ . Next we verify condition (A) and (D). Set  $R = 2(R_h + r)$  and  $c_3 = 0$ . Since two cylinders can only intersect if their distance is smaller than  $R$ , both conditions are satisfied. This argument follows analogously to our reasoning in the proof of Theorem 4.12. For the same reason, we can bound the first order difference operator by

$$|D_x \text{Iso}_{Z(\xi)}(W_s)| \leq \eta(\mathbb{B}_2(0, R)) \quad \mathbb{P}\text{-a.s.}$$

Set  $a := \mathbb{E}[\eta(\mathbb{B}_2(0, R))] = \gamma \cdot \lambda_2(\mathbb{B}_2(0, R))$  and  $x \in \mathbb{R}^2 \times \mathbb{M}_h^2$ . The number of isolated cylinders that can be connected by adding  $\text{Cyl}(x)$  to the model is limited by the total number of cylinders within maximum range. By using the fourth moment of the Poisson distributed random variable  $\eta(\mathbb{B}_2(0, R))$ , we get

$$\mathbb{E}[D_x \text{Iso}_{Z(\xi)}(W_s)^4] \leq a^4 + 6a^3 + 7a^2 + a.$$

Thus condition (C) is satisfied with  $c_2 := a^4 + 6a^3 + 7a^2 + a + 1$ . To verify (B), we use a strategy applied in [Rei05] and disassemble  $[-\frac{s}{2}, \frac{s}{2}]^2$  into squares of side length  $6(R_h + r)$ . Without loss of generality we can assume  $s = n \cdot 6(R_h + r)$  for some  $n \in \mathbb{N}$ , as the area outside these squares is of no consequence to what follows. We index these sets by indices collected in the set  $I$ . For each  $i \in I$  consider  $C_i$ , a square of side length  $2(R_h + r)$  in the center of the corresponding greater square  $S_i$  of side length  $6(R_h + r)$ . We define the event

$$A_i = \{\eta(C_i) = 2, \eta(S_i \setminus C_i) = 0\},$$

which is illustrated in Figure 4.3. Let the  $\sigma$ -algebra  $\mathcal{F}$  contain information on basepoints and directions of all cylinders of  $Z(\xi)$ , except those with basepoint in a square  $S_i$  with  $\mathbb{1}(A_i) = 1$ . Now we decompose the variance

$$\begin{aligned} \mathbb{V}[\text{Iso}_{Z(\xi)}(W_s)] &= \mathbb{E}[\mathbb{V}[\text{Iso}_{Z(\xi)}(W_s) \mid \mathcal{F}]] + \mathbb{V}[\mathbb{E}[\text{Iso}_{Z(\xi)}(W_s) \mid \mathcal{F}]] \\ &\geq \mathbb{E}[\mathbb{V}[\text{Iso}_{Z(\xi)}(W_s) \mid \mathcal{F}]] \\ &= \mathbb{E} \left[ \sum_{\mathbb{1}(A_i)=1} \mathbb{V}_{X_{i,1}, X_{i,2}}[\text{Iso}_{Z(\xi)}(W_s)] \right] \end{aligned} \quad (4.10)$$

where the right hand side variance is taken with respect only to the two random elements  $X_{i,1}, X_{i,2} \in \mathbb{R}^2 \times \mathbb{M}_h^2$ , created by the event  $A_i$ . Since these two

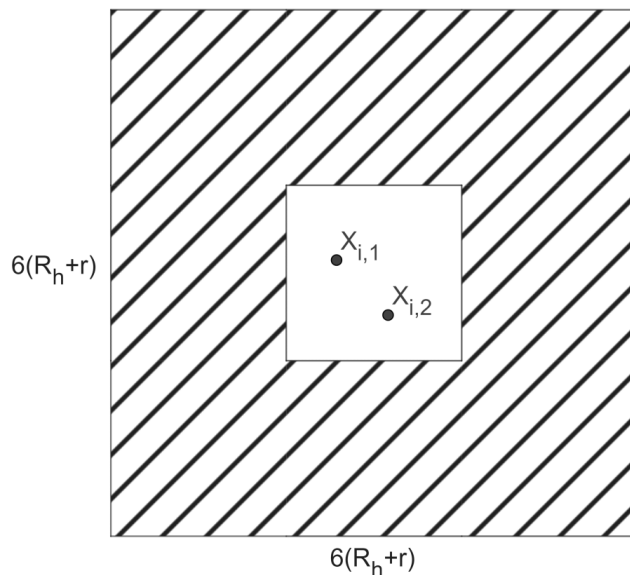


Figure 4.3: The event  $A_i$ . The two nodes in the center can only interact with one another, as the shaded area is conditioned to be empty and cannot be bridged by cylinders even with maximum scope.

cylinders can not intersect with any other cylinders of the model, the number of isolated nodes outside  $A_i$  is independent of that contributed by  $X_{i,1}$  and  $X_{i,2}$ . Let  $\Delta_{X_{i,1}, X_{i,2}} \text{Iso}_{Z(\xi)}(W_s)$  denote that contribution. Note that

$$\Delta_{X_{i,1}, X_{i,2}} \text{Iso}_{Z(\xi)}(W_s) = 2 \cdot \mathbb{1}(\text{Cyl}(X_{i,1}) \cap \text{Cyl}(X_{i,2}) = \emptyset). \quad (4.11)$$

This yields

$$\begin{aligned} \mathbb{V}_{X_{i,1}, X_{i,2}}[\text{Iso}_{Z(\xi)}(W_s)] &= \mathbb{V}_{X_{i,1}, X_{i,2}}[\text{Iso}_{Z(\xi - \delta_{X_{i,1}} - \delta_{X_{i,2}})}(W_s) + \Delta_{X_{i,1}, X_{i,2}} \text{Iso}_{Z(\xi)}(W_s)] \\ &= \mathbb{V}_{X_{i,1}, X_{i,2}}[\Delta_{X_{i,1}, X_{i,2}} \text{Iso}_{Z(\xi)}(W_s)] \\ \boxed{(4.11)} &= 4 \cdot \mathbb{P}[\text{Cyl}(X_{i,1}) \cap \text{Cyl}(X_{i,2}) = \emptyset] \cdot \mathbb{P}[\text{Cyl}(X_{i,1}) \cap \text{Cyl}(X_{i,2}) \neq \emptyset] \\ &=: c_4, \end{aligned}$$

since both probabilities clearly are strictly positive. Using this in (4.10) together with the stationarity and independence properties of  $\eta$  as well as  $|I| = \left(\frac{s}{6(R_h+r)}\right)^2$  we have

$$\begin{aligned} \mathbb{V}[\text{Iso}_{Z(\xi)}(W_s)] &\geq c_4 \cdot \sum_{i \in I} \mathbb{P}[A_i] \\ &\geq c_4 \cdot \sum_{i \in I} 2\gamma^2(R_h+r)^2 \exp(-4\gamma(R_h+r)^2) \cdot \exp(-32\gamma(R_h+r)^2) \end{aligned}$$

$$\geq c_4 \cdot \sum_{i \in I} c_5 = c_6 \cdot \left( \frac{s}{6(R_h + r)} \right)^2$$

$$\boxed{\lambda_3(W_s) = s^2 \cdot T} = \frac{c_6}{36T(R_h + r)^2} \lambda_3(W_s)$$

and thus condition (B).  $\square$

Again, the lower bound matches the order of the upper bound as given in Remark 4.11. Let us remark that the proof above was conceived with telecommunication networks in mind and thus formulated in the case  $d = 2$ . We however believe that the arguments can be easily transferred to arbitrary dimensions.

### 4.4.3. Proof for the Euler Characteristic

It remains to prove the limit theorem for the Euler characteristic.

*Proof of Theorem 4.15.* We aim to use Lemma 4.9 on  $f_{(\cdot)}$  for  $f_\xi : \mathcal{C}^3 \rightarrow \mathbb{Z}$  with

$$f_\xi(A) = \begin{cases} \chi(Z(\xi) \cap A), & \text{if } A \in \mathcal{R}^3 \\ 0, & \text{else.} \end{cases}$$

Since  $\eta$  has finite intensity, the properties of  $\chi$  imply that  $f(A) < \infty$  for all  $A \in \mathcal{C}^3$   $\mathbb{P}$ -a.s.. Once more we start by checking conditions (A) and (D). Again, set  $R = 2(R_h + r)$  and  $c_3 = 0$ . As  $\text{Cyl}(p, v) \cap W_s = \emptyset$  for any  $(p, v) \in \mathbb{R}^2 \times \mathbb{M}_h^2$  with  $|p| \geq R + s$ , condition (A) is satisfied.

Also, for  $(q, w) \in \mathbb{R}^2 \times \mathbb{M}_h^2$ ,  $\|p - q\| \geq R$  implies  $\text{Cyl}(p, v) \cap \text{Cyl}(q, w) = \emptyset$  and thus  $D_{(p,v)}(\chi(Z(\xi + \delta_{(q,w)}) \cap W_s)) - D_{(p,v)}(\chi(Z(\xi) \cap W_s)) = 0$   $\mathbb{P}$ -a.s.. To verify (C) we note that for  $x \in \mathbb{R}^2 \times \mathbb{M}_h^d$  the definition of  $\chi$  gives us

$$\begin{aligned} D_x \chi(Z(\xi) \cap W_s) &= \chi(Z(\xi + \delta_x) \cap W_s) - \chi(Z(\xi) \cap W_s) \\ &= \chi((Z(\xi) \cup \text{Cyl}(x)) \cap W_s) - \chi(Z(\xi) \cap W_s) \\ &= \chi((Z(\xi) \cap W_s) \cup (\text{Cyl}(x) \cap W_s)) - \chi(Z(\xi) \cap W_s) \\ \boxed{\text{Definition 4.14}} &= \chi(\text{Cyl}(x) \cap W_s) - \chi(Z(\xi) \cap \text{Cyl}(x) \cap W_s) \quad \mathbb{P}\text{-a.s..} \end{aligned}$$

Furthermore, it holds true that  $\chi(\text{Cyl}(x) \cap W_s) = \mathbb{1}(\text{Cyl}(x) \cap W_s \neq \emptyset)$  and since  $\chi(Z(\xi) \cap \text{Cyl}(x) \cap W_s)$  counts the number of disjoint intersections of  $\text{Cyl}(x) \cap W_s$  with cylinders of  $Z(\xi)$  we also have

$$\chi(Z(\xi) \cap \text{Cyl}(x) \cap W_s) \leq \sum_{y \in \xi} \mathbb{1}(\text{Cyl}(y) \cap \text{Cyl}(x) \neq \emptyset) \leq \eta(\mathbb{B}_2(0, R)) \quad \mathbb{P}\text{-a.s..}$$

To this, we have to add the number of cylinders added by the difference operators emerging in condition (C). Thus the condition is fulfilled with

$$c_2 := \mathbb{E}[(2 + \eta(\mathbb{B}_2(0, R)))^4].$$

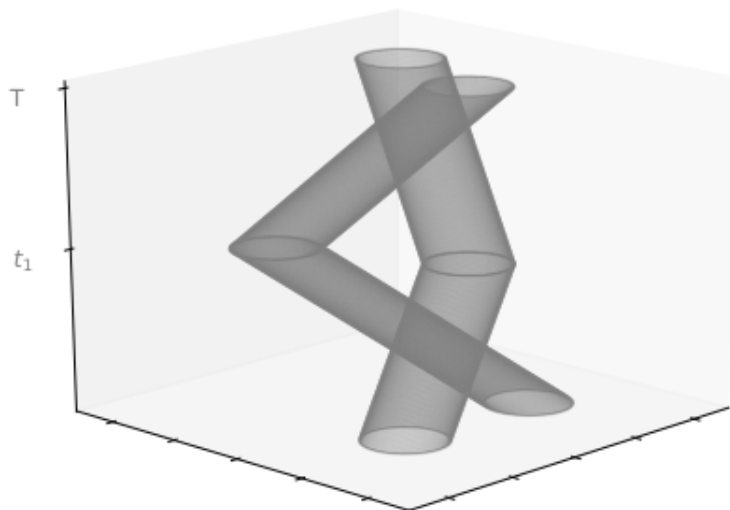


Figure 4.4: An excerpt of the TBC model in the expanded setting.

To verify (B) we use the same strategy as in the proof of Theorem 4.13 and now have to consider  $\mathbb{V}_{X_{i,1}, X_{i,2}}[\chi(Z(\xi) \cap W_s)]$ . Again, since the cylinders created by  $X_{i,1}$  and  $X_{i,2}$  can not intersect, we can use the additivity of the Euler characteristic to get

$$\begin{aligned} & \mathbb{V}_{X_{i,1}, X_{i,2}}[\chi(Z(\xi) \cap W_s)] \\ &= \mathbb{V}_{X_{i,1}, X_{i,2}}[\chi(Z(\xi - \delta_{X_{i,1}} - \delta_{X_{i,2}}) \cap W_s) + \Delta_{X_{i,1}, X_{i,2}}\chi(Z(\xi) \cap W_s)] \\ &= \mathbb{V}_{X_{i,1}, X_{i,2}}[\Delta_{X_{i,1}, X_{i,2}}\chi(Z(\xi) \cap W_s)]. \end{aligned}$$

Since  $\Delta_{X_{i,1}, X_{i,2}}\chi(Z(\xi) \cap W_s) \in \{1, 2\}$  we get

$$\begin{aligned} & \mathbb{V}_{X_{i,1}, X_{i,2}}[\chi(Z(\xi) \cap W_s)] \\ &= 5 \cdot \mathbb{P}[\text{Cyl}(X_{i,1}) \cap \text{Cyl}(X_{i,2}) = \emptyset] \cdot \mathbb{P}[\text{Cyl}(X_{i,1}) \cap \text{Cyl}(X_{i,2}) \neq \emptyset]. \end{aligned}$$

Thus condition (B) follows as it did for Theorem 4.13.  $\square$

Note that, again, the order of the lower bound on the variance coincides with that of the upper bound found in Remark 4.11.

## 4.5. Stacked Time Bounded Cylinders

Up to this point our model supports movements in one direction only. To allow for the nodes to change direction we iterate the marking process, giving a node a new direction vector at fixed points in time. These times can be given deterministically or randomly, but independent of all other random variables. In view of application,

one could think of a deterministic setting like a daily routine or an exponentially distributed random variable for the time distances.

### 4.5.1. Construction of the Cylinderstacks

Set  $t_0 := 0$ ,  $t_{K+1} := T$  and let  $T_K = (t_0, t_1, t_2, \dots, t_{K+1})$ , for some  $K \in \mathbb{N}$ , be a strictly monotone sequence of times in  $[0, T]$ . Now recall the definition of a cylinder as given in Definition 4.1. We will now modify it to reflect the expanded setting. To a point  $p \in \eta$  let  $V = (v_0, \dots, v_K)$  be the vector of directions taken, that is  $v_i \in \mathbb{M}_h^d$  for  $i \in \{0, \dots, K\}$ . Consider the projection  $\pi : \mathbb{M}_h^d \rightarrow [0, 1]$  onto the velocity, that is  $\pi(v) = v_{d+1}$  for  $v \in \mathbb{M}_h^d$ , and define  $\hat{p}_0 \in \mathbb{R}^{d+1}$  as the vector  $p$  but with an additional coordinate with value zero. Then

$$\hat{p}_k := \hat{p}_0 + \sum_{j=0}^{k-1} \frac{|t_{j+1} - t_j|}{\pi(v_j)} v_j.$$

In the context of random networks, think of this point as the location at time  $t_k$  of a node starting its journey in  $p$ . We are now in a position to modify Definition 4.1 for this expanded setting.

**Definition 4.16.** *Given a radius  $r \geq 0$  and  $T_K$  as above, the values of the function*

$$\begin{aligned} \text{Cyl}_{r, T_K} : \mathbb{R}^{d+1} \times (\mathbb{M}_h^d)^K &\rightarrow \mathcal{C}^{d+1} \\ (p, V) &\mapsto \bigcup_{k=0}^K \bigcup_{u \in [0, 1]} \left( \left( \hat{p}_k + \frac{u|t_{k+1} - t_k|}{\pi(v_k)} \cdot v_k \right) + \mathbb{B}_d(r) \right) \end{aligned}$$

are the **time bounded cylinderstacks**.

Our idea is that at every time  $t \in T_K$  a cylinder has the opportunity to change direction and will do so with probability  $q \in [0, 1]$ . A new direction is always drawn with respect to the probability measure  $\mathbb{Q}$  introduced in section 4.2. Thus the aforementioned vector  $V = (v_0, \dots, v_K) \in (\mathbb{M}_h^d)^K$  is drawn with respect to the probability measure

$$\mathbb{Q}_K := \mathbb{Q} \otimes (1 - q)\delta_{v_0} + q\mathbb{Q} \otimes \dots \otimes (1 - q)\delta_{v_{K-1}} + q\mathbb{Q}.$$

We can now give analogues to Definition 4.2 and Lemma 4.3.

**Definition 4.17.** *Let  $\eta$  be defined as in Section 4.2 and  $\mathbb{Q}_K$  as above. Mark every point in the support of  $\eta$  with a direction from  $\mathbb{M}_h^d$ , randomly with respect to  $\mathbb{Q}_K$ . The resulting marked point process  $\xi_K$  defined on  $\mathbb{R}^d \times (\mathbb{M}_h^d)^K$  is called the **process of time bounded cylinderstacks**.*

**Lemma 4.18.**  *$\xi_K$  is a Poisson point process with intensity measure  $\Lambda_K = \gamma\lambda_d \otimes \mathbb{Q}_K$ .*

*Proof.* Since  $\mathbb{Q}_K$  is independent of the Poisson process  $\eta$  we have an independent marking again and thus the statement follows as it did for Lemma 4.3.  $\square$

That the process of time bounded cylinderstacks preserves the Poisson properties of the original point process seems remarkable, but can be intuitively explained by using thinnings, see Example 2.9. Since for  $t_1 \geq T$  the model remains unchanged let us consider  $t_1 < T$ . We start with the point process  $\xi$  as introduced in Definition 4.2. From Lemma 4.3 we know that  $\xi$  is a Poisson point process. Now we take a  $q$ -thinning of  $\xi$ , namely a Bernoulli experiment with parameter  $q$  which decides for each point of the Poisson process if it belongs to  $\xi(q)$  or  $\xi - \xi(q)$ . Theorem 2.10 implies that both  $\xi(q)$  and  $\xi - \xi(q)$  are Poisson processes.

For the points in  $\xi(q)$  we now choose a new direction and by adding this into another component of the marking, we get a new marked point process which we call  $\xi(q)^M$ . Analogously to the single direction case Theorem 2.7 implies that this process is Poisson. For points in  $\xi - \xi(q)$  the direction stays the same, nevertheless, as for  $\xi(q)$  we add the previous direction as a new marking and again obtain a marked point process  $\xi(1 - q)^M$ . As a superposition of two Poisson processes  $\xi_1 := \xi(q)^M \oplus \xi(1 - q)^M$  is also Poisson. We proceed in thinning, marking and gluing together for each time step  $t_i < T$  and obtain the Poisson process of cylinderstacks. We can now conveniently define the expanded model as follows.

**Definition 4.19.** *With the point process  $\xi_K$  given as above, the **stacked time bounded cylinder (sTBC) model** is the random set*

$$Z(\xi_K) := \bigcup_{(p,V) \in \xi_K} \text{Cyl}(p, V).$$

*In this notation we identify the random measure  $\xi_K$  with its support.*

With these definitions we can now rephrase Lemma 4.9 to work with our modifications.

**Lemma 4.20.** *Let  $f : \mathcal{C}^{d+1} \rightarrow \mathbb{R}$ ,  $s \geq 1$  and  $W_s = [-\frac{s}{2}, \frac{s}{2}]^d \times [0, T]$ . Assume that  $|f(A)| < \infty$  for all  $A \in \mathcal{C}^{d+1}$  and that there exist constants  $c_1, c_2, c_3$  and  $R \in \mathbb{R}$  such that the following conditions are met for all  $x = (p, V), y = (q, W) \in \mathbb{R}^d \times (\mathbb{M}_h^d)^K$ :*

- (A)  $D_x f(Z(\xi_K) \cap W_s) = 0$   $\mathbb{P}$ -a.s. for  $\|p\| > R + s$ ,
- (B)  $\mathbb{V}[f(Z(\xi_K) \cap W_s)] \geq c_1 \cdot \lambda_{d+1}(W_s)$ ,
- (C)  $\max\{\mathbb{E}[D_x f(Z(\xi_K) \cap W_s)^4], \mathbb{E}[D_x f(Z(\xi_K + \delta_y) \cap W_s)^4]\} \leq c_2$ ,
- (D)  $\|p - q\| > R \Rightarrow \mathbb{E}[(D_{x,y}^2 f(Z(\xi_K) \cap W_s))^4] \leq \frac{c_3}{\lambda_{d+1}(W_s)^4}$ .

Then, there is a constant  $c \in \mathbb{R}$  such that

$$d_W \left( \frac{f(Z(\xi_K) \cap W_s) - \mathbb{E}[f(Z(\xi_K) \cap W_s)]}{\sqrt{\mathbb{V}[f(Z(\xi_K) \cap W_s)]}}, N \right) \leq \frac{c}{\sqrt{\lambda_{d+1}(W_s)}}.$$

As the proof in section 4.3 relies only on the assumed bounds and not on how the model is constructed, we can use the same techniques and estimates we used there and prove this lemma analogously.

### 4.5.2. Covered Volume

As usual, let  $W_s := [-\frac{s}{2}, \frac{s}{2}]^d \times [0, T]$ . We will now study the covered volume of the sTBC model that is the random variable

$$\lambda_{d+1}(Z(\xi_K) \cap W_s).$$

As this is an additive function our strategy for working with this quantity will be to split the sTBC model into TBC models and evaluate the volume for each of them. To that end let  $Z_t(\xi)$  denote the TBC model with time horizon  $t \geq 0$ . We will first apply our strategy when computing the expectation of the volume. Using (4.1) and Fubini we have

$$\begin{aligned} \mathbb{E}[\lambda_{d+1}(Z(\xi_K) \cap W_s)] &= \mathbb{E} \left[ \int_{W_s} \mathbb{1}(x \in Z(\xi_K)) \, dx \right] \\ &= \mathbb{E} \left[ \sum_{k=0}^K \int_{[-\frac{s}{2}, \frac{s}{2}]^d \times [t_k, t_{k+1}]} \mathbb{1}(x \in Z_{|t_{k+1}-t_k|}(\xi)) \, dx \right] \\ \boxed{\text{Fubini and (4.1)}} &= (1 - \exp(-\gamma \cdot r^d \kappa_d)) \cdot \sum_{k=0}^K \lambda_{d+1} \left( [-\frac{s}{2}, \frac{s}{2}]^d \times [t_k, t_{k+1}] \right) \\ &= (1 - \exp(-\gamma \cdot r^d \kappa_d)) \cdot \lambda_{d+1}(W_s). \end{aligned}$$

We see that the expected volume remains unchanged, which is unsurprising given the homogeneous nature of our model.

**Theorem 4.21.** *Let  $N$  denote a standard normal random variable and assume  $r < s$ . There exists a constant  $c \in \mathbb{R}_+$  such that*

$$d_W \left( \frac{\lambda_{d+1}(Z(\xi_K) \cap W_s) - \mathbb{E}[\lambda_{d+1}(Z(\xi_K) \cap W_s)]}{\sqrt{\mathbb{V}[\lambda_{d+1}(Z(\xi_K) \cap W_s)]}}, N \right) \leq \frac{c}{\sqrt{\lambda_{d+1}(W_s)}}.$$

*Proof.* We use Lemma 4.20 on the function  $f = \lambda_{d+1}$ . We can verify conditions (A) and (D) by the same observation we made in the proof of Theorem 4.12, again using  $R = 2(R_h + r)$  and  $c_3 = 0$ . The same is true for condition (C) which once more is satisfied with  $c_2 := \left(\frac{T \cdot r^d \kappa_d}{h}\right)^4$ . To verify (B) we have to make some adjustments but start as before with

$$\begin{aligned} & \mathbb{V}[\lambda_{d+1}(Z(\xi_K) \cup W_s)] \\ &= \int_{W_s^2} \mathbb{P}(x \notin Z(\xi_K), y \notin Z(\xi_K)) - \mathbb{P}(x \notin Z(\xi_K))\mathbb{P}(y \notin Z(\xi_K)) \lambda_{d+1}^2(d(x, y)). \end{aligned}$$

Given a point  $y \in W_s$ , let  $t_-^y, t_+^y \in T_K$  such that  $t_-^y \leq y_{d+1} \leq t_+^y$ ,  $t_-^y \neq t_+^y$  and there is no element of  $T_K$  in the interval  $(t_-^y, t_+^y)$ . We have

$$\begin{aligned} & \mathbb{V}[\lambda_{d+1}(Z(\xi_K) \cap W_s)] \\ &= \int_{W_s^2} \mathbb{P}(x \notin Z(\xi_K), y \notin Z(\xi_K)) - \mathbb{P}(x \notin Z(\xi_K))\mathbb{P}(y \notin Z(\xi_K)) \lambda_{d+1}^2(d(x, y)) \\ &\geq \int_{W_s} \int_{[-\frac{s}{2}, \frac{s}{2}]^d \times [t_-^y, t_+^y]} \mathbb{P}(x \notin Z_{|t_+^y - t_-^y|}(\xi), y \notin Z_{|t_+^y - t_-^y|}(\xi)) \\ &\quad - \mathbb{P}(x \notin Z_{|t_+^y - t_-^y|}(\xi))\mathbb{P}(y \notin Z_{|t_+^y - t_-^y|}(\xi)) \lambda_{d+1}(dx) \lambda_{d+1}(dy). \end{aligned}$$

Note that the bound of the inner integral now ensures that  $x$  and  $y$  share a time slot in the stacked cylinder model. Because of this we can argue as in the single direction case and derive the constant  $\tau > 0$  such that  $p_{xy} - p_x p_y \geq \tau$  for all  $x \in \mathbb{B}_{d+1}(y, \frac{r}{2}) \cap ([-\frac{s}{2}, \frac{s}{2}]^d \times [t_-^y, t_+^y])$  and  $y \in W_s$ . As before we then have

$$\begin{aligned} & \lambda_{d+1}(\mathbb{B}_d(y, \frac{r}{2}) \cap ([-\frac{s}{2}, \frac{s}{2}]^d \times [t_-^y, t_+^y])) \\ &\geq \frac{1}{2^{d+1}} \cdot \lambda_{d+1}(\mathbb{B}_{d+1}(0, \min\{\frac{r}{2}, t_+^y - t_-^y\})) \\ &= \frac{\kappa_{d+1} \cdot \min\{\frac{r}{2}, t_+^y - t_-^y\}^{d+1}}{2^{d+1}} \end{aligned}$$

and thus

$$\begin{aligned} & \mathbb{V}[\lambda_{d+1}(Z(\xi_K) \cap W_s)] \\ &\geq \tau \cdot \int_{W_s} \mathbb{E}[\lambda_{d+1}(\mathbb{B}_d(y, r) \cap ([-\frac{s}{2}, \frac{s}{2}]^d \times [t_-^y, t_+^y]))] \lambda_{d+1}(d(y)) \\ &\geq \frac{\tau \cdot \kappa_{d+1} \cdot \mathbb{E}[\min\{r, Y\}^{d+1}]}{2^{d+1}} \cdot \lambda_{d+1}(W_s) =: c_1 \cdot \lambda_{d+1}(W_s) \end{aligned}$$

with the random variable  $Y := \min_k \{|t_{k+1} - t_k|\}$ . □



### 4.5.3. Isolated Cylinders

We are now interested in the isolated stacks in the sTBC model. The point process of isolated cylinder stacks with basepoint in  $A \subset \mathbb{R}^d$  is given by

$$\mu(A) = \int_{A \times (\mathbb{M}_h^d)^K} \mathbb{1}(\text{Cyl}(x) \cap Z(\xi_K - \delta_x) = \emptyset) \xi_K(dx).$$

The next theorem shows asymptotic normality of  $\text{Iso}_{Z(\xi_K)}(W_s) = \mu(W_s)$ .

**Theorem 4.22.** *Assume  $d = 2$ ,  $s \geq 6(R_h + r)$  and let  $N$  denote a standard normal random variable. There exists a constant  $c \in \mathbb{R}_+$  such that*

$$d_W \left( \frac{\text{Iso}_{Z(\xi_K)}(W_s) - \mathbb{E}[\text{Iso}_{Z(\xi_K)}(W_s)]}{\sqrt{\mathbb{V}[\text{Iso}_{Z(\xi_K)}(W_s)]}}, N \right) \leq \frac{c}{\sqrt{\lambda_{d+1}(W_s)}}.$$

*Proof.* Note that the maximum scope of a cylinder remains unchanged in the multi-directional setting. Thus, conditions (A), (C) and (D) are derived in the same way as in the proof of Theorem 4.13, using the same choices for  $R$ ,  $c_2$  and  $c_3$ . To verify (B) we use the same strategy as before and get to

$$\begin{aligned} & \mathbb{V}_{X_{i,1}, X_{i,2}}[\text{Iso}_{Z(\xi_K)}(W_s)] \\ &= 4 \cdot \mathbb{P}[\text{Cyl}(X_{i,1}) \cap \text{Cyl}(X_{i,2}) = \emptyset] \cdot \mathbb{P}[\text{Cyl}(X_{i,1}) \cap \text{Cyl}(X_{i,2}) \neq \emptyset]. \end{aligned}$$

Even in this modified setting it is clear that these probabilities are not zero, as they can be estimated using  $r$  and  $R$ . It follows that (B) holds true, which concludes the proof.  $\square$

# Chapter 5

## Closing Remarks

It was the aim of this work to consider problems arising from the practical study of telecommunication networks and revise them using rigorous mathematics. We have identified obstruction and mobility as intimidating challenges to the modelling of these networks. Obstruction makes it harder for nodes to connect putting the robustness of the network at risk. Mobility is a difficult aspect to handle mathematically as traditional models show shortcomings when trying to analyse their behavior over the complete timeframe.

We treated obstruction by taking a second look at an existing model and revisited its percolation properties. We presented new thresholds for the sub- and supercritical regimes. In the subcritical case we extended known bounds to arbitrary dimensions. After that we began our analysis of asymptotic distributions in modified Boolean models and proved a limit theorem for the covered volume of the random set associated to the obstructed Gilbert graph. We applied results derived from the Malliavin-Stein method to achieve this.

Then we presented a new approach to mobility modelling and introduced the time bounded cylinder model. Our setting allows for a connectivity analysis over a prolonged period of time. We proceeded to generalize our technique used to derive the limit theorem in the chapter before and applied it to the TBC model. We used it to prove asymptotics for important properties of the model, like the covered volume and isolated nodes.

There are a number of ways to build on the work done in this thesis. For the obstructed Gilbert graph the supercritical regimes for higher dimensions remains an open problem. However, our approach was to compare the connectivity graph with a fitting, 2-dimensional site percolation model. This approach can not be easily applied to higher dimensions as site percolation thresholds become increasingly hard to derive. The number of isolated nodes would be a natural candidate for another limit theorem.

When it comes to the time bounded cylinders the most natural way to build on our work would be to adapt the model for other, more sophisticated mobility

schemes. We see our introduction of the stacked cylinder model as a good starting point to do so. Another way to further extend this work would be to take a closer look at its topological properties. With our central limit theorem for its Euler characteristic we took a first step in this direction.

# Chapter 6

## Addendum - Simulation Techniques

In preparation of this thesis the author has employed a number of simulation techniques to obtain a better understanding of the topics covered in this work. In this chapter we will present some of these techniques and give short examples of their implementation. All implementations can be found on the authors Github page at <https://github.com/stbussmann/CarcaSim>.

### 6.1. Poisson Point Processes

To simulate a (inhomogeneous) Poisson point process on a bounded window of observation  $W \subset \mathbb{R}^2$ , we can exploit the independence property and disassemble the window into a large number of disjoint cells. Then the distribution of the number of Poisson points in each of these cells is independent from the other ones. Assume  $C = [x_1, x_2) \times [y_1, y_2)$  to be one of these cells and  $f : \mathbb{R}^2 \rightarrow \mathbb{R}$  the given intensity function. We use Fubini's Theorem to calculate

$$\gamma_C = \int_C f(x, y) d(x, y) = \int_{x_1}^{x_2} \int_{y_1}^{y_2} f(x, y) d(y) d(x).$$

Then we assign the cell a random number  $p_C$  with respect to a Poisson probability measure with parameter  $\gamma_C$ . After that,  $p_C$  points  $(x, y)$  are created by sampling  $x$  from a uniform distribution on  $[x_1, x_2)$  and  $y$  from a uniform distribution on  $[y_1, y_2)$ . The union over all these points created for every cell is the Poisson point process. It is clear that the trustworthiness of this simulation is heavily dependent on how many cells we choose to evaluate. This is illustrated in Figure 6.1 below. By the additivity of integration the number of generated points will be accurate no matter how many cells we use. However, their position might be flawed in the inhomogeneous case. The error in the  $x$  and  $y$  coordinates of a point is bounded by the width respectively the height of a cell.

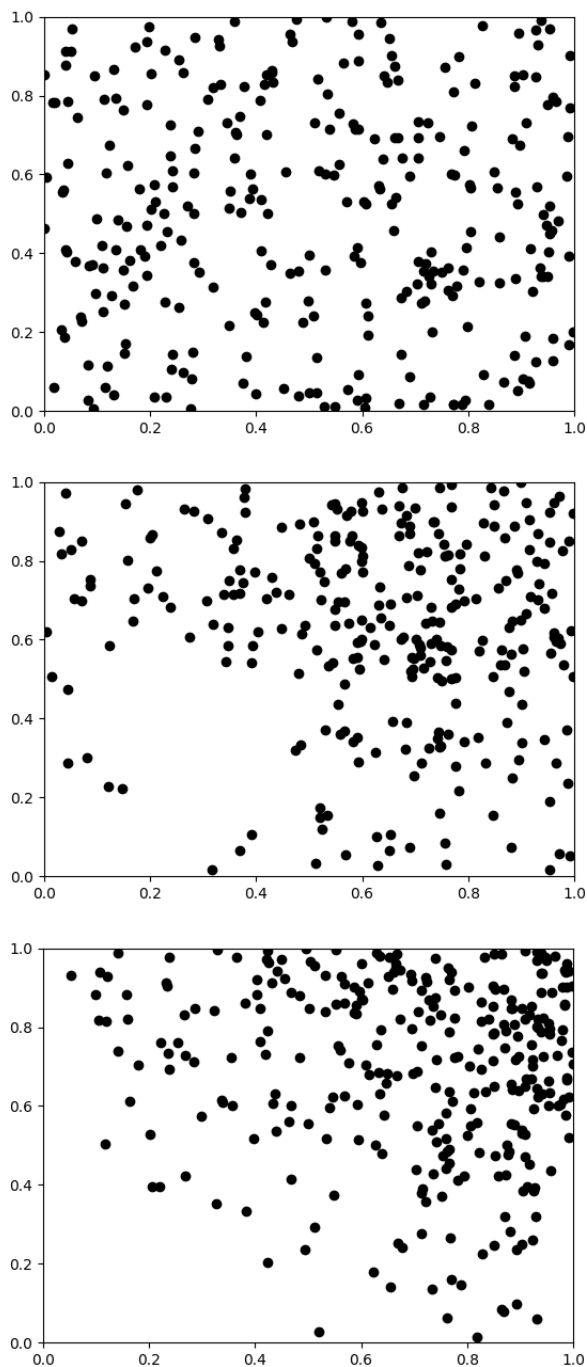


Figure 6.1: Poisson processes generated by the presented algorithm using intensity function  $200 \cdot (x + y)^3$ . The upper picture shows grid size  $1 \times 1$ , the middle one  $2 \times 2$  and the lower one  $1024 \times 1024$ .

**Algorithm 1:** Poisson point process

**Input:** Height and width of observation window, intensity function  $f$ , number of cells  $n_x$  in  $x$ - and  $n_y$  in  $y$ -direction.

**Output:** A list  $S$  of the random points created by the Poisson point process.

**begin**

- Get cell width  $c_x$  (height  $c_y$ ) by dividing width (height) of the observation window by  $n_x$  ( $n_y$ ).
- Initialize an empty list  $S$ .
- for**  $i$  from 0 to  $n_x - 1$  **do**
  - for**  $j$  from 0 to  $n_y - 1$  **do**
    - Calculate  $p = \int_{i \cdot c_x}^{(i+1) \cdot c_x} \int_{j \cdot c_y}^{(j+1) \cdot c_y} f(x, y) \, dy \, dx$ .
    - Sample  $s$  from a Poisson distribution with parameter  $p$ .
    - for**  $k$  from 0 to  $s$  **do**
      - Append a point with  $x$ -coordinate sampled from a uniform distribution on  $[i \cdot c_x, (i + 1) \cdot c_x]$  and  $y$ -coordinate sampled from a uniform distribution on  $[j \cdot c_y, (j + 1) \cdot c_y]$  to  $S$ .

The biggest computational challenge is the integration of the intensity function. Luckily this can be done with relative ease using numerical methods. The Python package SciPy for example offers the function `dblquad` to do this.

## 6.2. Connected components

Next we show how to handle components in a connectivity graph. Algorithm 2 below is an adaptation of a strategy presented in [New10, p.620] and allows us to discern the component structure of the graph. We can use this algorithm to get some insight into percolation properties of the model if we take the following result into consideration.

**Theorem 6.1** ([DCRT20, Theorem 1.4]). *Consider a Boolean model  $(\eta, r, \gamma)$  in  $\mathbb{R}^2$  as given in Definition 2.15 and assume the model to be in the subcritical regime. Let  $0 \leftrightarrow \partial \mathbb{B}_2(r)$  denote the event that there is a component in the Boolean model that connects the origin to the boundary of the ball with radius  $r \geq 1$ . Then there exists a  $c > 0$  such that*

$$\mathbb{P}(0 \leftrightarrow \partial \mathbb{B}_2(r)) \leq e^{-cr}.$$

This tells us that the probability to get a component with diameter  $2r$  decays exponentially in  $r$  whenever we are in the subcritical regime. Because of this if we choose a window of observation large enough and if the simulated model creates a crossing component from the left boundary to the right, we have a good probability to be in the supercritical regime.

**Algorithm 2:** Determining the Graph Structure**Input:** Set of nodes  $V$ . Connectivity radius  $r$ .**Output:** A list  $C$  of the components, which are given by lists of individual points.**begin**

- Initialize the index  $k = 0$ .
- Initialize an empty list  $C$
- for**  $v \in V$  **do**
  - Append an empty list to  $C$ .
  - Attach the tuple  $(v, k)$  to  $C[k]$ .
  - for** *all vertices  $w$  that have been added before  $v$*  **do**
    - if**  $\|v - w\| \leq 2 \cdot r$  **then**
      - Check component sizes of  $v$  and  $w$ .
      - Append all points in the smaller component to the bigger one and update their index to match their new component.
      - Remove all points from the smaller component.
- Increase  $k$  by one.

In this context we would like to mention the Python package Shapely which allows for the handling of two-dimensional geometric objects. In particular it allows for set operations. We can create an object for each individual ball and take the union over these balls to get a representation of the Boolean model created by the simulation. Shapely stores the model in one of two classes, both introduced by Shapely itself. If the whole model is connected we get a Polygon object, which provides convenient methods for analytics, like a method to calculate the covered area for example. If the model decomposes into connected components we get a Multipolygon object. These are iterable and contain a Polygon object representing each component. Shapely thus allows us to simulate a Boolean model in great detail and offers powerful tools for its analysis. However, this naturally comes at the cost of slower computation when compared to more specialized algorithms.

### 6.3. The Carcassonne Grid

In Chapter 3 we discussed our approach to model obstruction in telecommunication networks. The obstructed Gilbert graph is not the only model we have considered however, in this section we introduce our approach to handle obstruction via a Boolean model using star-shaped communication areas.

We start with some grid on  $\mathbb{R}^2$  where the cells have some fixed side length  $s > 0$  and declare a random variable  $X(i, j)$  for each cell, indexed by the point in that cell with maximal absolute coordinates. This random variable takes values in  $\mathcal{C}^2$  the system of compact subsets of  $\mathbb{R}^2$ .

$x(1,0)$	$x(1,1)$	$x(2,1)$
$x(0,0)$	$x(1,0)$	$x(2,0)$

Figure 6.2: Excerpt of the grid used and its assigned random variables.

Now given a node  $x = (x_1, x_2) \in \mathbb{R}^2$ , its area of communication is the random set

$$S_x = x + X(\lceil x_1 \rceil, \lceil x_2 \rceil).$$

The idea behind this approach was that nodes located in close proximity to one another should be assigned the same or a similar communication zone. Naturally this introduces a great deal of dependency into the model. The grid was thought of as a way to introduce such dependency in a simple and controlled fashion.

The sets we assign to nodes are created in the following way. We fix real numbers  $0 < r_- \leq r_+ < \infty$  and refer to  $r_-$  as the inradius of a communication zone and  $r_+$  as its outradius. Now we fix an even  $k \in \mathbb{N}$  and randomly choose  $k$  points given by their polar coordinates. The distance from the origin for each point is chosen with respect to a uniform distribution on  $[r_-, r_+]$ . The angle of the  $i$ -th point is chosen according to a uniform distribution on  $[(i-1) \cdot \frac{2\pi}{k}, i \cdot \frac{2\pi}{k})$ . Illustration 6.3 clarifies this procedure.

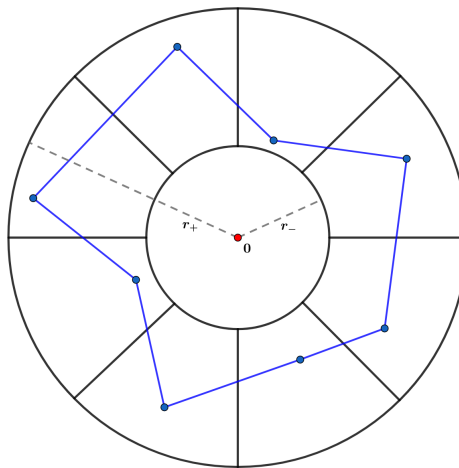


Figure 6.3: Illustration of the generating technique used for the communication zones. The blue polygon marks the boundary of the zone.



Note that how irregular these shapes are is highly dependent on  $k$  and the difference  $|r_+ - r_-|$ . For nodes created by a Poisson point process, large  $k$  and  $r_+ \approx r_-$  this procedure approximates the classical Boolean model.

In our work we used this setting to gain some insight into the influence of obstruction on telecommunication networks. Studied quantities were the covered volume and the number of isolated nodes. Our setup for this was as follows: we have a simulation area of  $1\text{km}^2$  and cells of sidelength 5m. We fix an outradius  $r_+$  of 30m and set  $r_- = \Delta \cdot r_+$  for  $\Delta \in \{0.2, 0.4, 0.6, 0.8, 1\}$ . For each value of  $\Delta$  we did 300 iterations of the following procedure:

1. We placed a grid over the simulation area and realized the corresponding random variables as instructed above.
2. A deterministic number of nodes was placed in the area at random and homogeneously.
3. Communication zones were assigned accordingly.
4. The number of isolated nodes and the covered volume were calculated.

After that we averaged volume and isolated nodes over the 300 samples created for each  $\Delta$ . The resulting numbers give us an idea of the impact obstruction has on the connectivity of the simulated network. The following tables summarize our results for 250 and 1000 nodes respectively.

$\Delta$	Avg. Covered Volume	Avg. Number of Isolated Nodes
0.2	223504.69	125.14
0.4	293257.59	116.62
0.6	360932.42	107.88
0.8	432018.29	98.68
1.0	509706.59	88.27

Table 6.1: Results for 250 nodes.

$\Delta$	Avg. Covered Volume	Avg. Number of Isolated Nodes
0.2	641991.60	159.24
0.4	758830.91	142.57
0.6	853257.23	126.70
0.8	925718.70	111.59
1.0	979453.36	96.24

Table 6.2: Results for 1000 nodes.

The data clearly shows that the introduction of obstructed communication zones has a substantial influence on connectivity in the network. Furthermore, the data seems to suggest asymptotic normality of both the distribution of the volume and of the isolated nodes as a kernel density estimation shows:

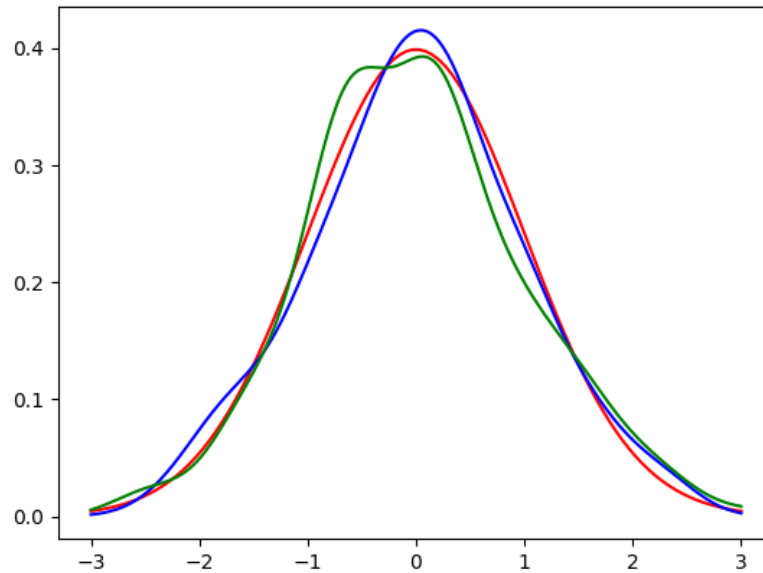


Figure 6.4: In this picture we see the density function of standard normal distribution in red and kernel density estimators of the standardized volume (blue) and isolated nodes (green). This is in the case  $\Delta = 0.2$  and 1000 nodes.

In line with these observations [LRP17, Theorem 6.1] shows asymptotic normality of both the distribution of the volume and of the isolated nodes for Boolean models with general grains (i.i.d. compact sets) in the binomial setting. These results motivated us to further investigate obstruction in telecommunication networks, leading to the theorems presented in Chapter 3. We also used the Carcassonne simulation technique on mobility traces generated by BonnMotion, thus studying the impact of mobility. This inspired the TBC model and the results derived in Chapter 4.

# List of Figures

2.1	Two realizations of Poisson point processes observed in the cube $[0, 1]^2$ . To the left we see the stationary case with intensity 200. To the right we see the case where the intensity measure is given by $\Lambda(A) = 200 \cdot \int_A (x + y)^3 \, d(x, y)$ , $A \subset [0, 1]^2$ . . . . .	14
2.2	Excerpt of a Boolean model in $\mathbb{R}^2$ . . . . .	16
2.3	Visualization of the bond percolation model on the 2-dimensional lattice. The black bonds are open, the grey ones closed. On the left we have $p = 0.2$ , to the right $p = 0.5$ . . . . .	19
2.4	Illustration of site percolation on a triangular lattice. The black vertices are open, grey ones are closed. Same for the edges. . . . .	20
2.5	Two Boolean models with identical radius. The left one has too low intensity to form an unbounded component. The right, denser one has formed one, which is marked in black. . . . .	21
3.1	An example of a tree and its generations. . . . .	32
3.2	Illustration of the construction used in the proof of Theorem 3.6. In the center we have the point $x$ and the blue shaded area is the mentioned intersection $A_x$ of open balls. . . . .	35
3.3	Variance estimation for $d = 2$ . The shaded area marks $H_{\frac{2}{2}}^2(r)$ . . . . .	39
4.1	The blue shaded area is the set of possible directions when $d = 2$ . . . . .	44
4.2	In the left picture we see a cylinder with basepoint $\hat{p}_0$ and direction $v$ . The arrow marks the displaced vector $p + v$ . To the right we have an excerpt of a TBC model $Z$ constructed on $\mathbb{R}^2$ . . . . .	46
4.3	The event $A_i$ . The two nodes in the center can only interact with one another, as the shaded area is conditioned to be empty and cannot be bridged by cylinders even with maximum scope. . . . .	58
4.4	An excerpt of the TBC model in the expanded setting. . . . .	60
6.1	Poisson processes generated by the presented algorithm using intensity function $200 \cdot (x + y)^3$ . The upper picture shows grid size $1 \times 1$ , the middle one $2 \times 2$ and the lower one $1024 \times 1024$ . . . . .	69
6.2	Excerpt of the grid used and its assigned random variables. . . . .	72

---

6.3	Illustration of the generating technique used for the communication zones. The blue polygon marks the boundary of the zone. . . . .	72
6.4	In this picture we see the density function of standard normal distribution in red and kernel density estimators of the standardized volume (blue) and isolated nodes (green). This is in the case $\Delta = 0.2$ and 1000 nodes. . . . .	74

Figures 2.1, 2.5, 4.2 and 4.5 have been generated using Python scripts written by the author of the thesis. Packages used were NumPy, Matplotlib and Shapely. All other figures have been generated using GeoGebra.

# Bibliography

- [ABD21] N. Aschenbruck, S. Bussmann, and H. Döring. Asymptotics of a time bounded cylinder model. Electronic preprint arXiv:2105.13916, 2021.
- [ABV<sup>+</sup>12] D. Anthony, W.P. Bennett, M.C. Vuran, M.B. Dwyer, S. Elbaum, A. Lacy, M. Engels, and W. Wehtje. Sensing through the continent: Towards monitoring migratory birds using cellular sensor networks. *2012 ACM/IEEE 11th International Conference on Information Processing in Sensor Networks (IPSN)*, pages 329–340, 2012.
- [BBGT20] A. Baci, C. Betken, A. Gusakova, and C. Thäle. Concentration inequalities for functionals of Poisson cylinder processes. *Electronic Journal of Probability*, 25:1–27, 2020.
- [Bla17] Bartłomiej Błaszczyszyn. Lecture Notes on Random Geometric Models — Random Graphs, Point Processes and Stochastic Geometry. Lecture, 2017.
- [BP16] S. Bourguin and G. Peccati. The Malliavin-Stein method on the Poisson space. In *Stochastic analysis for Poisson point processes*, volume 7 of *Bocconi Springer Ser.*, pages 185–228. Bocconi Univ. Press, 2016.
- [BT16] E. Broman and J. Tykesson. Connectedness of Poisson cylinders in Euclidean space. *Annals de l’Institut Henry Poincaré Probabilités et Statistiques*, 52:102–126, 2016.
- [CBD02] T. Camp, J. Boleng, and V. Davies. A survey of mobility models for ad hoc network research. *Wireless communications and mobile computing*, 2(5):483–502, 2002.
- [DCRT20] H. Duminil-Copin, A. Raoufi, and V. Tassion. Subcritical phase of  $d$ -dimensional Poisson Boolean percolation and its vacant set. *Annales Henri Lebesgue*, 3:677–700, 07 2020.
- [DFHO<sup>+</sup>18] J. Dede, A. Förster, E. Hernández-Orallo, J. Herrera-Tapia, K. Kuladinithi, V. Kuppusamy, P. Manzoni, A. bin Muslim, A. Udugama,

- and Z. Vatandas. Simulating opportunistic networks: Survey and future directions. *IEEE Communications Surveys Tutorials*, 20(2):1547–1573, 2018.
- [DFK16] H. Döring, G. Faraud, and W. König. Connection times in large ad-hoc mobile networks. *Bernoulli*, 22(4):2143 – 2176, 2016.
- [Die18] R. Diestel. *Graph Theory*. Graduate Texts in Mathematics. Springer Berlin Heidelberg, 2018.
- [DMPG09] J. Díaz, D. Mitsche, and X. Pérez-Giménez. Large connectivity for dynamic random geometric graphs. *IEEE Trans. Mob. Comput.*, 8:821–835, 06 2009.
- [FH21] D. Flimmel and L. Heinrich. On the variance of the area of planar cylinder processes driven by Brillinger-mixing point processes. Electronic preprint arXiv:2104.10224, 2021.
- [Gil61] E.N. Gilbert. Random plane networks. *Journal of the Society for Industrial and Applied Mathematics*, 9:533–543, 1961.
- [Hae12] M. Haenggi. *Stochastic Geometry for Wireless Networks*. Cambridge University Press, 2012.
- [HJC19] C. Hirsch, B. Jahnel, and E. Cali. Continuum percolation for Cox point processes. *Stochastic Processes and their Applications*, 129(10):3941–3966, 2019.
- [HJC21] C. Hirsch, B. Jahnel, and E. Cali. Percolation and connection times in multi-scale dynamic networks. Electronic preprint arXiv:2103.03171, 2021.
- [HS09] L. Heinrich and M. Spiess. BerryEsseen bounds and Cramér-type large deviations for the volume distribution of Poisson cylinder processes. *Lithuanian Mathematical Journal*, 49:381–398, 2009.
- [HS13] L. Heinrich and M. Spiess. Central limit theorems for volume and surface content of stationary Poisson cylinder processes in expanding domains. *Advances in Applied Probability*, 45:312–331, 2013.
- [JBRAS05] A.P. Jardosh, E.M. Belding-Royer, K.C. Almeroth, and S. Suri. Real-world environment models for mobile network evaluation. *IEEE Journal on Selected Areas in Communications*, 23:622 – 632, 2005.
- [JK20] B. Jahnel and W. König. *Probabilistic Methods in Telecommunications*, pages 43–71. Birkhäuser Basel, 06 2020.

- [Kes80] H. Kesten. The critical probability of bond percolation on the square lattice equals  $\frac{1}{2}$ . *Communications in Mathematical Physics*, 74:41–59, 1980.
- [Kes82] H. Kesten. *Percolation Theory for Mathematicians*. Progress in probability and statistics. Birkhäuser, 1982.
- [Las16] G. Last. Stochastic analysis for Poisson processes. In: *Stochastic Analysis for Poisson Processes*, Bocconi & Springer Series Vol.7, 2016.
- [Li11] S. Li. Concise formulas for the area and volume of a hyperspherical cap. *Asian Journal of Mathematics and Statistics*, 4:66–70, 2011.
- [LJ19] A. Lohachab and A. Jangra. Opportunistic Internet of Things (IoT): Demystifying the effective possibilities of opportunistic networks towards IoT. In *2019 6th International Conference on Signal Processing and Integrated Networks (SPIN)*, pages 1100–1105, 2019.
- [LP18] G. Last and M. Penrose. *Lectures on the Poisson process*, volume 7 of *Institute of Mathematical Statistics Textbooks*. Cambridge University Press, Cambridge, 2018.
- [LPS16] G. Last, G. Peccati, and M. Schulte. Normal approximation on Poisson spaces: Mehler’s formula, second order Poincaré inequalities and stabilization. *Probability Theory and Related Fields*, 165(3-4):667–723, 2016.
- [LRP17] R. Lachièze-Rey and G. Peccati. New Berry-Esseen bounds for functionals of binomial point processes. *The Annals of Applied Probability*, 27:1992–2031, 2017.
- [Mal78] P. Malliavin. Stochastic calculus of variation and hypoelliptic operators. Proceedings of the International Symposium on Stochastic Differential Equations, Kyoto, 1976, 1978.
- [MFM<sup>+</sup>14] V. Mota, C. Felipe, D. Macedo, J.M. Nogueira, and A. Loureiro. Protocols, mobility models and tools in opportunistic networks: A survey. *Computer Communications*, 48, 07 2014.
- [MR96] R. Meester and R. Roy. *Continuum Percolation*. Cambridge Tracts in Mathematics. Cambridge University Press, 1996.
- [New10] M.E.J. Newman. *Networks : An Introduction*. Oxford University Press, 2010.
- [Pen03] M.D. Penrose. *Random Geometric Graphs*, volume 5 of *Oxford Studies in Probability*. Oxford University Press, Oxford, 2003.

- [PR16] G. Peccati and M. Reitzner. *Stochastic analysis for Poisson point processes: Malliavin calculus, Wiener-Itô chaos expansions and stochastic geometry*. Bocconi & Springer Series. Springer International Publishing, 2016.
- [PSTU10] G. Peccati, J. L. Solé, M. S. Taqqu, and F. Utzet. Steins method and Normal approximation of Poisson functionals. *The Annals of Probability*, 38(2):443 – 478, 2010.
- [Rei05] M. Reitzner. Central limit theorems for random polytopes. *Probability Theory and Related Fields*, 133:483507, 2005.
- [RMSM01] E.M. Royer, P.M. Melliar-Smith, and L.E. Moser. An analysis of the optimum node density for ad hoc mobile networks. *ICC 2001. IEEE International Conference on Communications. Conference Record (Cat. No.01CH37240)*, 3:857–861, 2001.
- [Ros11] N. Ross. Fundamentals of Stein’s method. *Probability Surveys*, 8:210–293, 2011.
- [SA19] M. Schwamborn and N. Aschenbruck. On modeling and impact of geographic restrictions for human mobility in opportunistic networks. *Performance Evaluation*, 130:17–31, 2019.
- [Ste72] C. Stein. A bound for the error in the normal approximation to the distribution of a sum of dependent random variables. Proc. 6th Berkeley Sympos. math. Statist. Probab., Univ. Calif. 1970, 2, 583-602 (1972)., 1972.
- [SW08] R. Schneider and W. Weil. *Stochastic and integral geometry*. Probability and its Applications (New York). Springer-Verlag, Berlin, 2008.
- [Wei87] W. Weil. Point processes of cylinders, particles and flats. *Acta Applicandae Mathematicae*, 9:103–136, 1987.
- [YSBRL19] M. Yemini, A. Somekh-Baruch, C. Reuven, and A. Leshem. The simultaneous connectivity of cognitive networks. *IEEE Transactions on Information Theory*, 65(11):6911 – 6930, 2019.



## ANLAGE

### **Erklärung über die Eigenständigkeit der erbrachten wissenschaftlichen Leistung**

Ich erkläre hiermit, dass ich die vorliegende Arbeit ohne unzulässige Hilfe Dritter und ohne Benutzung anderer als der angegebenen Hilfsmittel angefertigt habe. Die aus anderen Quellen direkt oder indirekt übernommenen Daten und Konzepte sind unter Angabe der Quelle gekennzeichnet.

Weitere Personen waren an der inhaltlichen materiellen Erstellung der vorliegenden Arbeit nicht beteiligt. Insbesondere habe ich hierfür nicht die entgeltliche Hilfe von Vermittlungs- bzw. Beratungsdiensten (Promotionsberater oder andere Personen) in Anspruch genommen. Niemand hat von mir unmittelbar oder mittelbar geldwerte Leistungen für Arbeiten erhalten, die im Zusammenhang mit dem Inhalt der vorgelegten Dissertation stehen.

Die Arbeit wurde bisher weder im In- noch im Ausland in gleicher oder ähnlicher Form einer anderen Prüfungsbehörde vorgelegt.

.....  
(Ort, Datum)

.....  
(Unterschrift)